CalVal Jason-1

Jason-1 validation and cross calibration activities [Annual Report 2013]

Contract No 104685 - lot1.2A

Reference : CLS.DOS/NT/ 13-226

Nomenclature : SALP-RP-MA-EA-22269-CLS

Issue : 1rev 1

Date : April 15, 2014

CLS - 8-10 Rue Hermès - Parc Technologique du Canal - 31520 Ramonville St-Agne - FRANCE
Telephone 33 5 61 39 47 00 / Fax 33 5 61 75 10 14

Chronology Issues :		
Issue :	Date :	Reason for change :
1.0	30/10/2013	Created
1.1	15/04/2014	Revision, taking into account remarks from N. Picot

People involved in this issue :		
Written by :	H. Roinard	CLS
	G. Valladeau	CLS
	J.F. Legeais	CLS
	S. Philipps	CLS
	M. Ablain	CLS
Checked by :	S. d'Alessio	CLS
Approved by :	J.P. Dumont	CLS
	M. Ablain	CLS
Application authorized by :		

Index sheet :	
Context	
Keywords	Jason-1, Calval, orbits, 59-day signal
hyperlink	

Distribution :		
Company	Means of distribution	Names
CLS/DOS	1 electonic copy	G. DIBARBOURE
	1 electonic copy	V. ROSMORDUC
DT/AQM (DOC/CLS)	DOCUMENTATION	1 printed copy + 1 cd-rom
CNES	1 electronic copy	thierry.guinle@cnes.fr
CNES	1 electronic copy	emilie.bronner@cnes.fr
CNES	1 electronic copy	nicolas.picot@cnes.fr
CNES	1 electronic copy	aqgp_rs@cnes.fr
CNES	1 electronic copy	dominique.chermain@cnes.fr
CNES	1 electronic copy	delphine.vergnoux@cnes.fr

.

List of tables and figures :

List of Tables

List of Figures

Contents

1. Introduction

This document presents the synthesis report concerning validation activities of Jason-1 GDRs under SALP contract (N° 104685 Lot1.2A) supported by CNES at the CLS Space Oceanography Division. It is divided into several parts concerning mainly CAL/VAL Jason-1 activities, but when useful, results from Topex/Poseidon and Jason-2 are also shown for comparison.

Since the beginning of the mission, Jason-1 data have been analyzed and monitored in order to assess the quality of Jason-1 GDR products (AVISO and PODAAC User handbook, [1]) for oceanographic applications.
Since May 2012, Jason-1 was on a geodetic orbit. To distiguish this geodetic phase from the previous repeat ground-track, numbering of the geodetic orbit period starts with cycle 500. Furthermore from cycle 500 onwards, the orbit standard is switched to POE standard D and the mean sea surface available in the GDRs is CNES-CLS-2011. The repeat period of the geodetic orbit is 406 days, but GDRs are distributed using the 10.9 days sub-cycle. Therefore Jason-1 GDRs during the geodetic phase contain 280 tracks per cycle. For more information about the Jason-1 geodetic mission, see the technical note issued by E. Bronner and G. Dibarboure [2].
This report is basically concerned with long-term monitoring of the Jason-1 altimeter system, from all GDR data until the end of the mission, that is for 10 years of data on repetitive orbit (cycles 1 to 374, corresponding to period from January 2002 to March 2012) and 14 months of data on geodetic orbit (cycles 500 to 537, corresponding to period from May 2012 to June 2013).
This includes careful monitoring of all altimeter and radiometer parameters, performance assessment, geophysical evaluation and cross-calibration with T/P measurements (as long as T/P data were available). For comparison and cross-calibration with Jason-2 data, see [4]. For comparison and cross-calibration with Envisat data (until Envisat shut down on 8th of April 2012), see [6].
Note that in this report, on figures showing cycle per cycle monitoring, the x-axis was shifted for the geodetic period by 119 cycles, in order to prevent a (artificial) gap between the last cycle on the repeat ground-track (cycle 374) and the first cycle on the geodetic orbit (cycle 500).
After loss of telemetry on 21 June 2013, Jason-1 was passivated and decommissioned on 01 July 2013, with the last command sent at 16:37:40 UTC.

Moreover specific studies are presented in this document :

- Estimation of the jump in GMSL at move to geodetic orbit [8.1.]
- Comparison between GDR-D orbit standard and current GDR-C orbit standard [8.2.].
- Towards a new Jason-1 orbit solution using different ponderation strategies of DORIS beacons in South Atlantic Anomaly for climate studies [8.3.]

This work is routinely performed at CLS and in this frame, besides continuous analyzes in terms of altimeter data quality, Jason-1 GDR Quality Assessment Reports (e.g. Ablain et al. 2013 [7]) are produced and associated to data dissemination. Even if only low order statistics are mainly presented here, other analyzes including histograms, plots and maps are continuously produced and used in the quality assessment process.
The work performed in terms of data quality assessment also includes cross-calibration analyzes mainly with the T/P mission until November 2005 (end of the T/P mission). Even if T/P mission is finished, cross-calibration analyzes are useful for the reprocessing activities in order to study the sea state bias or the relative SSH bias for instance. Cross-calibration analyzes with Jason-2 are also performed, but shown in annual report of Jason-2 (see [4]).

Indeed, it is well recognized that the usefulness of any altimeter data only makes sense in a multi-mission context, given the growing importance of scientific needs and applications, particularly for operational oceanography. One major objective of the Jason-1 mission is to continue the T/P high precision altimetry and to allow combination with other missions (ENVISAT, Jason-2). This kind of comparisons between different altimeter missions flying together provides a large number of estimations and consequently efficient long term monitoring of instrument measurements. Of course, other sources of comparisons are also needed, using independent datasets (e.g. Queffeulou et al. 2004 [8], Ray and Beckley 2003 [9], Arnault et al. 2004 [10], Provost et al. 2004[11], Durrant et al. 2009 [12], Abdalla et al. 2010 [13]). [15] and [17] show comparisons between altimeter data and in-situ data (respectively tide gauges measurements and T/S profiles).

2. Processing status

2.1. IGDR, GDR and CAL/VAL Processing

To date, the whole mission of Jason-1 (GDR products) is available in version "c" of CMA ground processing software, though there are some differences from the move to the geodetic orbit onwards. The purpose of this document is to report the major features of the data quality from the Jason-1 mission. Moreover, the document is associated with comparison results from T/P GDRs. All these cycle reports are available on AVISO website: http://www.aviso.altimetry.fr/en/home.html. In addition to these reports, several meeting (CAVE, OSTST) have been performed to inform the Jason-1 GDR's users about the main results and the studies in progress.

2.1.1. Models and Standards History

Three versions of the Jason-1 Interim Geophysical Data Records (IGDRs) and Geophysical Data Records (GDRs) have been generated to date. These three versions are identified by the version numbers "a", "b" and "c" in the name of the data products. For example, version "a" GDRs are named "JA1_GDR_2Pa", version "b" GDRs are named "JA1_GDR_2Pb", and version "c" GDRs are named "JA1_GDR_2Pc". All versions adopt an identical data record format as described in Jason-1 User Handbook and differ only in the models and standards that they adopt. Version "a" I/GDRs were the first version released soon after launch. Version "b" I/GDRs were first implemented operationally from the start of cycle 140 for the IGDRs and cycle 136 for the GDRs. Reprocessing to generate version "b" GDRs for cycles 1-135 were performed in 2006 and 2007 in order to generate a consistent data set. Version "c" I/GDRs were first operationally implemented from mid cycle 237 for the IGDRs and cycle 233 for the GDRs. Reprocessing to generate version "c" GDRs for cycles 1-232 were performed from June 2008 to January 2010 in order to generate a consistent data set. Table 1 below summarizes the models and standards that are adopted in these three versions of the Jason-1 I/GDRs. More details on some of these models are provided in Jason-1 User Handbook document ([1]).
Furthermore, from cycle 500 onwards, the orbit standard is switched to POE standard D and the mean sea surface available in the GDRs is CNES-CLS-2011.

Model	Product Version "a"	Product Version "b"	Product Version "c"
Orbit	JGM3 Gravity Field DORIS tracking data for IGDRs DORIS+SLR tracking data for GDRs	EIGEN-CG03C Gravity Field DORIS tracking data for IGDRs DORIS+SLR+GPS tracking data for GDRs	EIGEN-GL04S with time-varying gravity DORIS tracking data for IGDRs DORIS+SLR+GPS tracking data for GDRs with increased weight of D/L

.../...

Model	Product Version "a"	Product Version "b"	Product Version "c"
			from cycle 500 onwards, switched to POE standard D (EIGEN-GRGS_RL02bis_MEAN-FIELD (2011))
Altimeter Re-tracking	MLE3 + 1st order Brown model (mis-pointing estimated separately)	MLE4 + 2nd order Brown model : MLE4 simultaneously retrieves the 4 parameters that can be inverted from the altimeter wave-forms: epoch, SWH, Sigma0 and mispointing angle. This algorithm is more robust for large off-nadir angles (up to 0.8°).	Identical to version "b"
Altimeter Instru-ment Corrections	Consistent with MLE3 retracking algorithm.	Consistent with MLE4 retracking algorithm.	Identical to version "b". A new correction is available in the product to account for the apparent datation bias (field 28). Users are advised to add this correction to the Ku-band altimeter range, as it is not a component of the net instrument correction that has already been applied to the provided Ku-band range
Jason Microwave Radiometer Parameters	Using calibration pa-rameters derived from cycles 1-30.	Using calibration pa-rameters derived from cycles 1-115.	Using calibration pa-rameters derived from cycles 1-227. From GDR cycle 500 on-wards, a new calibra-tion file is applied.
			.../...

Model	Product Version "a"	Product Version "b"	Product Version "c"
Dry Troposphere Range Correction	From ECMWF atmospheric pressures.	From ECMWF atmospheric pressures and model for S1 and S2 atmospheric tides.	From ECMWF atmospheric pressures and model for S1 and S2 atmospheric tides. Uses new ECMWF delivery to correct for spurious oscillation effects.
Wet Troposphere Range Correction from Model	From ECMWF model	From ECMWF model.	Identical to version "b"
Back up model for Ku-band ionospheric range correction.	Derived from DORIS measurements.	Derived from DORIS measurements.	Derived from JPL's Global Ionosphere Model (GIM) maps
Sea State Bias Model	Empirical model derived from cycles 19-30 of version "a" data.	Empirical model derived from cycles 11-100 of MLE3 altimeter data with version "b" geophysical models.	Empirical model derived from cycles 11-100 of MLE4 altimeter data with version "c" geophysical models
Mean Sea Surface Model	GSFC00.1	CLS01	Identical to version "b" until cycle 374, and switched to CNES-CLS-2011 from cycle 500 onwards
Along Track Mean Sea Surface Model	None (set to default)	None (set to default)	None (set to default)
Geoid	EGM96	EGM96	Identical to version "b"
Bathymetry Model	DTM2000.1	DTM2000.1	Identical to version "b"
Mean Dynamic Topography	None (was a spare)	None (was a spare)	Rio 2005 solution
Inverse Barometer Correction	Computed from ECMWF atmospheric pressures	Computed from ECMWF atmospheric pressures after removing model for S1 and S2 atmospheric tides.	Identical to Version "b" but using new ECMWF delivery to correct for spurious oscillation effects

.../...

Model	Product Version "a"	Product Version "b"	Product Version "c"
Non-tidal High-frequency De-aliasing Correction	None (set to default)	Mog2D ocean model on GDRs, none (set to default) on IGDRs. Ocean model forced by ECMWF atmospheric pressures after removing model for S1 and S2 atmospheric tides.	High resolution Mog2D model for both IGDR and GDR products
Tide Solution 1	GOT99	GOT00.2 + S1 ocean tide . S1 load tide ignored.	Identical to version "b"
Tide Solution 2	FES99	FES2004 + S1 and M4 ocean tides. S1 and M4 load tides ignored.	FES2004 + S1 and M4 ocean tides. S1, K2 and loading tides have been updated
Equilibrium long-period ocean tide model.	From Cartwright and Taylor tidal potential.	From Cartwright and Taylor tidal potential.	Identical to version "b"
Non-equilibrium long-period ocean tide model.	None (set to default)	Mm, Mf, Mtm, and Msqm from FES2004.	Identical to version "b"
Solid Earth Tide Model	From Cartwright and Taylor tidal potential.	From Cartwright and Taylor tidal potential.	Identical to version "b"
Pole Tide Model	Equilibrium model	Equilibrium model.	Identical to version "b"
Wind Speed from Model	ECMWF model	ECMWF model	Identical to version "b"
Altimeter Wind Speed	Table derived from TOPEX/POSEIDON data.	Table derived from version "a" Jason-1 GDR data.	Identical to version "b"
Rain Flag	Derived from TOPEX/POSEIDON data.	Derived from version "a" Jason-1 GDRs.	Derived from version "b" Jason-1 GDRs using the AGC instead of sigma naught values

.../...

Model	Product Version "a"	Product Version "b"	Product Version "c"
Ice Flag	Climatology table	Climatology table	New flag based on the comparison of the model wet tropospheric correction and of a radiometer bi frequency wet tropospheric correction (derived from 23.8 GHz and 34.0 GHz), accounting for a backup solution based on climatologic estimates of the latitudinal boundary of the ice shelf, and from altimeter wind speed.

Table 1: *M*odels and standards adopted for the Jason-1 product version "a", "b", and "c"

2.1.2. Differences in editing procedure for the different GDR product versions

For GDR version "c" the same editing criteria and thresholds like in GDR version "b" should be used. Since GDR version "b" the MLE4 retracking algorithm is used. It is based on a second-order altimeter echo model and is more robust for large off-nadir angles (up to 0.8 degrees). For product version "a" (CMA version 6.3), the maximum threshold on square off-nadir angle proposed in Jason-1 User Handbook document was set to 0.16 deg^2 (inline with MLE3 retrackig algorithm specifications). Since GDR version "b", this threshold is too restrictive and has been set to 0.64 deg^2 (inline with MLE4 retrackig algorithm specifications).

However, this editing criteria had the side effect of removing some bad measurements impacted by rain cells, sigma0 blooms or ice. With the new threshold (0.64 deg^2), these measurements are not rejected anymore.

2.1.3. Impact of product versions

The main changes between GDRs version "a" and "b" were the new orbit, the retracking of the wave forms with MLE4 algorithm, and new geophysical corrections. This had not only an impact on editing procedure, but also on crossover performances. For version "c", the main changes are the new orbit, new JMR calibration and new sea state bias. For information concerning reprocessing in version "b", please refer to [18] or [20]. Concerning reprocessing in version "c", please refer to [21] or [22].

2.1.4. Impact of the move to geodetic orbit

Since May 2012, Jason-1 has been moved on a geodetic orbit after more than 10 years on a repetitive orbit. For more information about the Jason-1 geodetic mission, see the technical note issued by E. Bronner and G. Dibarboure [2]. This induces a few differences to be taken into account in the products.

- The repeat period of the geodetic orbit is 406 days, but GDRs are distributed using the 10.9 days sub-cycle. Therefore Jason-1 GDRs during the geodetic phase contain 280 tracks per cycle.
- From cycle 500 onwards, the orbit standard is switched to POE standard D and the mean sea surface available in the GDRs is CNES-CLS-2011.
- Figure 1 shows the drift of pass 001 ground-track from 10.9-days pseudo-cycles 500 to 537.

Note that on this new orbit, there are overflights of Jason-1 by Jason-2 every 33 days: in order to avoid interferences on Jason-2 (reference mission), Jason-1 altimeter is switched to INIT MODE for 3 hours during the overflight period, so that no altimeter data are acquired [2].

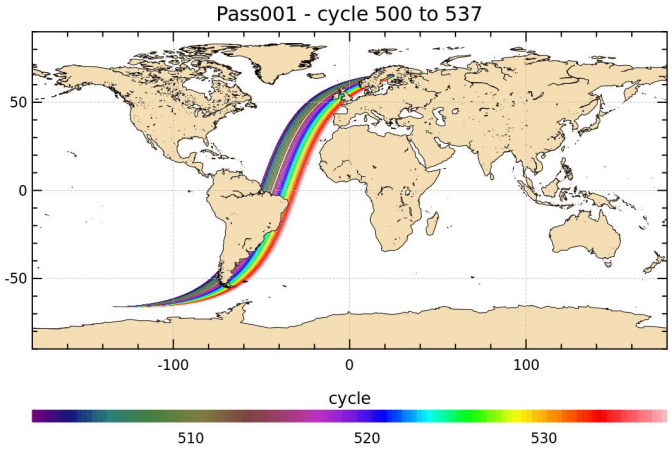

Figure 1: *Evolution of the ground track of pass 001 for cycles 500 to 537*

2.2. CAL/VAL status

2.2.1. Missing measurements

This section presents a summary of major satellite events that occurred from cycle 1 to 537. Table 2 gives a status about the number of missing passes (or partly missing) for GDRs version "c" and the associated events for each cycle.
Gyro calibration, Star Tracker unavailability and ground processing issues were the main events which produced missing data from cycle 1 to 73 (2002 and 2003).
During year 2004 (cycle 73 to 110), 2 safe hold mode incidents have produced 15 days of missing data due to a wheel anomaly. As result of this incident, only 3 wheels have been available but this has had no impact on scientific applications.
During year 2005 (110-146), most of incidents are due to SEU. The altimeter was reinitialized automatically without C-band. Few passes have only been impacted each time, and they are rejected because of the lack of C-band data, and therefore lack of dual-frequency ionospheric correction.
During year 2006 (cycles 147 - 183) Jason-1 experienced a safe hold mode (cycle 177 to 179) producing 17 days of missing data due to mass memory error. In addition 2 altimeter SEU occurred. It also happened that small data gaps occur (less than one minute duration).
During 2007 (cycles 183 to 220) Jason-1 had experienced several altimeter SEU.
In 2008 (cycles 220 to 257), there were two major events : the altimeter switch-off in May, due to the close encounter with drifting TOPEX/Poseidon, and a safehold mode in August.
During 2009 (cycles 257 to 294), Jason-1 was moved from its original groundtrack to its new interleaved groundtrack from 26th January to 14th February 2009. During most of this time, no altimeter or radiometer data is available. Furthermore, the satellite experienced a safehold mode in September 2009 producing 10 days of missing data.
During 2010 (cycles 294 to 331) Jason-1 was particularly impacted by degraded performances of its Star Trackers and Gyro wheels, especially when the satellite is in yaw fix mode. This lead to high mispointing, which caused sometimes altimeter lost of track and altimeter incidences. To avoid the possibility of a spacecraft safe hold, Jason-1 swaped on 14th of April 2010 from Gyro wheel 1 to redundant Gyro wheel 3. Furthermore, during cycle 315 (July 2010), Jason-1 performed several out of plane maneuvers in order to deplete fuel (to reduce risk of explosion in case of loss of control). Groundtrack departed up to 7 km from nominal groundtrack.
During 2011 (cycles 331 to 368) Jason-1 continued the out of plane maneuvers in order to deplete fuel. The cycles impacted by these maneuvers are 356, and 358-360. Mispointing behavior was good in 2011.
During 2012 (cycles 368 to 521) Jason-1 turned into a first safe hold mode between 2012-02-16 and 2012-02-29 - no measurement is available from 2012-02-16 16:39:05 to 29-02-2012 10:28:44 (cycles 373 and 374)- and into a second safe hold mode since 2012-03-03 no measurement is available on its repetitive orbit from 2012-03-03 12:59:12 (during cycle 374) onwards. It was then decided to move Jason-1 to a geodetic orbit. Jason-1 science data on the geodetic orbit are available from 07-05-2012 16:00:01 (from cycle number 500) onwards.
Only half a year is available for year 2013 (cycles 521 to 537). Jason-1 was in Safe Hold Mode from 28/02/2013 to 18/03/2013. And after loss of telemetry on 21 June 2013, Jason-1 was passivated and decommissioned on 01 July 2013, with the last command sent at 16:37:40 UTC. During 2013, cycles 517 to 537 were analysed.
The following table gives an overview over missing data and why it is missing.

Jason-1 Cycles	Number of completely missing passes	Number of partly missing passes	Events
001	2	7	Science telemetry unavailability
002	14	3	On board Doris anomaly
003	0	2	Gyro-calibration
004	2	5	Gyro-calibration and Science telemetry unavailability
006	1	4	Altimeter echo data unavailability
007	0	2	Science telemetry unavailability
008	2	5	Ground processing issue
009	3	4	Poseidon-2 altimeter SEU and Gyro-calibration
010	0	2	Gyro-calibration
015	0	1	Ground processing issue
019	0	1	Ground processing issue
021	0	1	Star tracker unavailability
023	0	1	Ground processing issue
026	0	2	Gyro-calibration
027	0	2	Gyro-calibration
031	0	1	Star tracker unavailability
038	0	4	Ground processing issue
039	0	1	Gyro-calibration
042	5	2	Poseidon-2 altimeter SEU
045	0	3	Gyro-calibration
046	0	1	Poseidon-2 altimeter SEU
048	0	1	Gyro-calibration
062	0	1	Ground processing issue
064	0	2	Exceptional calibrations
068	38	0	Safe Hold Mode (19/11/03)
069	208	1	Safe Hold Mode
075	4	0	Poseidon-2 altimeter SEU

.../...

Jason-1 Cycles	Number of completely missing passes	Number of partly missing passes	Events
077	69	0	Safe Hold Mode (15/02/04 to 21/02/04)
078	82	0	Safe Hold Mode (15/02/04 to 21/02/04)
080	0	1	Calibration over ocean
082	54	1	Failure in module 3 of PLTM2
087	0	1	Calibration over ocean
091	2	4	DORIS instrument switch to redundancy and altimeter incident (no C band information)
094	0	1	Altimeter incident or star tracker unavailability
099	0	1	Altimeter incident or star tracker unavailability
101	0	1	Altimeter incident or star tracker unavailability
102	1	0	Altimeter SEU (no C band information)
103	0	2	Altimeter SEU (no C band information)
104	0	1	No data between 21:29:18 and 21:30:07 on November 8th pass 189
106	3	2	Altimeter SEU (no C band information)
108	0	2	Altimeter SEU (no C band information)
114	3	1	Altimeter SEU (no C band information)
115	0	4	2 altimeter SEU incidents (C band) and altimeter initialization procedure.
118	6	2	Altimeter SEU (no C band information)
131	0	7	TRSR2 “elephant packets” anomaly
132	0	1	Altimeter SEU (no C band information)
133	0	2	Altimeter SEU (no C band information)
136	104	2	Altimeter SEU (no C band information), Platform incident (20/09/05 to 28/09/05)
137	91	2	Platform incident (20/09/05 to 28/09/05)
161	0	5	TRSR elephant packets

.../...

Jason-1 Cycles	Number of completely missing passes	Number of partly missing passes	Events
165	0	1	(planned) Poseidon calibration (board filter)
173	0	3	Altimeter SEU (no C band information)
177	141	1	Safe Hold Mode (30/10/2006 to 16/11/2006)
178	254	0	Safe Hold Mode (30/10/2006 to 16/11/2006)
179	45	1	Safe Hold Mode (30/10/2006 to 16/11/2006)
181	5	2	Altimeter SEU
185	0	3	calibration over ocean
191	0	2	Altimeter SEU
192	0	1	calibration over ocean
198	1	1	Altimeter SEU
200	0	3	calibration over ocean
206	0	2	Altimeter SEU
219	2	0	Missing telemetry
222	0	2	calibrations over ocean
231	0	1	erroneous command sent by JTCCS
233	142	2	altimeter switch off (TP/J1 close encounter)
234	0	1	calibration
242	84	1	Safe Hold Mode
243	254	0	Safe Hold Mode
254	1	1	Altimeter SEU
260	254	0	**Jason-1 moves to its new interleaved ground-track**
261	254	0	**Jason-1 moves to its new interleaved ground-track**
262	12	4	Jason-1 moves to its new interleaved ground-track + calibrations over ocean
263	0	4	calibrations over ocean
276	0	2	calibrations over ocean
283	26	1	Safe Hold Mode (2009-09-15 to 2009-09-24)

.../...

Jason-1 Cycles	Number of completely missing passes	Number of partly missing passes	Events
284	233	0	Safe Hold Mode (2009-09-15 to 2009-09-24)
290	0	2	Altimeter SEU
301	0	3	Altimeter SEU + restart
304	0	42	Due to on-orbit degradation of star trackers and gyro wheel performances, altimeter lost track
305	0	5	Due to on-orbit degradation of star trackers and gyro wheel performances, altimeter lost track
		2	calibrations over ocean
306	0	3	Altimeter SEU + restart
310	39	53	Due to on-orbit degradation of star trackers performances, altimeter lost track + altimeter incidents + reinits
312	0	3	Altimeter SEU + restart
315	12	28	Due to on-orbit degradation of star trackers performances, altimeter lost track + altimeter incidents
316	0	5	calibrations + missing PLTM (probably linked to high mispointing)
318	0	2	calibrations over ocean
319	1	2	gyroscope calibration
324	0	2	calibrations over ocean
343	0	2	Due to calibrations, passes 106 and 107 are partially missing with respectively 62% and 23% of missing measurements over ocean
356	0	1	Due to missing PLTM there are 2 small (less than 2 minutes) data gaps on 2011-09-06 between 06 :20 :56 and 06 :22 :15 and between 06 :32 :46 and 06 :34 :38 (pass 153).
359	4	1	Passes 181 to 184 are completely missing and pass 180 is partly missing (24% of ocean measurements). These passes are missing related to DORIS DIODE autoinit mode, where precise datation is not possible

.../...

Jason-1 Cycles	Number of completely missing passes	Number of partly missing passes	Events
363	0	2	Due to calibrations, passes 106 and 107 are partly missing with respectively 68% and 15% of missing ocean measurements
373	233	1	Safe Hold Mode (2012-02-16 to 2012-02-29)
374	174	2	Safe Hold Mode (2012-03-03 to 2012-05-07)
375 to 499			Safe Hold Mode (2012-03-03 to 2012-05-07) **Move to geodetic orbit and change in numerotation**
500	3	3	CCI data are only available from 2012-05-07 16h onwards (impacting passes 001 and 002) Due to Jason-2 overflight, Jason-1 altimeter was in INIT mode on 2012-05-15 between 14:37:00 and 17:44:54. (impacting passes 206 to 209)
501	0	2	Due to calibrations,passes 172 and 174 are partly missing with respectively 69% and 67% of missing ocean measurements
502	0	1	Pass 034 has about 2m30 (2012-05-30 17h30m02 to 17h32m31) of missing ocean data due to a routine calibration done over ocean (instead of land).
503	1	2	Due to Jason-2 overflight, Jason-1 altimeter was in INIT mode on 2012-06-18 between 01:43:12 and 03:07:54. Pass 226 is completely missing and passes 225 and 227 are partly missing with 7% and 43% of missing ocean measurements.
504	0	2	Due to special calibrations, passes 198 and 199 are partly missing with respectively 68% and 21% of missing ocean data.
506	2	2	Due to Jason-2 overflight, Jason-1 altimeter was in INIT mode on 2012-07-21 between 11:47:39 and 14:02:25, so that passes 244 and 245 are totally missing and passes 243 and 246 are partly missing with respectively 17.23% and 5.08% of missing ocean data.

.../...

Jason-1 Cycles	Number of completely missing passes	Number of partly missing passes	Events
509	2	4	Poseidon incident lead to missing ocean measurements on passes 257 (54%), 258 (100%), and 259 (38%) Due to Jason-2 overflight, Jason-1 altimeter was in INIT mode on 2012-08-23 from 22:45:28 to 23:58:52,that leads to missing ocean measurements on passes 262 (24%), 263 (100%), and 264 (26%).
513	2	1	Due to Jason-2 overflight, Jason-1 altimeter was in INIT mode on 2012-09-26 from 08:49:29 to 10:50:54, passes 001 and 002 and part of pass 003 are missing (respectively 100%, 100% and 10.92% of missing measurements over sea).
516	1	1	Due to Jason-2 overflight, Jason-1 altimeter was in INIT mode on 2012-10-29 between 19:48 and 20:48 so that pass 20 is completely missing, and pass 21 is partly missing (with 31.28% of missing ocean measurements).
519	2	0	Due to Jason-2 overflight, Jason-1 altimeter was in INIT mode on 2012-12-02 between 05:48 and 07:44 so that passes 38 and 39 are missing.
520	0	1	Due to special calibrations, pass 46 is partly missing with 68.6% of missing ocean measurements.
522	3	0	Due to Jason-2 overflight, Jason-1 altimeter was in INIT mode on 2013-01-04 from 15:47:59 to 18:36:00, so that passes 56 to 58 are missing.
525	3	0	Due to Jason-2 overflight, Jason-1 altimeter was in INIT mode on 2013-02-07 from 01:48 to 04:39, so that passes 74 to 76 are missing
527	1	213	Due to Jason-1 in Safe Hold Mode, pass 67 is partly missing (5.8% of missing ocean measurements) and passes 68 to 280 are completely missing.

.../...

Jason-1 Cycles	Number of completely missing passes	Number of partly missing passes	Events
528	1	244	Due to Safe Hold Mode, passes 1 to 244 are missing and pass 245 has 29% of missing measurements over ocean.
531	2	1	Due to Jason-2 overflight, Jason-1 altimeter was in INIT mode between 2013-04-14 22:45 and 2013-04-15 01:33, so that passes 112 and 113 are missing and pass 111 has 99.1% of missing measurements over sea.
534	3	1	Due to Jason-2 overflight, Jason-1 altimeter was in INIT mode on 2013-05-18 between 09:38 and 12:30, so that passes 130,131,132 are missing and pass 133 has 11.7% of missing measurements over sea.
537	129	1	Due to Jason-2 overflight, Jason-1 altimeter was in INIT mode on 2013-06-20 between 19:39 and 21:33, so that passes 148 and 149 are missing. Due to loss of telemetry on 2013-06-21 00:56:54 onwards, pass 153 has 9.6% of missing measurements over sea and there are no data pass 154 onwards.

Table 2: *M*issing pass status

2.2.2. Edited measurements

Table 3 indicates the cycles which have a larger amount of removed data due to editing criteria (see section 3.2.1.). Most of the occurrences correspond to dual-frequency ionospheric correction at default value (altimeter SEU) or missing radiometer wet troposphere correction (following safehold modes).
Notice that since cycle 78, the satellite operates with only 3 wheels: the maneuver impact (burn maneuver, yaw transition) is greater than before on the attitude control. Consequently for GDR "a" (which used MLE3 ground retracking algorithm), some measurements could be edited due to higher mispointing values when a maneuver occurs. Since the GDR "b" release, improvements in ground retracking algorithm have been set up and improvements on Star Tracker behavior have been performed in 2006. Therefore for the current GDR version ("c" release), generally only few measurements were edited by mispointing criterion until 2010. Jason-1 experienced high mispointing for several cycles in 2010, leading in some cases to edited measurements or even altimeter loss of tracking. Improvements on Star Tracker behavior and gyro performances have been performed at the end of 2010 so that mispointing was greatly improved.

Jason-1 Cycles	Comments
001	Passes 252 to 254 are edited due to radiometer wet troposphere correction at default value.
006	Pass 56 (in the Pacific ocean) is partly edited due to the bad quality of data. Indeed, the altimetric parameters values are out of the thresholds.
008	All the altimetric parameters are edited for 10% of pass 252 due to the bad quality of all the altimetric parameters as a result of a Star Tracker incident leading to a quite high off nadir angle.
009	Passes 004 and 005 partly edited by dual-ionospheric correction at default value (no c-band information).
021	Small part of pass 210 is edited after checking the square of the mispointing angle criterion.
069	Passes 209 to 211 are edited due to the radiometer wet troposphere correction at default value. This is linked to the safe hold mode on cycle 69 : the JMR has been set on 2 hours after the altimeter.
078	Passes 83 to 85 are edited due to the radiometer wet troposphere correction at default value. This is linked to the safe hold mode on cycle 88 : the JMR has been set on 2 hours after the altimeter.
091	Passes 126, 127 and partly 130 are edited by dual-ionospheric correction at default value (no c-band information).
102	Passes 187, 188 and partly 189 are edited by dual-ionospheric correction at default value (no c-band information).
103	Passes 29 to 31 are edited by dual-ionospheric correction at default value (no c-band information).
108	Passes 16 and 17, as well as part of passes 15 and 18 are edited by dual-ionospheric correction at default value (no c-band information).
115	Passes 19 to 21 and 29 to 31 are edited by dual-ionospheric correction at default value (no c-band information).
133	Pass 13 is partly edited due to dual-ionospheric correction at default value (no c-band information).
137	Passes 92, 93 and partly 94 are edited by radiometer wet tropospheric correction, since the radiometer was later switched on than the other instruments.
173	Due to an altimeter upset (no c-band information), the dual-frequency ionospheric correction is partially missing for passes 65 and 68 and fully for passes 66 and 67.
175	Pass 9 is partly edited by mispointing criterion out of threshold (probably aberrant quaternion).
	.../...

Jason-1 Cycles	Comments
179	As radiometer was only switch on later, passes 046 to 058, as well as part of pass 059 are edited by radiometer wet troposphere correction at default values.
181	Pass 247 is partly edited by dual-frequency ionosphere at default value (no C-band information).
198	Pass 073 is partly edited by dual-frequency ionosphere at default value (no C-band information).
212	Pass 187 is entirely edited: one half by altimetric parameters at default value, other half by apparent squared mispointing values out of thresholds. Pass 186 is partly edited by apparent squared mispointing values out of thresholds.
220	Pass 189 is partly edited by altimetric parameters at default value.
224	Passes 30 and 163 are partly edited by altimetric parameters at default value. Just before and after these parts, they are edited by outbounded apparent squared mispointing values.
256	On passes 003 and 111 a portion is edited by several altimetric parameters at default value due to high mispointing (probably related to maneuver burn and yaw flip).
262	Passes 116 to 120 are completely edited by SLA out of thresholds (related to the last orbit change maneuvers).
279	On passes 241 and 242 a portion is edited by several altimetric parameters at default value due to high mispointing (probably related to yaw flip maneuver).
284	As radiometer was only switch on later after safehold, passes 234 to 236, as well as part of pass 237 are edited by radiometer wet troposphere correction at default values.
292	Pass 137 is partially edited by apparent squared mispointing out of threshold (related to Yaw flip maneuver).
301	Following altimeter reinit on 2010-03-04 at 04:40, though measurements are available since 04:53:11, they are edited till 07:03:27 as due to high off-nadir angles all altimeter parameters are at default values (passes 007, 008 and most of pass 009).
304	Due to high off-nadir angles, several passes are partly edited as altimeter parameters are at default values or mispointing are out of thresholds.
305	Due to high off-nadir angles, several passes are partly edited as altimeter parameters are at default values or mispointing are out of thresholds.
306	Following both altimeter reinit on 2010-04-26 at 09:57:03 and 11:22:13, though measurements are available since 10:00:49, they are edited till 11:43:09 as all altimeter parameters are at default values (passes 100, 101 and part of pass 102 over North America).

.../...

Jason-1 Cycles	Comments
310	Apparent squared mispointing is very high for passes 62 to 216 (period between yaw flip and yaw ramp), leading to edited (altimeter parameters at default values) or missing measurements on many passes during this period .
312	Following altimeter incident there were altimeter reinit on 2010-06-28 at 17:03:26 and altimeter restart at 17:25:18. Though measurements are available since 17:07:00, they are edited because all altimeter parameters are at default values till 17:27:42 (pass 198 over North Atlantic).
315	Several passes are completely edited by SLA out of thresholds (2,27,29,54,57,182,183) or SLA pass statistics out of thresholds (3,4,28,53,55,136,160). Furthermore several passes are partly edited by SLA out of threshold. This is caused by the maneuvers. Several passes are completely (123,151,178,191,198,204,221,230,233) and several partly edited by altimeter parameters at default values. This is causes by high mispointing (too high for MLE4 algorithm). Passes 177 and 178 are partly edited by radiometer wet troposphere correction at default value.
316	Part of pass 1 is edited by the square of the off-nadir angle. Several part of passes (2, 3, 8, 10, 12, and 217) are edited as altimetric parameters are at default value (degraded star tracker performances).
327	Due to mispointing out of threshold, passes 115 and 239 are partly edited, respectively on 2010-11-21 and 2010-11-26.
328	Pass 011 is partially edited due to the Yaw Flip maneuver on 2010-11-27 from 01:53:34 to 02:12:37.
338	The star tracker performance seems to be degraded on pass 202, with very low tracking performance. This loss of STR tracking generated large off-nadir mispointing. Apparent squared mispointing is thus high, but still within thresholds. On pass 228 apparent squared mispointing is very high, leading to edited measurements (altimeter parameters at default values).
339	Due to mispointing out of thresholds, part of pass 088 is edited south of Australia and New-Zealand).
350	Apparent squared mispointing is very high on several passes, it is out of threshold or at default value in northern Pacific for passes 004, 006, and 032. For passes 004 and 006, altimeter parameters are partly at default value. This is probably due to low star tracker availability.
356	Due to inclination maneuvers the following passes were partially or entirely invalidated: passes 120 to 123, 145 to 148, 196 to 199.
358	Due to inclination maneuvers, the following passes were partially or entirely invalidated: passes 226 to 229 and 252 to 254.

.../...

Jason-1 Cycles	Comments
359	A portion of pass 101 has about 10 minutes of radiometer wet troposphere correction at default values. Due to inclination maneuvers 24 passes were partially or entirely invalidated: passes 001, 074 to 077, 101 to 104, 124 to 127, 150 to 153, 176 to 179, 252 to 254.
360	Due to inclination maneuvers 27 passes were partially or entirely invalidated: passes 001, 025 to 028, 051 to 054, 077 to 080, 101 to 104, 178 to 183, 204 to 206, and 231.
361	A small part of pass 143 (South Pacific, near Antarctica) is edited by significant wave height higher than 11 m. This is probably due to meteorological conditions
362	A very small part of pass 063 (North Atlantic) is edited by Significant Wave Height higher than 11 m. This is probably related to meteorological conditions.
366	Several small portions of passes 39, 46, 63, 139 and 163 are edited in North Atlantic and small portions of passes 42 and 49 are edited in southern Indian Ocean (near Antarctic) by SWH $>$ 11m. Due to meteorological conditions.
367	Several small portions of passes 121, 165 and 170 from 23/12 and 24/12 edited in North Atlantic by SWH $>$ 11m. Due to meteorological conditions.
368	A portion of pass 122 in North Atlantic is edited by SWH $>$ 11m, probably due to meteorological conditions.
369	A small part of pass 206 is edited (near the California peninsula) by several altimeter parameters out of thresholds or with default values (due to sigma0 bloom).
374	Several passes (094,095,096,098) have some portions of data edited due to radiometer wet troposphere at 0 or default values. This was already the case for the IGDR data. These passes are just after the switch-on of the radiometer. So the radiometer is likely not yet stabilized.
508	Small parts of passes are edited in south pacific due to significant wave height $> 11m$ or low backscattering coefficient, probably related to meteorological conditions.
509	Following the Poseidon incident, the altimeter parameters are at default values on pass 259 until the restart from ground.
513	Some parts of passes are rejected in Japan Sea, Pilippines Sea and East China Sea due to wet troposphere correction out of thresholds. This is coherent with a high level of water vapor that has been seen thanks to other instruments (Asian typhoon).
514	A part of passes 193 and 230 are rejected in north pacific ocean at the south of Japan due to wet troposphere correction out of thresholds (Asian typhoon).

.../...

Jason-1 Cycles	Comments
523	Small parts of passes are edited cause of backscattering coefficient and significant wave height in north pacific and nord atlantic, probably related to meteorological conditions.
524	Some parts of passes are edited by significant wave height out of thresholds in northern atlantic, probably related to meteorological conditions.
525	Some parts of passes are edited by significant wave height out of thresholds ($> 11m$) in northern atlantic, probably related to meteorological conditions.
528	JMR restarted on 18-03-2013 at 11:03:24 and the first available JMR measurement in the product is on 18-03-2013 at 11:04:19 so that measurements are rejected due to radiometer wet troposphere at default value from 10:59:50 to 11:04:18.
531	Pass 213 is partly edited due to mispointing at default value or out of thresholds, this is probably due to star tracker unavailability.

Table 3: *E*dited measurement status

3. Data coverage and edited measurements

3.1. Missing measurements

3.1.1. Over ocean

Determination of missing measurements relative to the theoretically expected orbit ground pattern is used to detect missing telemetry in Jason-1 datasets due to altimetry events for instance. This procedure is applied cycle per cycle and leads to the results plotted on the left figure 2. It represents the percentage of missing measurements relative to the theory, when limited to ocean surfaces. A small annual cycle is visible, which is due to sea ice (as Jason-1 does not track very well over sea ice). The mean value is about 4% over the repetitive period and 7.7% over the end-of-life orbit period, but this figure is not significant due to several events when the measurements are missing. All these events are described on table 2. Moreover, events which occurred during 2013 are also indicated by colored lines and stripes on bottom part of figure 2.
On figure 2 on the right, the percentage of missing measurements is plotted without taking into account the cycles where instrumental events or other anomalies occurred. Moreover shallow waters and high latitudes have been removed. This allows us to detect small data gaps in open ocean. The mean value is about 0.03%. This weak percentage of missing measurements is mainly explained by the rain cells, sea ice or sigma0 blooms. These sea states can disturb significantly the Ku band waveform shape leading to a non significant measure.
Another reason for these small data gaps in open ocean are datation gaps, which occur occasionally. Since cycle 500 onwards, there are overflights of Jason-1 by Jason-2 every 33 days: in order to avoid interferences on Jason-2 (reference mission), Jason-1 altimeter is switched to INIT MODE for 3 hours during the overflight period [2].
Note that on the following figures, showing cycle per cycle monitoring, the x-axis was shifted for the geodetic period by 119 cycles, in order to prevent a (artificial) gap between the last cycle on the repeat ground-track (cycle 374) and the first cycle on the geodetic orbit (cycle 500).

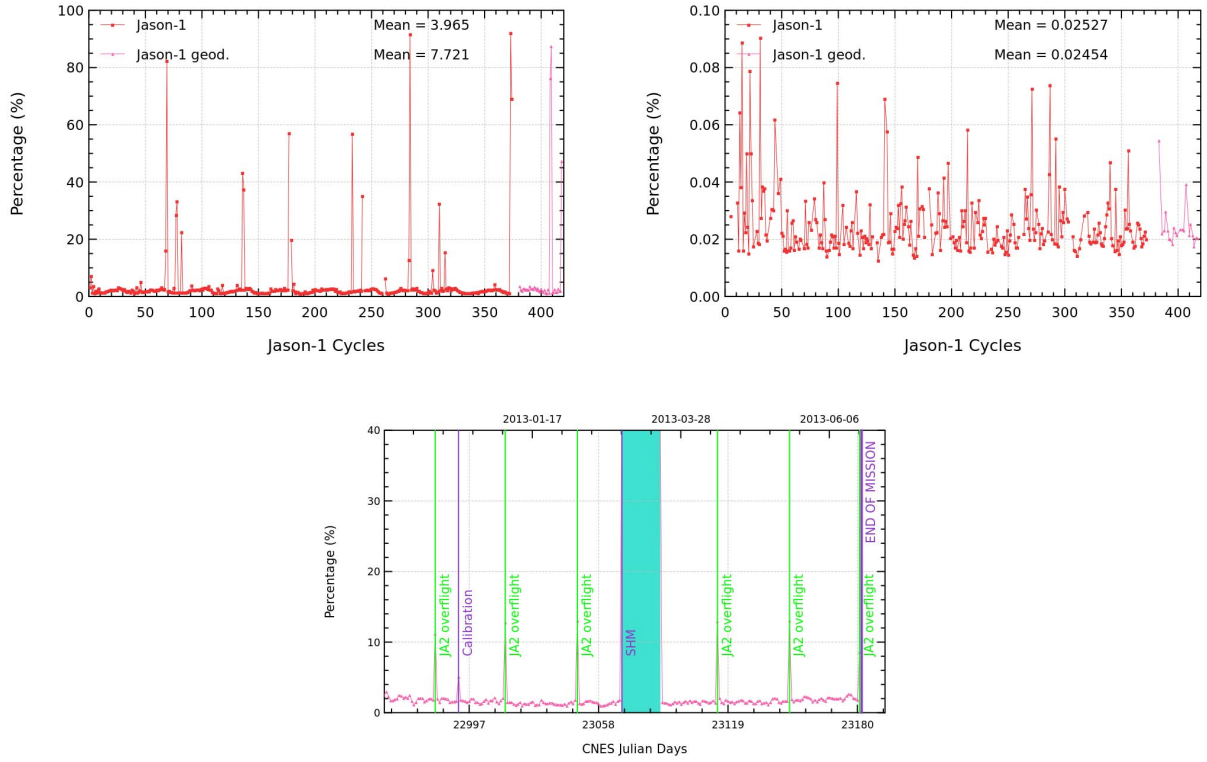

Figure 2: *Percentage of missing measurements over ocean on cyclic basis over the whole mission period with all data (top left) and without particular cycles with incident (top right) and on a daily basis for cycle 517 to 537 (bottom).*

3.1.2. Over land and ocean

Figure 3 shows the percentage of missing measurements for Jason-1 and T/P (all surfaces) computed with respect to a theoretical possible number of measurements. Due to differences between tracker algorithms, the number of data is greater for T/P (excepted when T/P experienced problems, especially since the tape recorders were no longer in service (T/P cycle 444, Jason-1 cycle 101)) than for Jason-1. Differences appear on land surfaces as shown in figure 4.

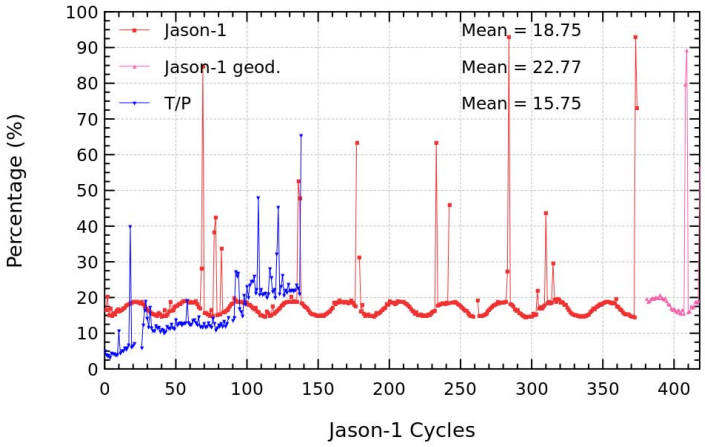

Figure 3: *Percentage of missing measurements over ocean and land for J1 and T/P*

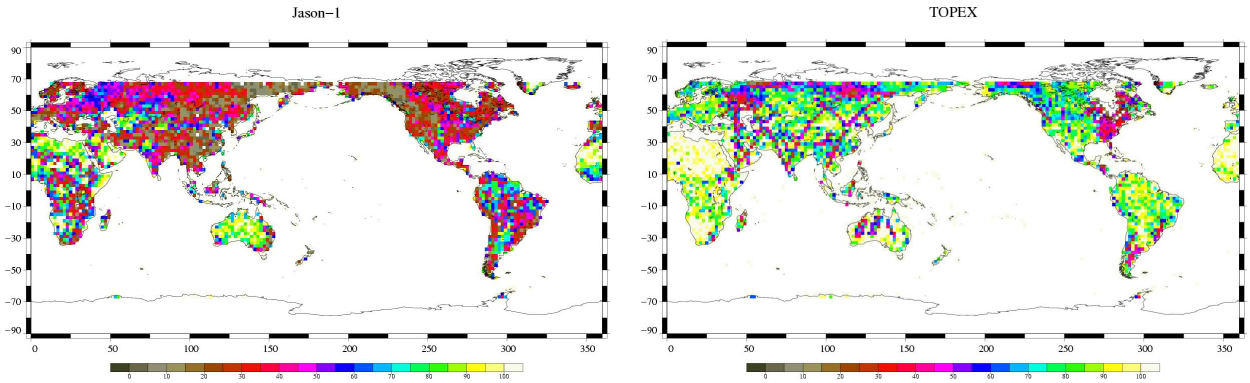

Figure 4: *Map of percentage of available measurements over land for Jason-1 on cycle 61 (left) and for TOPEX on cycle 404 (right)*

3.2. Edited measurements

3.2.1. Editing criteria definition

Editing criteria are used to select valid measurements over ocean. The editing process is divided into 4 parts. First, only measurements over ocean and lakes are kept (see section 3.2.2.). Second, the quality criteria concern the flags which are described in section 3.2.3. and 3.2.4. Then, threshold criteria are applied on altimeter, radiometer and geophysical parameters and are described in table 4. Moreover, a spline criterion is applied to remove the remaining spurious data. These criteria are also defined in AVISO and PODAAC User handbook. For each criterion, the cycle per cycle percentage of edited measurements has been monitored. This allows detection of anomalies in the number of removed data, which could come from instrumental, geophysical or algorithmic changes.

Parameter	Min thresholds	Max thresholds	mean edited on repetitive orbit period	mean edited on geodetic orbit period
Sea surface height	$-130\,m$	$100\,m$	0.93%	0.77%
Sea level anomaly	$-10\,m$	$10.0\,m$	1.17%	0.88%
Number measurements of range	10	*Not applicable*	1.29%	1.11%
Standard deviation of range	$0\,m$	$0.2\,m$	1.47%	1.31%
Square off-nadir angle	$-0.2\,deg2$	$0.64\,deg2$	0.68%	0.50%
Dry troposphere correction	$-2.5\,m$	$-1.9\,m$	0.00%	0.00%
Inverted barometer correction	$-2.0\,m$	$2.0\,m$	0.00%	0.00%
JMR wet troposphere correction	$-0.5m$	$-0.001\,m$	0.15%	0.06%
Ionosphere correction	$-0.4\,m$	$0.04\,m$	1.26%	1.05%
Significant waveheight	$0.0\,m$	$11.0\,m$	0.71%	0.57%
Sea State Bias	$-0.5\,m$	$0.0\,m$	0.62%	0.49%
Number measurements of Ku-band Sigma0	10	*Not applicable*	1.28%	1.10%
Standard deviation of Ku-band Sigma0	$0\,dB$	$1.0\,dB$	1.80%	1.59%
Ku-band Sigma0 [1]	$7.0\,dB$	$30.0\,dB$	0.66%	0.52%
Ocean tide	$-5.0\,m$	$5.0\,m$	0.06%	0.06%
Equilibrium tide	$-0.5\,m$	$0.5\,m$	0.00%	0.00%
Earth tide	$-1.0\,m$	$1.0\,m$	0.00%	0.00%
Pole tide	$-15.0\,m$	$15.0\,m$	0.00%	0.00%
Altimeter wind speed	$0\,m.s^{-1}$	$30.0\,m.s^{-1}$	1.07%	0.93%
All together	-	-	3.18%	2.81%

Table 4: *E*diting criteria

[1]The thresholds used for the Ku-band Sigma0 are the same than for T/P, but the sigma0 bias between Jason-1 and T/P (about 2.4 dB) is applied.

.

3.2.2. Selection of measurements over ocean and lakes

In order to remove data over land, a land-water mask is used. Only measurements over ocean or lakes are kept. Indeed, this allows us to keep more data near the coasts and then detecting potential anomalies in these areas. Furthermore, there is no impact on global performance estimates since the most significant results are derived from analyzes in deep ocean areas. Figure 5 (left) displays the cycle per cycle percentage of measurements eliminated by this selection. It shows a seasonal signal which is due to the varying number of measurements available in the GDRs and varies not only over ocean but also over land. After removing the annual signal, there is no trend noticeable (see figure 5).

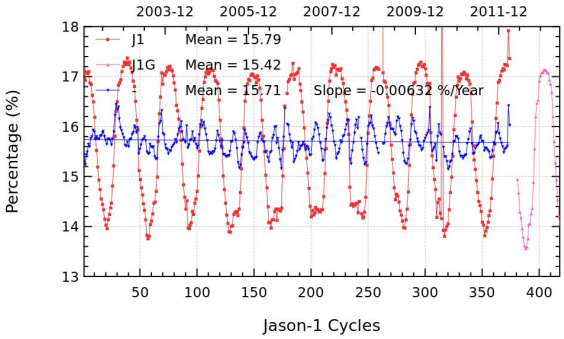

Figure 5: *Cycle per cycle percentage of eliminated measurements during selection of ocean/lake measurements with annual signal (in red: repetitive orbit, in pink: geodetic orbit) and trend of eliminated measurements after removing annual signal (in blue).*

3.2.3. Flagging quality criteria: Ice flag

The ice flag is used to remove the sea ice data. Figure 6 shows the cycle per cycle percentage of measurements edited by this criterion. On figure 6, an annual cycle is visible. Indeed, the maximum number of points over ice is reached during the northern fall. As Jason-1 takes measurements between 66° north and south, it does not detect thawing of sea ice (due to global warming), which takes place especially in northern hemisphere beyond 66°N.
For some cycles (304, 310 and 315), the percentage of edited measurements by ice flag is increased. This is not related to real sea ice. It is related to high mispointing (number of elementary range measurements used in computation of ice flag is zero due to high mispointing). The ice flag edited measurements are plotted on figure 6 for one cycle.

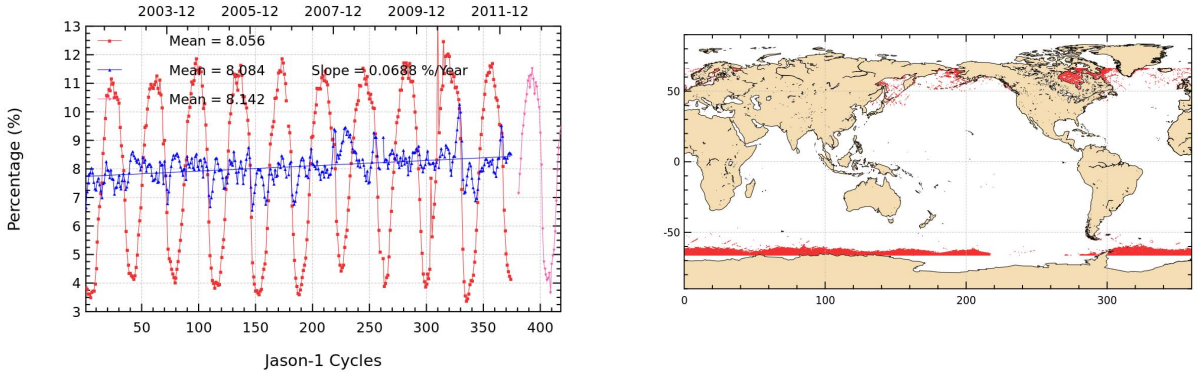

Figure 6: *Cycle per cycle percentage of edited measurements by ice flag criterion with (in red: repetitive orbit, in pink: geodetic orbit) and without (blue) annual and semi-annual signal (left), Map of edited measurements by ice flag criterion on cycle 536 (right).*

3.2.4. Flagging quality criteria: Rain flag

The rain flag is not used for data selection since it is quite restrictive. It is thus recommended not to be used by users. The rain flag has changed in version "c" making it even more restrictive. The percentage of rain edited measurements is plotted in figure 7 over cycles 517 to 537 (covering 225 days). It shows that measurements are especially edited near coasts, but also in the equatorial zone and open ocean. The rain flag seems to be too strict, using it would lead to editing 11.1% of additional measurements over the period from cycle 517 to cycle 537.

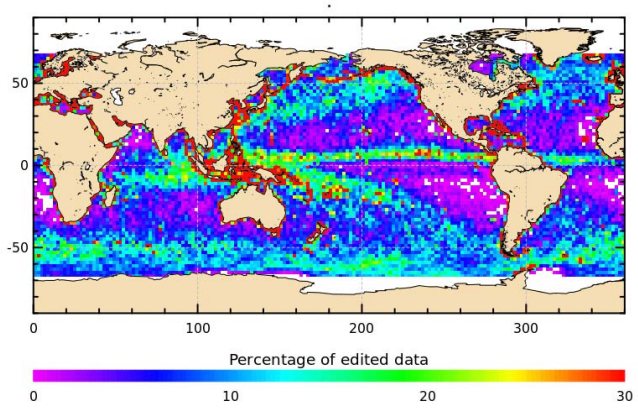

Figure 7: *Map of percentage of edited measurements by rain flag criterion over a 8-month period (cycles 517 to 537).*

3.2.5. Threshold criteria: Global

Instrumental and geophysical parameters have also been analyzed from comparison with thresholds, after selecting only ocean/lake measurements and applying flagging quality criteria (ice flag). Note that no measurements are edited by threshold criteria on the following corrections : dry troposphere correction, inverted barometer correction, equilibrium tide, earth and pole tide, which are all model corrections. Indeed these parameters are only verified in order to detect data at default values, which might happen during a processing anomaly.

The percentage of measurements edited by each criterion has been monitored on a cycle per cycle basis (figure 8). The mean percentage of edited measurements is about 3.2%. An annual cycle is visible due to the seasonal sea ice coverage in the northern hemisphere. Indeed most of northern hemisphere coasts are without ice during its summer. Consequently some of these coastal measurements are edited by the thresholds criteria in summer instead of the ice flag in winter. This seasonal effect visible in the statistics is not balanced by the southern hemisphere coasts due to the shore distribution between both hemispheres.
Note that for some cycles, the percentage of edited measurements is higher than usual. Concerning cycles 69, 179 and 284, this is mostly due to the lack of radiometer wet troposphere correction, as after safehold modes radiometer is usually switched on some time after the altimeter, see also section 3.2.10.. For cycles 304, 310 and 315, edited measurements are partly due to mispointing out of thresholds. As during 2010 squared off-nadir angle got for several cycles very high, MLE4 retracking could sometimes no longer retrieve altimeter parameters, they are therefore at default value and edited. In the following sections, all altimeter parameters show an increased percentage of edited measurements for the period of cycles 304 to 316, and especially for cycles 304, 310 and 315. During year 2013, pass 213 of cycle 531 is partly edited due to mispointing at default value or out of thresholds probably due to star tracker unavailability. As a consequence, this pass is visible on the maps of edited measurements from pass 517 to 537 in the following parts dealing with altimeter parameters.

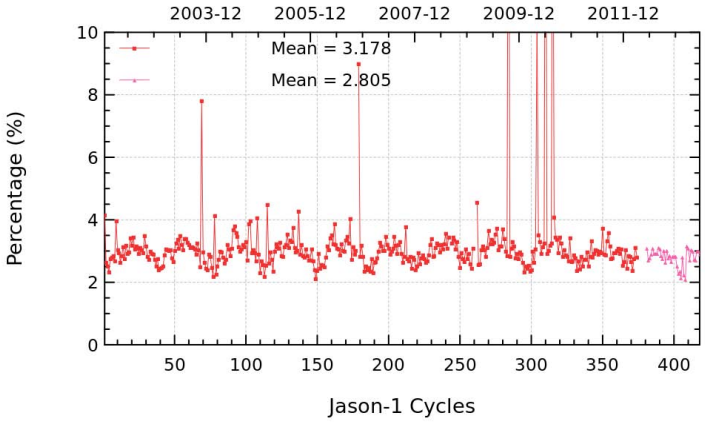

Figure 8: *Cycle per cycle percentage of edited measurements by threshold criteria*

3.2.6. Threshold criteria: 20-Hz measurements number

The percentage of edited measurements because of a too low number of 20-Hz measurements is represented on left side of figure 9. Neither a trend nor any anomaly has been detected, except for cycle 212 and period between cycles 304 and 316. Indeed during cycle 212, about half of a pass had all altimetric parameters set at default values, due to satellite off-pointing. During cycles 304 to 316, several portions of passes were concerned.
The map of measurements edited by the 20-Hz measurements number criterion is plotted on the right panel of figure 9 and shows correlation with heavy rain, wet areas, sigma0 bloom as well as coastal regions. Indeed the waveforms are distorted by rain cells, which makes them often unexploitable for SSH calculation. In consequence edited measurements due to several altimetric criteria are often correlated with wet areas. As the number of 20-Hz range measurements is one of the criteria used for the computation of the sea ice flag (in sea ice regions, if the 20-Hz elementary Ku-band range number is less than 10, the data is flagged as sea ice) - using the same threshold as during the threshold editing step - right of figure 9 shows no data edited by 20-Hz elementary Ku-band range number in possible sea ice regions (as they were already edited by the ice flag).

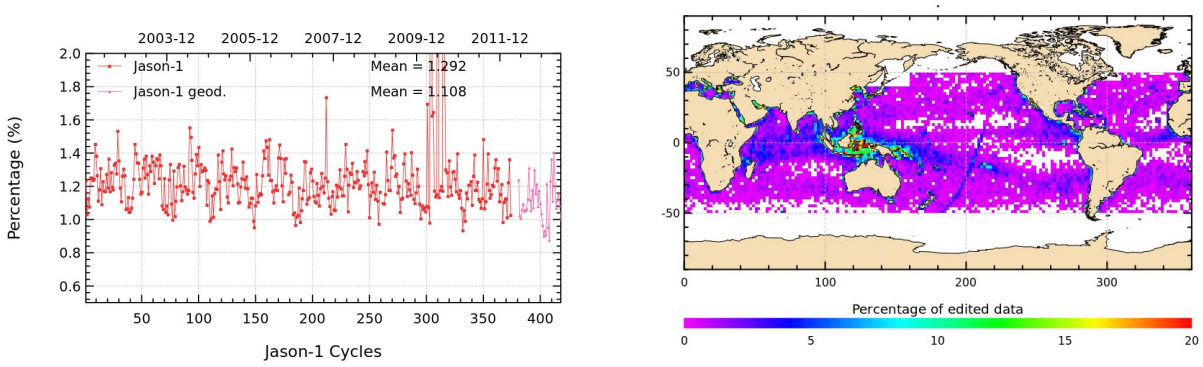

Figure 9: *Cycle per cycle percentage of edited measurements by 20-Hz measurements number criterion (left). Right: Map of percentage of edited measurements by 20-Hz measurements number criterion over an eight-months period (cycles 517 to 537).*

3.2.7. Threshold criteria: 20-Hz measurements standard deviation

The percentage of edited measurements due to 20-Hz measurements standard deviation criterion is shown in left of figure 10. The observed annual signal is linked to the seasonal variability associated with ice coverage. After removing the annual signal and not taking into account cycles which were impacted by very high mispointing (blue curve on the left of figure 10), no trend is visible.
Figure 10 (right part) shows a map of measurements edited by the 20-Hz measurements standard deviation criterion. Edited measurements are mainly correlated with wet areas or sigma0 bloom events.

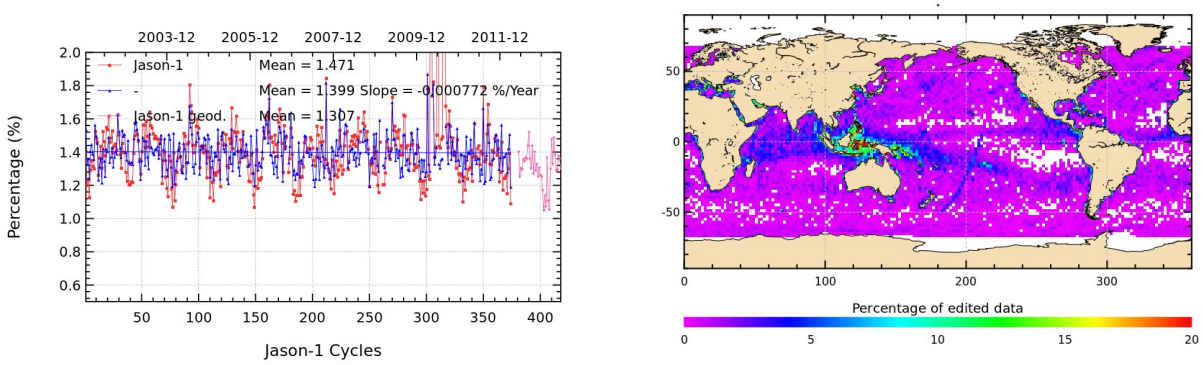

Figure 10: *Cycle per cycle percentage of edited measurements by 20-Hz measurements standard deviation criterion with (in red: repetitive orbit, in pink: geodetic orbit) and without (in blue) annual signal (left) , Map of percentage of edited measurements by 20-Hz measurements standard deviation criterion over an eight-months period (cycles 517 to 537) (right).*

3.2.8. Threshold criteria: Significant wave height

The percentage of edited measurements due to significant wave height criterion is represented in figure 11. It is about 0.71% and no drift has been detected over the repetitive orbit period, and 0.57% since the beginning of the geodetic period. This small decrease in edited data due to significant wave height criterion is due to a decrease of data at default values during the period of the geodetic mission. Peaks visible for cyles 304 to 316 are due to altimeter parameters at default values caused by very high mispointing. Smaller peaks visible for cycles 212 and 224 are also due to a portion of a pass at default values. The effect is barely visible on the global rejected measurements figure 8 for cycle 212, and unseen for cycle 224, because of the weak impact of the SWH criterion with regard to the global editing criteria. Figure 11 (right part) shows that measurements edited by SWH criterion are especially found near coasts in the equatorial regions.

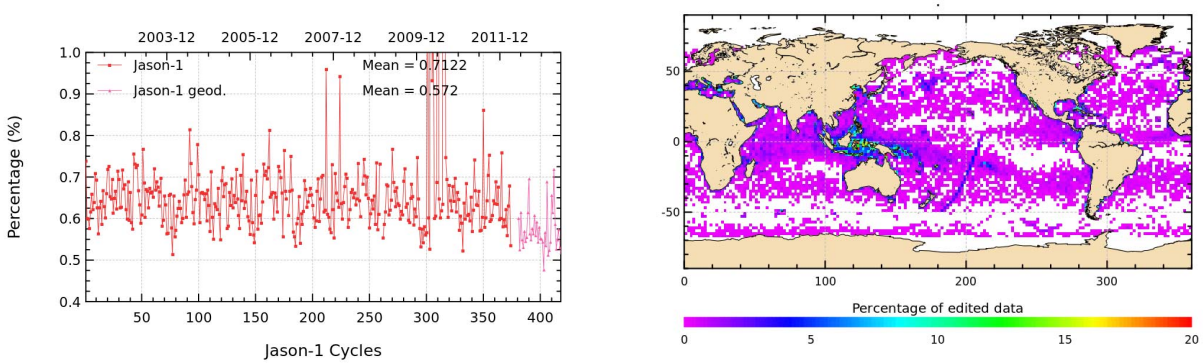

Figure 11: *Left: Cycle per cycle percentage of edited measurements by SWH criterion. Right: Map of percentage of edited measurements by SWH criterion over an eight-months period (cycles 517 to 537).*

3.2.9. Backscatter coefficient

The percentage of edited measurements due to backscatter coefficient criterion is represented in figure 12. It is about 0.66% and shows no drift over the repetitive period. The peaks visible for cycles 212 and 224 are due to a portion of a pass at default values. This is also the case for the peaks of cycles 304 to 316. Since the beginning of the geodetic period, it is about 0.52%. The right part of figure 12 shows that measurements edited by backscatter coefficient criterion are especially found near coasts in the equatorial regions.

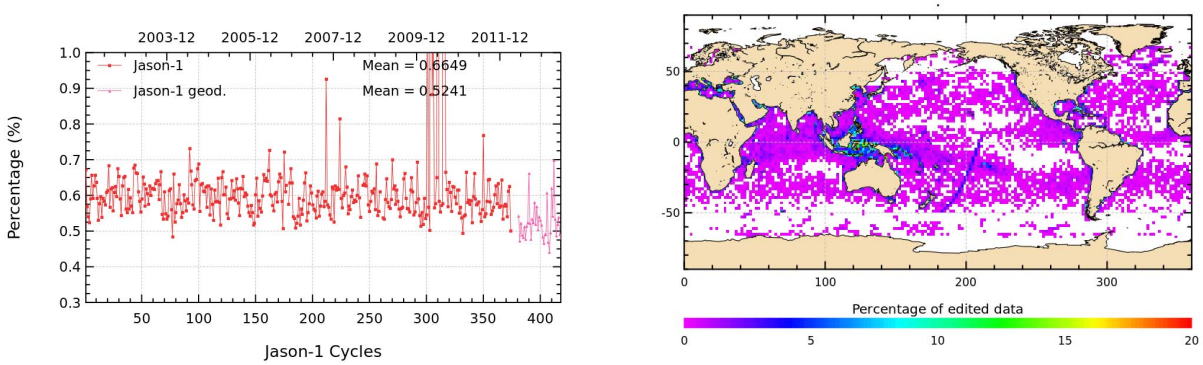

Figure 12: *Cycle per cycle percentage of edited measurements by Sigma0 criterion (left). Right: Map of percentage of edited measurements by Sigma0 criterion over an eight-months period (cycles 517 to 537).*

3.2.10. Radiometer wet troposphere correction

The percentage of edited measurements due to radiometer wet troposphere correction criterion is represented in figure 13. It is about 0.15% over the repetitive period. When removing cycles which experienced problems, percentage of edited measurements drops to 0.05%. It is about 0.05% over the geodetic period. The figure shows irregular oscillations which are not correlated to annual cycle. The map 13 shows that only few measurements are edited by radiometer wet troposphere correction criterion.
Notice that for some cycles the percentage of edited measurements is higher than usual. This is often linked to the Jason safe hold mode on some of these cycles (69, 78, 137, 179, 284, 316): the radiometer has been set on 2 hours later than the altimeter. As a result, the radiometer wet troposphere correction has been set to default value during this period and these measurements have been edited. As concerned cycle 528, the percentage of edited measurements is higher than usual because of Jason SHM too, but in this case JMR was restarted only 5 minutes after the first data so that there are less edited measurements than in the previous mentionned cases.

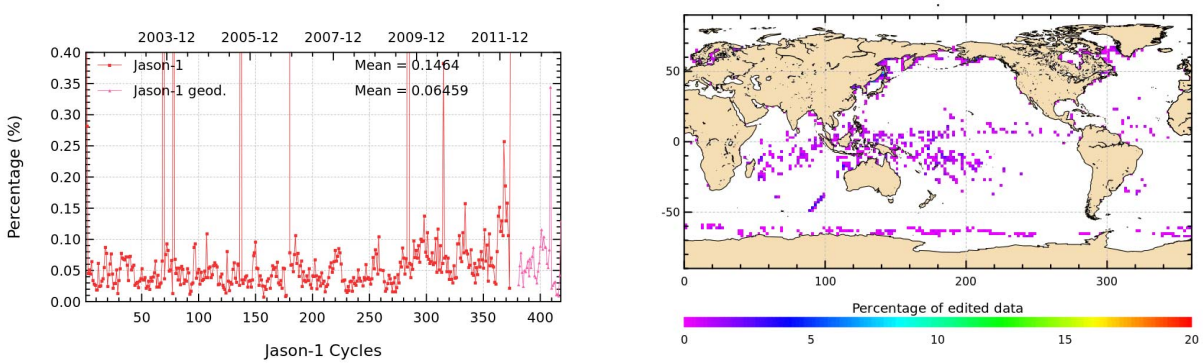

Figure 13: *Cycle per cycle percentage of edited measurements by radiometer wet troposphere criterion (left). Map of percentage of edited measurements by radiometer wet troposphere criterion over an eight-months period (cycles 517 to 537).*

Around cycle 284, there seems to be a slight increase of edited measurements, probably due to the use of a new JMR calibration file after safe hold event in September 2009. There are more points for which wet troposphere correction is set to zero for $|latitude| > 50^o$ and points for which it is out of thresholds in tropical area and for $|latitude| > 50^o$.

A second increase is visible about cycle 363, the reason of this increase is unknown.

3.2.11. Dual frequency ionosphere correction

The editing procedure is applied to the dual frequency ionosphere correction as it is available in the GDR products (before filtering). The percentage of edited measurements due to dual frequency ionosphere correction criterion is represented in figure 14. It is about 1.26% and shows no drift over the repetitive period. The map 14 shows that measurements edited by dual frequency ionosphere correction are mostly found in equatorial regions.
Notice that for cycles 9, 91, 102, 103, 108, 115, 133, 173, 198, 212, 301, 304-306, 310, 315 and 316 the percentage of edited measurements is higher than usual. Till cycle 198, this is linked to an altimeter SEU occurred on these cycles. The dual frequency ionospheric correction is not available during a few hours following the altimeter incidents (lack of C-band parameters requirering ground TC to resume nominal configurations). Peaks from cycle 212 onwards are mostly due to altimeter parameters at default value related to very high mispointing (see section 3.2.6.). The percentage of edited measurements due to dual frequency ionosphere correction criterion is about 1.052% since the move to geodetic orbit.

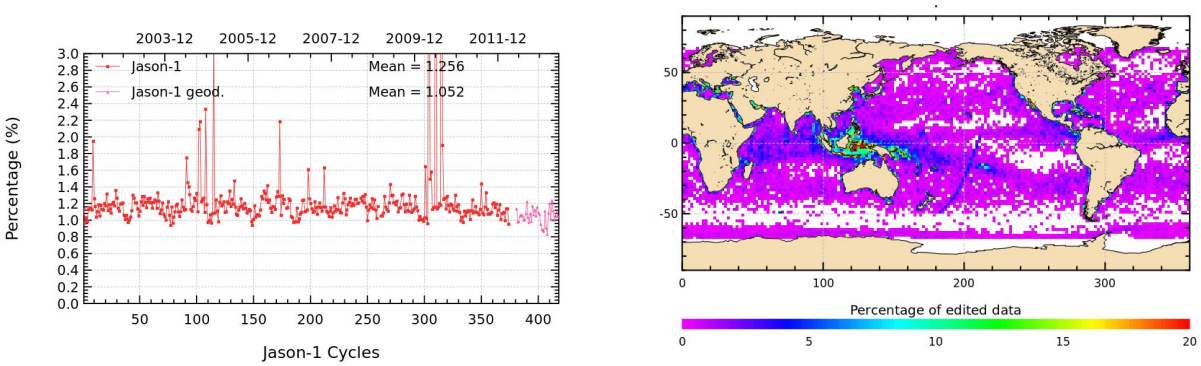

Figure 14: *Cycle per cycle percentage of edited measurements by dual frequency ionosphere criterion (left). Map of percentage of edited measurements by dual frequency ionosphere criterion over an eight-months period (cycles 517 to 537).*

3.2.12. Square off-nadir angle

The percentage of edited measurements due to square off-nadir angle criterion is represented in figure 15. It is about 0.68% over the repetitive period and 0.5% since the beginning of the geodetic orbit period. During 2010, Jason-1 experienced very high off-nadir angles due to low star tracker and gyro performances, especially for period between cycles 304 and 316. Mispointing was greatly improved end of 2010. During 2011, there were only a couple of cycles impacted by increased mispointing values. The map 15 shows that edited measurements are mostly found in coastal regions. During year 2013, pass 213 of cycle 531 is partly edited due to mispointing at default value or out of thresholds probably due to star tracker unavailability. As a consequence, this pass is visible on the map of edited measurements from pass 517 to 537 of figure 15.

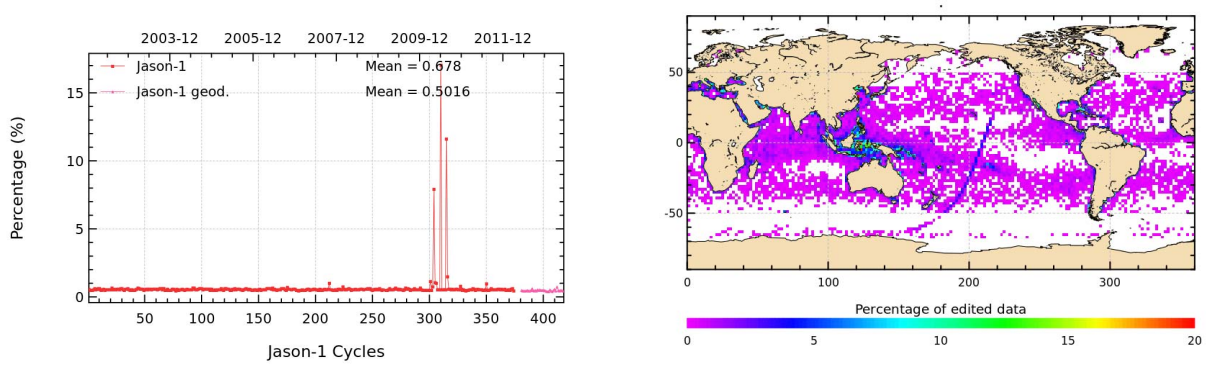

Figure 15: *Cycle per cycle percentage of edited measurements by square off-nadir angle criterion (left). Right: Map of percentage of edited measurements by square off-nadir angle criterion over an eight-months period (cycles 517 to 537).*

3.2.13. Altimeter wind speed

The percentage of edited measurements due to altimeter wind speed criterion is represented in figure 16. It is about 1.07% and shows no drift over the repetitive period. Since the move to the end-of-life orbit, the percentage of edited measurements due to altimeter wind speed criterion is about 0.93%. Measurements are generally edited because they have default values, as happened due to very high mispointing for period between cycles 304 to 316. Otherwise, this is the case when sigma0 itself is at default value, or when it shows very high values (higher than 25 dB), which occur during sigma bloom and also over sea ice. The annual cycle is probably due to sea ice, which was not detected by the ice flag.
Note that percentage of edited altimeter wind speed is higher than that of edited sea state bias. This is very likely related to the fact that in ground processing software, slightly negative altimeter wind speed values may occur, for which a sea state bias value is computed. Nevertheless in binary Jason-1 GDR product, the slightly negative wind speed values are replaced by the default value (and are therefore edited).

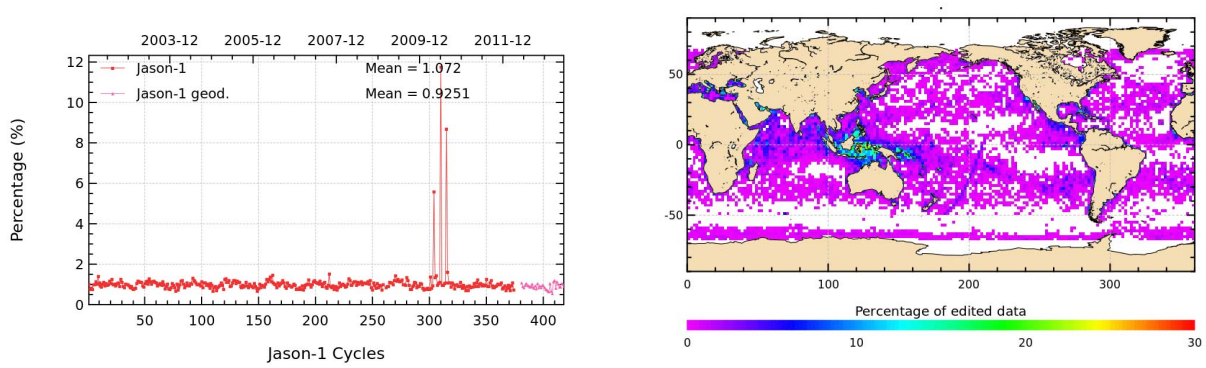

Figure 16: *Cycle per cycle percentage of edited measurements by altimeter wind speed criterion (left). Right: Map of percentage of edited measurements by altimeter wind speed criterion over an eight-months period (cycles 517 to 537).*

3.2.14. Sea state bias correction

The percentage of edited measurements due to sea state bias correction criterion is represented in figure 17. The percentage of edited measurements is about 0.62% over the repetitive period and 0.49% since the move to the geodetic orbit, and shows no drift. But as other parameters, it was impacted by altimeter parameters at default values during period between cycles 304 and 316. The map 17 (right side) shows that edited measurements are mostly found in equatorial regions near coasts.
The map 17 showing percentage of measurements edited by sea state bias criterion is highly correlated with the map 16.

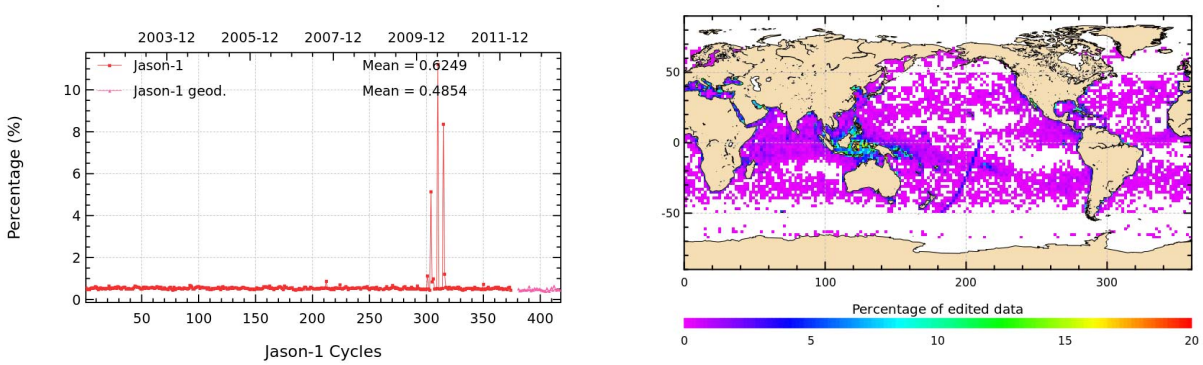

Figure 17: *Cycle per cycle percentage of edited measurements by sea state bias criterion (left). Right: Map of percentage of edited measurements by sea state bias criterion over an eight-months period (cycles 517 to 537).*

3.2.15. Ocean tide correction

The percentage of edited measurements due to ocean tide correction criterion is represented in figure 18. It is about 0.06% over all the mission period and shows a little jump but no drift. A slight decrease in edited measurements is visible since cycle 262 (change of Jason-1 ground-track). The level of edited measurements has also increased since the move of Jason-1 to geodetic orbit. This is related to the new ground track, which no longer overflows the same areas.
The ocean tide correction is a model output, there should therefore be no edited measurements. Indeed there are no measurements edited in open ocean areas, but only very few near coasts or in lakes or rivers (see map 18). These measurements are mostly at default values.
Generally approximatively the same amount of measurements is edited by ocean tide correction for each cycle. The small annual signal visible in figure 18 comes from the seasonal fluctuation of available ocean data (due to seasonal fluctuation of sea ice coverage).

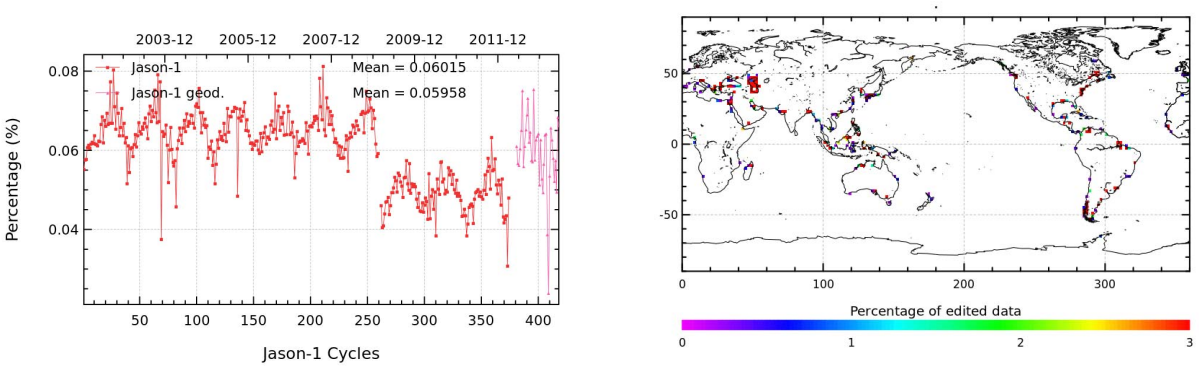

Figure 18: *Cycle per cycle percentage of edited measurements by ocean tide criterion (left). Right: Map of percentage of edited measurements by ocean tide criterion over an eight-months period (cycles 517 to 537).*

3.2.16. Sea surface height

The percentage of edited measurements due to sea surface height criterion is represented in figure 19. It is about 0.93% over the repetitive orbit and shows no drift. There is however an annual signal visible. For the peaks see section 3.2.12.. Concerning the geodetic period, the percentage of edited measurements due to sea surface height criterion is about 0.77%.
Besides anomalies due to poor star tracker and gyro performances, the measurements edited by sea surface height criterion are mostly found near coasts in equatorial regions (see map 19).

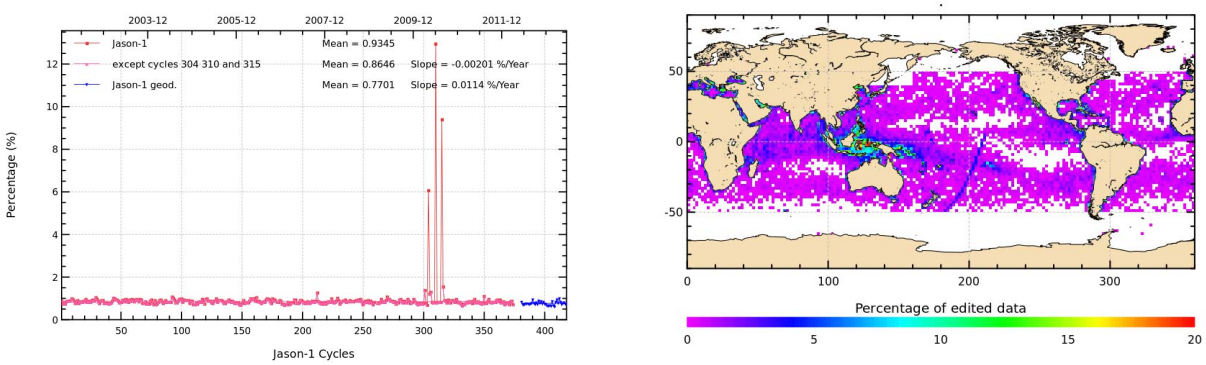

Figure 19: *Cycle per cycle percentage of edited measurements by sea surface height criterion (left). Right: Map of percentage of edited measurements by sea surface height criterion over an eight-months period (cycles 517 to 537).*

3.2.17. Sea level anomaly

The percentage of edited measurements due to sea level anomaly criterion is represented in figure 20. It is about 1.17% over the repetitive orbit and shows no drift. It is 0.88% since the move to the geodetic orbit. The percentage of about 1% is due to the fact that the SLA clip contains many of the parameters used for editing. Whereas the map in figure 20 allows us to plot the measurements edited due to sea level anomaly out of thresholds (after applying all other threshold criteria), these are generally only very few measurements (mostly around Caspian Sea).

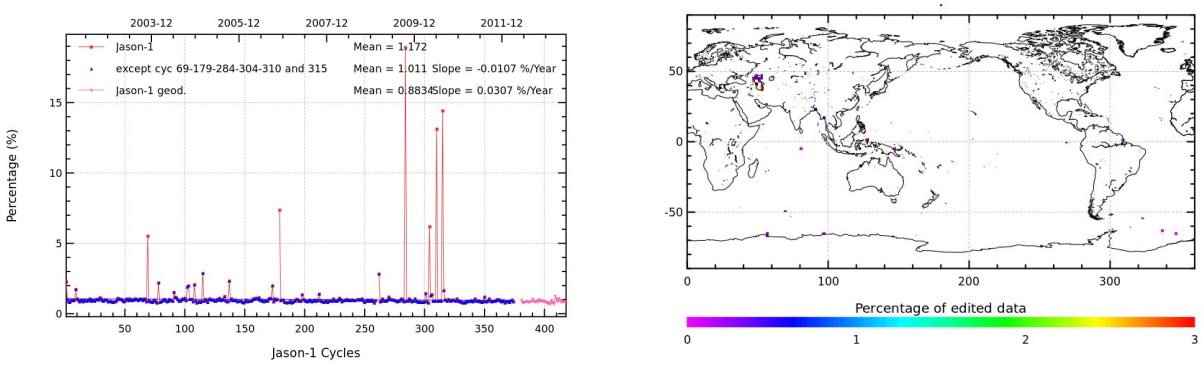

Figure 20: *Cycle per cycle percentage of edited measurements by sea level anomaly criterion (left). Right: Map of percentage of edited measurements by sea level anomaly criterion (after applying all other threshold criteria) over an eight-months period (cycles 517 to 537).*

4. Monitoring of altimeter and radiometer parameters

4.1. Methodology

Both mean and standard deviation of the main parameters of Jason-1 have been monitored since the beginning of the mission. Moreover, a comparison with T/P parameters has been performed: it allows us to monitor the bias between the parameters of the 2 missions. The comparison is done till the end of scientific mission of T/P, which occurred during Jason-1 cycle 138. Two different methods have been used to compute the bias:

- During the verification phase (cycles 1 to 21), Jason-1 and T/P are on the same ground track and are spaced out about 1 minute apart. The mean of the T/P − Jason-1 differences can be computed using a point by point repeat track analysis.
- From cycle Jason-1 22 (Cycle T/P 365), the 15th of August 2002, a maneuver sequence was conducted over 30 days to move T/P to the new Tandem Mission orbit : further on T/P was located one half of the TP/Jason-1 track spacing to the West of Jason-1. Geographical variations are then too strong to directly compare Jason-1 and T/P parameters on a point by point basis. Therefore cycle per cycle differences have been carried out to monitor Jason-1 and T/P differences, but data gaps on both satellites have been taken into account.

For comparison between Jason-1 and Jason-2 please see annual Jason-2 report ([3]).

Note that as for the previous chapter, on the figures showing cycle per cycle monitoring, the x-axis is shifted for the geodetic period by 119 cycles, in order to prevent a (artificial) gap between the last cycle on the repeat ground-track (cycle 374) and the first cycle on the geodetic orbit (cycle 500).

4.2. 20 Hz Measurements

The monitoring of the number and the standard deviation of 20 Hz elementary range measurements used to derive 1 Hz data is presented here. These two parameters are computed during the altimeter ground processing. Before a regression is performed to derive the 1 Hz range from 20 Hz data, a MQE criterion is used to select valid 20 Hz measurements. This first step of selection thus consists in verifying that the 20 Hz waveforms can be effectively approximated by a Brown echo model (Brown, 1977 [23]) (Thibaut et al. 2002 [24]). Through an iterative regression process, elementary ranges too far from the regression line are discarded until convergence is reached. Thus, monitoring the number of 20 Hz range measurements and the standard deviation computed among them is likely to reveal changes at instrumental level.

4.2.1. 20 Hz measurements number in Ku-Band and C-Band

Figure 21 shows the cycle per cycle mean of 20-Hz measurements number in Ku-Band (on the left) and C-Band (on the right). A very weak seasonal signal is visible.

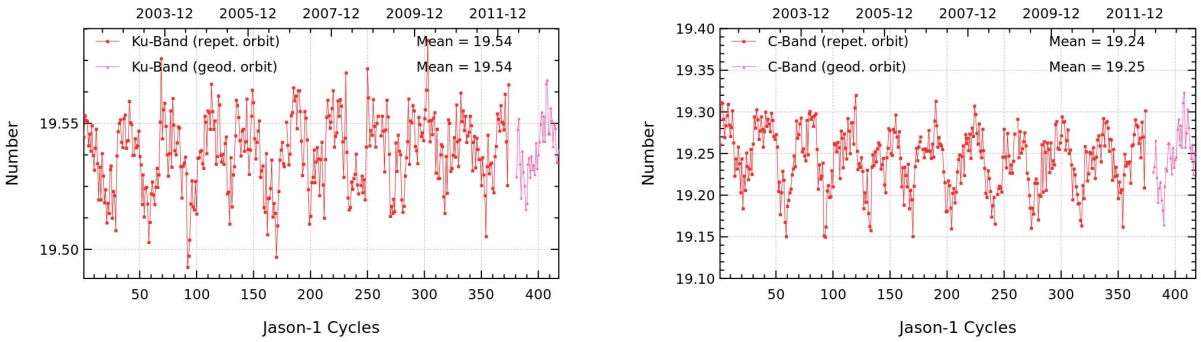

Figure 21: *Cycle per cycle mean of 20-Hz measurements number in Ku-Band (left) and C-Band (right)*

4.2.2. 20 Hz measurements standard deviation in Ku-Band and C-Band

Figure 22 shows the cycle per cycle standard deviation of the 20 Hz measurements in Ku-Band (on the left) and C-Band (on the right). Apart from a weak seasonal signal, neither trend nor any anomaly has been detected. C-Band standard deviation of the 20 Hz measurements rms is noisier than those of Ku-Band. This is directly linked to the C-band standard deviation which is higher than the Ku, as the onboard averaging is performed over less waveforms (90 Ku pulses for 15 C pulses) leading to an increased noise.

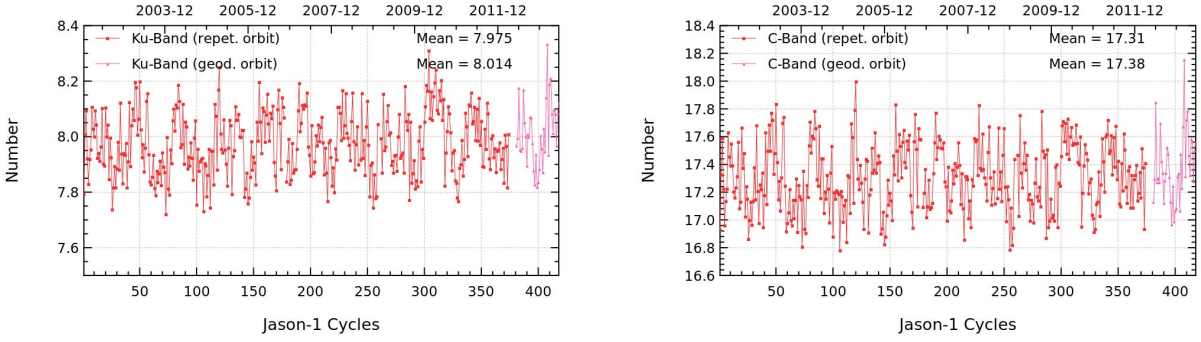

Figure 22: *Cycle per cycle mean of 20-Hz measurements standard deviation in Ku-Band (left) and C-Band (right)*

4.3. Off-Nadir Angle from waveforms

The off-nadir angle is estimated from the waveform shape during the altimeter processing. The square of the off-nadir angle, averaged on a one-cycle basis, has been plotted in figure 23. The mean values are slightly positive. This mean value is not significant in terms of actual platform mispointing. In fact squared attitude is what is retrieved from waveforms, not attitude. During about the 100 first cycles of the mission off-nadir angles are low and quite stable, except for cycle 69 related to a platform safehold mode. Between cycles 100 and 200, the off-nadir angle slightly increases and reaches more often strong values and between cycle 200 until end of year 2010, it is disturbed and reached very strong values. Indeed, there are periods where the combination of low Beta angles and Sun glint or Moon in the field of view significantly reduces the tracking performance of both star trackers, especially during fixed-yaw. Previously, in GDR version "a", when the off-nadir angle was larger than the 0.2 degree specification, error was introduced in the altimeter parameters as the off nadir was not taken into account in the ground processing (Vincent et al., 2003). Thus, an improvement of the retracking algorithm was made since GDR version "b" ([19]), to correct for estimations of altimeter parameters for mispointing angle errors up to 0.8 deg. (Amarouche et al. 2004 [25]).
During years 2008 and 2009, the satellite has experienced several severe mispointing cases, although the mispointing values remained within the threshold editing criteria (-0.2 to $0.64 deg^2$). This feature has been repeatedly pointed out, especially after maneuvers. Neither specific geographic pattern nor ascending/descending tracks systematisms are observed. The high mispointing values are related to low star tracker availability and gyro wheels behavior. During 2010, off-nadir angles were particularly high, leading even to altimeter lost of track. Since the end of 2010 thanks to improvements of star tracker performances and gyro wheels, mispointing is again quite low.

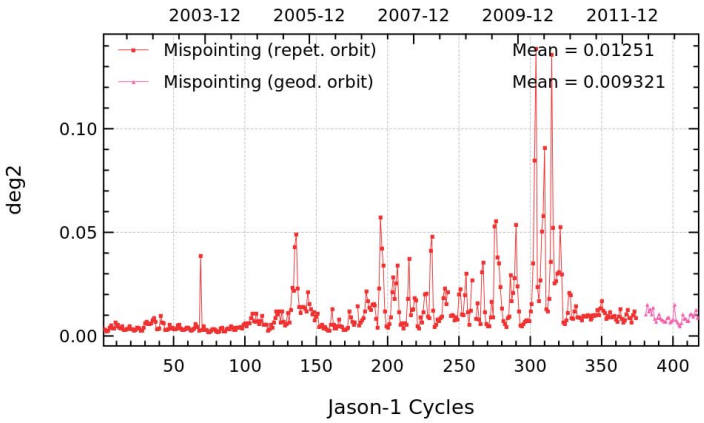

Figure 23: *Cycle mean of the square of the off-nadir angle deduced from waveforms (deg^2).*

4.4. Significant wave height

Jason-1 and T/P Ku SWH are compared in terms of global statistics in figure 24: cycle means of both missions are presented in a cycle basis, as well as mean differences between T/P and Jason-1. Global variations of the SWH statistics are the same on the two missions. A weak annual signal is visible. Jason-1 SWH shows almost no drift on the whole altimeter time period. The (TOPEX - Jason-1) SWH bias is about 5.4 cm. The estimate of the (Poseidon-1 - Poseidon-2) SWH difference is about 12 cm for Poseidon-2 cycle 18 not plotted here.

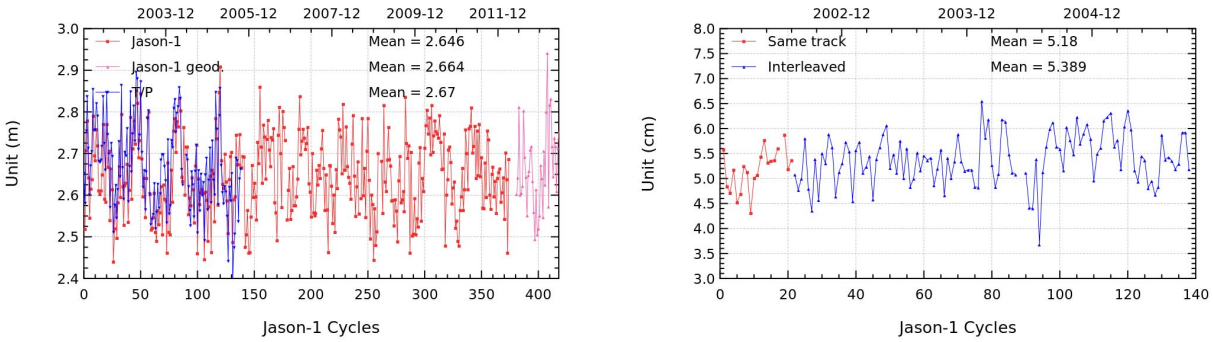

Figure 24: *Cycle per cycle mean (left), T/P−Jason mean differences (right) of Ku-band SWH*

Figure 25 shows global statistics of Jason-1 and T/P C-band SWH. The cycle per cycle mean of both missions shows a small annual signal (figure 25 top left). Jason-1 and T/P values are quite similar. The (TOPEX - Jason-1) C-band SWH mean bias is about 8 cm (figure 25 top right), with a drift of about -2 mm/yr.

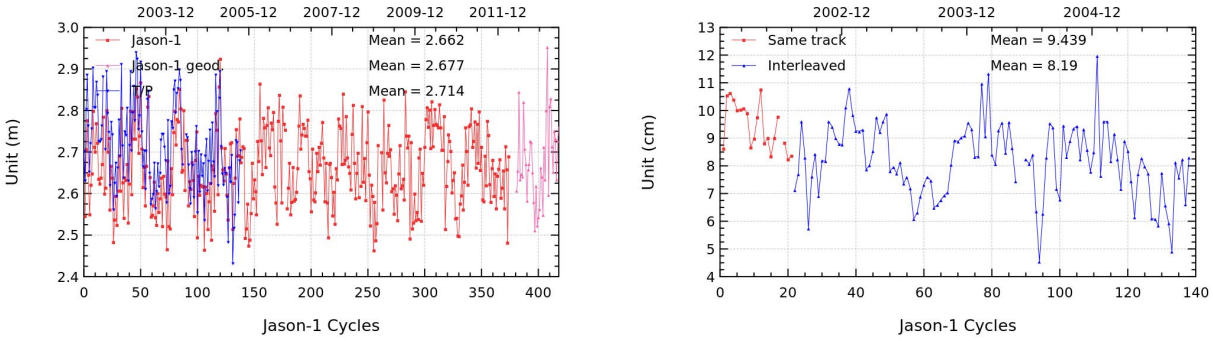

Figure 25: *Cycle per cycle mean (left), T/P−Jason mean differences (right) of C-band SWH*

Figure 26 shows global statistics of Ku-band minus C-band difference of SWH for Jason-1. The mean monitoring shows no drift (on the left) and the standard deviation (on the right) of the Ku-band minus C-band SWH shows a great annual signal related to geophysical annual cycle of waves.

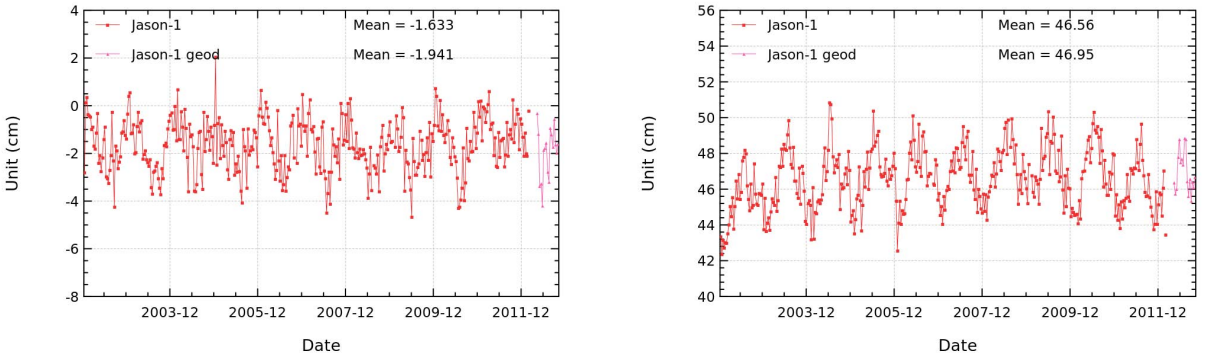

Figure 26: *Cycle per cycle mean **(right)** and standard deviation **(left)** of Ku-band SWH - C-band SWH differences*

4.5. Backscatter coefficient

4.5.1. Ku-band Sigma0

The cycle per cycle mean (figure 27: top panel on the left) for Jason-1 (red curve) Ku-band sigma0 is coherent with the TOPEX mean (blue curve). A small drift is visible for Jason-1. It is mostly due to geophysical evolutions, but also due to small sigma0 anomalies (see also [26]). In order to compare sigma0 parameters from both missions and keep a significant dynamic scale, TOPEX Ku-Sigma0 is biased by a 2.26 dB value to align TOPEX with the Jason-1 Sigma0. The bias between the two corrections (figure 27: top panel on the right) is quite stable about -2.5 dB.

Besides, the absolute bias is higher than usual from T/P cycle 433 to 437 (J1 cycles 90 to 94) by 0.1 dB: this is due to the TOPEX Sigma0. Indeed, the satellite attitude was impacted by a pitch wheel event linked to the T/P safe-hold mode occurred on cycle T/P 430 (see electronic communication: T/P Daily Status (26/07/2004)). This anomaly has probably biased the TOPEX sigma0 during this period. The T/P - Jason-1 backscattering difference is after this period slightly lower than before. This is probably also related to T/P (see figure comparing Topex altimeter wind speed and ERA-Interim wind speed in [26]). Jason-1 and T/P curves on bottom panel, showing the standard deviation differences, are very similar .

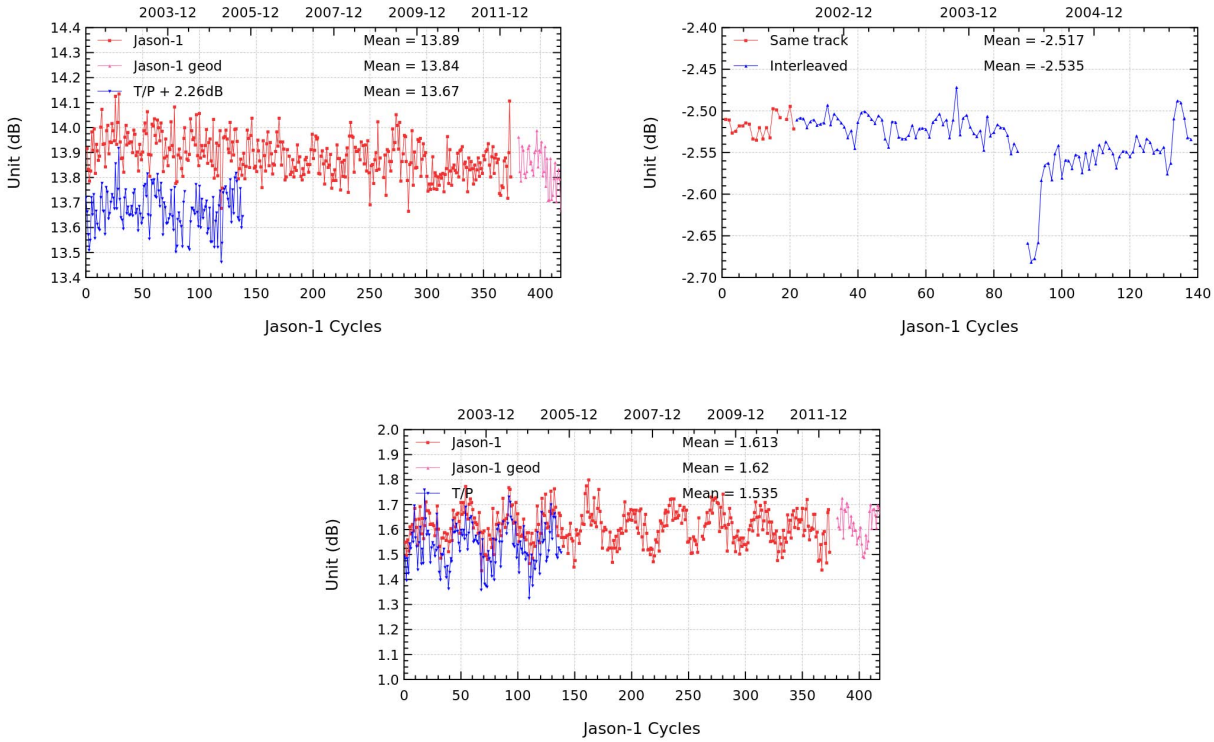

Figure 27: *Cycle per cycle mean (left), T/P−Jason mean differences (right), and standard deviation (bottom) of Ku-band Sigma0*

4.5.2. C-band Sigma0

The cycle per cycle mean (figure 28: top panel on the left) for Jason-1 (red curve) Ku-band sigma0 is coherent with the TOPEX mean (blue curve). The bias between the two corrections (figure 28: top panel on the right) decreases from -0.65 dB to -0.72 dB. This is due to the T/P C-band Sigma0 (Ablain et al. 2004 [27]).
Note that in science processing software a bias of approximately -0.28 dB is applied to the provided C-Band Sigma0 for any geophysical algorithms that require use of sigma0. Standard deviation of C-band sigma0 (figure 28: bottom) has similar values for both missions and shows an annual signal.

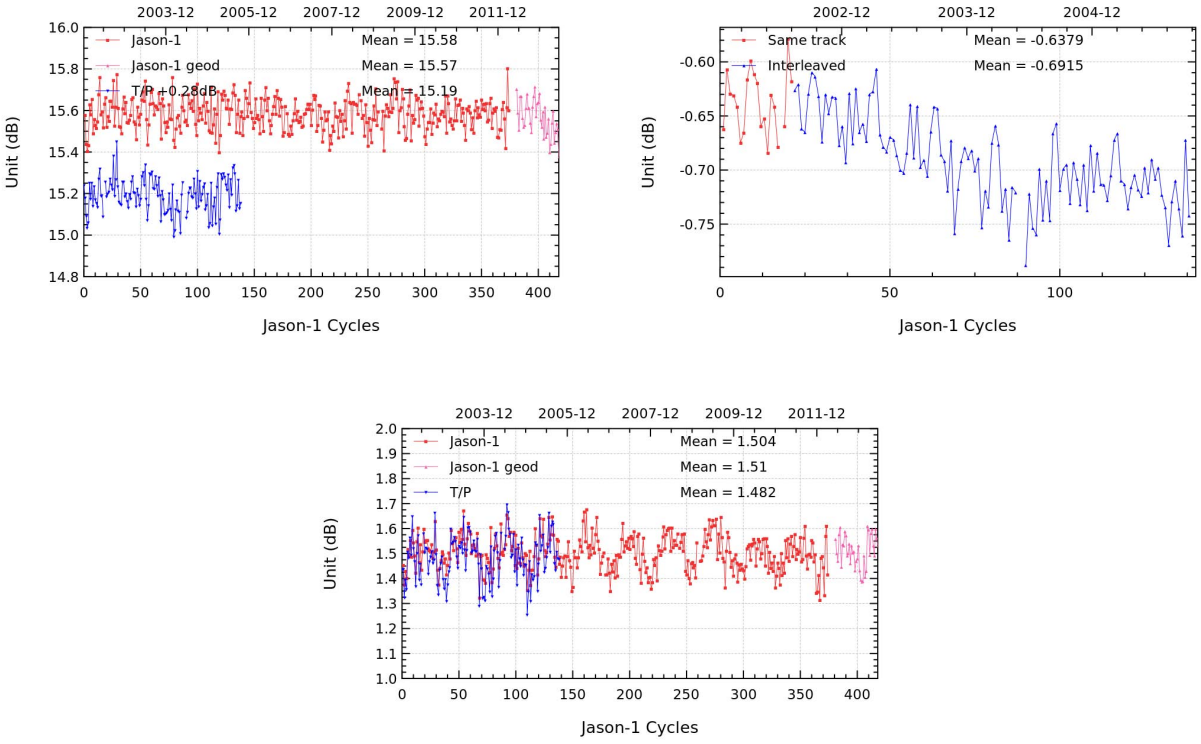

Figure 28: *Cycle per cycle mean (left), T/P−Jason mean differences (right), and standard deviation (bottom) of C-band SIGMA0*

4.6. Ionosphere correction

4.6.1. Dual-frequency ionosphere correction

The dual frequency ionosphere corrections derived from the TOPEX and Jason-1 altimeters have been monitored and compared in the same way (figure 29). The mean difference between TOPEX and Jason-1 estimates is about 1.5 mm, with cycle to cycle variations lower than 2 mm. There is nevertheless a small visible jump of 1 mm around Jason-1 cycle 90. Both corrections are very similar and vary according to the solar activity. Note that, as for TOPEX (Le Traon et al. 1994 [28]), it is recommended to filter the Jason-1 dual frequency ionosphere correction before using it as a SSH geophysical correction (Chambers et al. 2002 [29]). A low-pass filter has thus been used to remove the noise of the correction in all SSH results presented in the following sections. Note that in GDR-C product, the DORIS ionospheric correction is no longer available. It has been replaced by the GIM ionospheric correction (model), which displays better metrics than the DORIS' one.

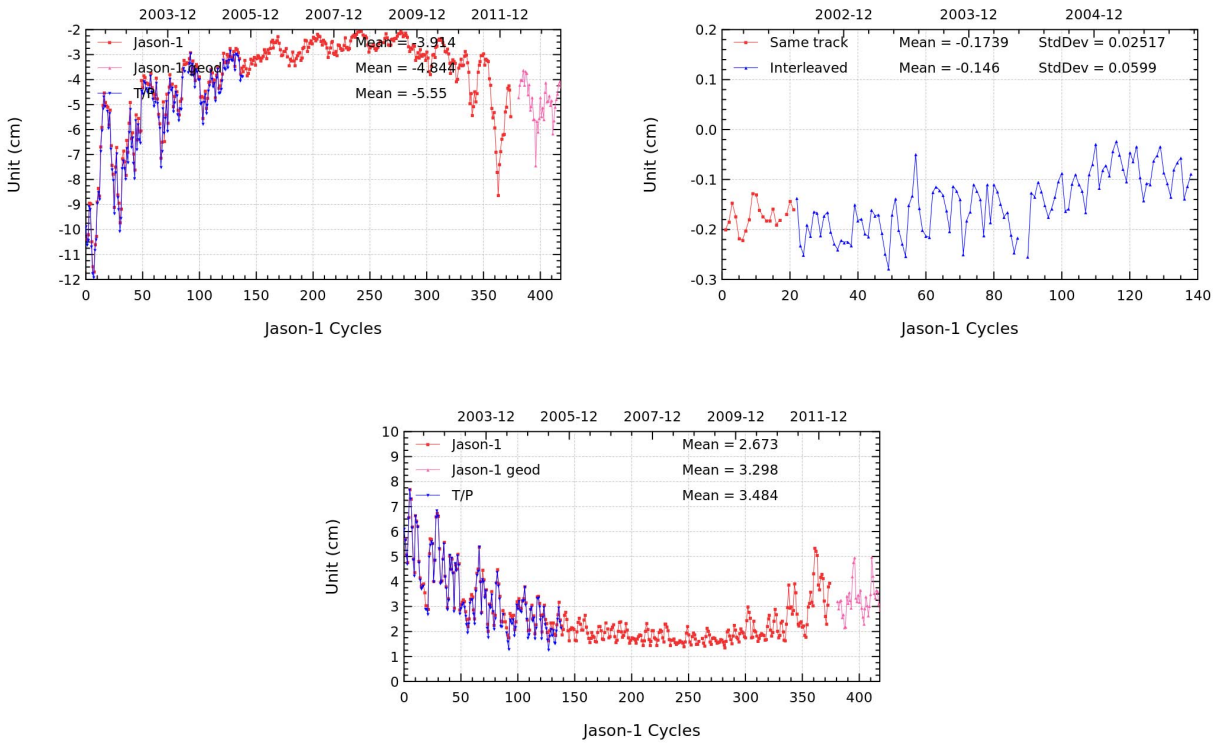

Figure 29: *Cycle per cycle mean (left), T/P−Jason mean differences (right), and standard deviation (bottom) of dual frequency ionosphere correction*

4.6.2. Comparison of GIM and filtered dual-frequency ionosphere corrections

Cycle by cycle statistics of the difference between filtered dual-frequency correction and gim correction are plotted on figure 30. The mean evolution (left part of the figure) shows first a decrease and then an increase of the correction differences with the minimum during year 2008, which is in accordance to the solar activity. The difference value stay under 1 cm over all the mission and the mean over the ten years of repetitive period is 0.12 cm, and for geodetic period, the mean is 0.26 cm.

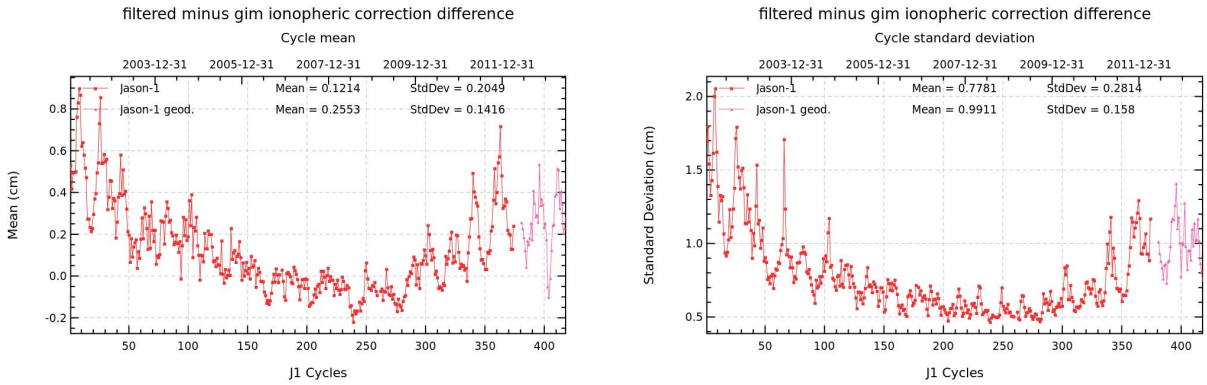

Figure 30: *Cycle per cycle mean (left), and standard deviation (right) of (filtered - gim) ionosphere correction difference*

In order to assess the evolution of the discrepancies between the two corrections, the mean differences have been computed according to several local time intervals of 4 hours. The computation has been performed through the entire mission. Each cycle gives an estimate of the mean difference between two solutions for every local time interval, it has been computed and leads to the results plotted on figure 31. Higher level of differences is observed for local day time hours around 12:00 and differences are lower for night time hours. Furthermore, following the solar activity in both cases, the differences between corrections first decreased from the beginning of the mission and then has increased with a turn about the end of year 2008, with an evolution over the period of about 4mm in case of night hours and 8mm around noun hours.

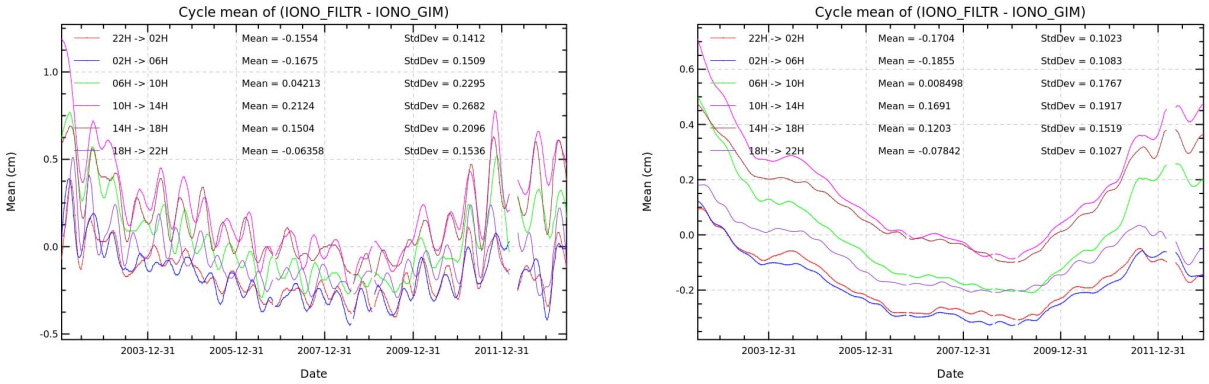

Figure 31: *Cycle per cycle mean of (filtered - gim) ionosphere correction difference as a function of local time, without smooth (left) and after smooth (right)*

4.7. JMR Wet troposphere correction comparison with ECMWF model

Wet troposphere correction is a very important variable for mean sea level trend calculation (see also [30]). Jason-1 satellite has beside the altimeter also a microwave radiometer (JMR) onboard in order to compute the radiometer wet troposphere correction. Furthermore ECMWF model wet troposphere correction is available in GDR products. Both corrections can be subject to jumps or drifts. Comparing both (as well as other radiometer corrections from e.g. Jason-2 or Envisat missions), can help to detect anomalies.
JMR is subject to jumps, or oscillations especially when thermal environment changes, such as after altimeter switch offs. Right side of figure 32 shows for instance oscillations of up to 7 mm just after August 2008 safe hold. These anomalies are generally corrected when GDR products are reprocessed. In the meanwhile, a JMR replacement product is available ([31]) which corrects for these instabilities. Furthermore, JMR continues to be sensitive to yaw maneuvers. On the other hand, ECMWF model is also subject to evolutions, which have an impact on wet troposphere correction. These evolutions are indicated by green lines in figure 32. A jump of several mm occurred after model version change of January 2002. The ECMWF model version change from 9th November 2010, induced a small jump of about 2 mm.

The improvements of the ECMWF model standards are visible on the standard deviation of wet troposphere correction difference (between radiometer and ECMWF model) which is shown on figure 32, left panel. At the beginning of 2003 standard deviation decreases from 1.4 cm to 1.1 cm. This corresponds to a model evolution. In the following, it continues to decrease. In 2009, an increase in standard deviation of radiometer minus ECMWF model wet troposphere differences (of about 0.1 cm) is noticeable. This corresponds to a model evolution on 10th March 2009 (see http://www.ecmwf.int/products/data/operationalsystem/evolution/evolution2009.html#10March2009). The model evolution of 9th November 2010 caused again a decrease of the standard deviation.

Behavior of wet troposphere correction is therefore continually monitored and comparison of the different radiometer and model wet tropospheric corrections are regularly done (see [32]).
Note that JMR has been recalibrated when Jason-1 moved to its geodetic orbit.
On the right hand side of figure 32, a zoom is done on 2013 for the radiometer-ECMWF wet troposphere difference. GDR and IGDR radiometer wet troposphere corrections are different since JA1 safe hold mode: as radiometer minus model wet troposphere difference was again very strongly impacted by yaw maneuvers, another new calibration file was used from 2013 safe hold mode onwards (the calibration files used in case of IGDR product and GDR product are different). This last new calibration reduces the effects of yaw maneuvers, but in spite of this evolution, the radiometer-ECMWF wet troposphere difference is still impacted by yaw maneuvers for the last 10 cycles of the mission (daily monitoring of radiometer – model wet troposphere correction showed impact of more than 1 cm during Yaw fix periods after March 2013 safehold). In addition, note that a pre/post safehold bias remains (which will be addressed by an end-of-mission dedicated recalibration of the JMR).

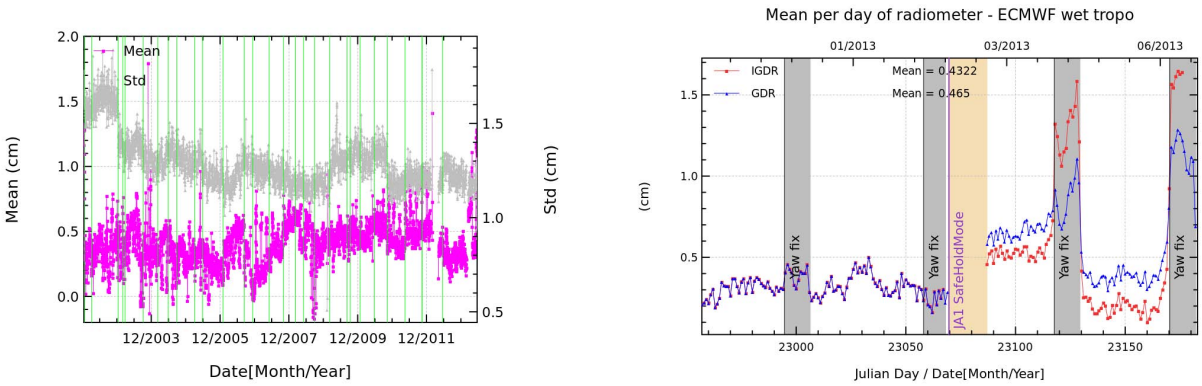

Figure 32: *Difference of radiometer and model wet tropospheric corrections. Left: daily mean and standard deviation over all the Jason-1 mission period. Green lines indicate ECMWF model version changes. Right: Daily mean during 2013. Red curve: IGDR data. Blue curve: GDR data. Gray stripes indicate periods, where Jason-1 is in fix mode.*

5. Crossover analysis

Crossover differences are systematically analyzed to estimate data quality and the Sea Surface Height (SSH) performances. Furthermore, T/P crossover performances (as long as they were available) have been monitored in order to compare both performances. SSH crossover differences are computed on a one cycle basis, with a maximum time lag of 10 days, in order to reduce the impact of ocean variability which is a source of error in the performance estimation. The main SSH calculation for Jason-1 and T/P are defined below. For TOPEX, Jason-1 standards have been used for the tidal and atmospheric corrections.

$$SSH = Orbit - Altimeter\_Range - \sum_{i=1}^{n} Correction_i$$

with Jason-1 orbit = POE_C_CNES orbit until cycle 374, Jason-1 orbit = POE_D_CNES orbit from cycle 500 onwards and

$$\begin{aligned}
\sum_{i=1}^{n} Correction_i \;=\; & \textit{Dry troposphere correction : } S1 \textit{ and } S2 \textit{ atmospheric tides applied} \\
+\; & \textit{Combined high resolution dynamical atmospheric correction} \\
+\; & \textit{Radiometer wet troposphere correction} \\
+\; & \textit{Filtered dual frequency ionospheric correction} \\
+\; & \textit{Non parametric sea state bias correction} \\
+\; & \textit{Geocentric ocean tide height, } GOT\ 2000 : \ S1 \textit{ atmospheric tide is applied} \\
+\; & \textit{Solid earth tide height} \\
+\; & \textit{Geocentric pole tide height}
\end{aligned}$$

5.1. Mean crossover differences

The mean of crossover differences represents the average of SSH differences between ascending and descending passes. It should not be significantly different from zero. More importantly, special care is given to the geographical homogeneity of the mean differences at crossovers. The map of the Jason-1 crossover differences averaged over the whole period of available GDR (cycle 1 to 537) has been plotted in figure 33 (on the left). It is quite homogeneous. Nevertheless some geographically correlated patterns are visible (as it is also the case for Jason-2 [3]). Since GDR version "c", a new empirically correction, called pseudo_datation_bias_corr_ku is available in the products, which corrects for a bias between northern and southern hemisphere previously observable. The origin of this pseudo time tag bias was found by CNES [33].
The cycle mean of Jason-1 SSH crossover differences is plotted for the whole Jason-1 period in figure 33 (right).

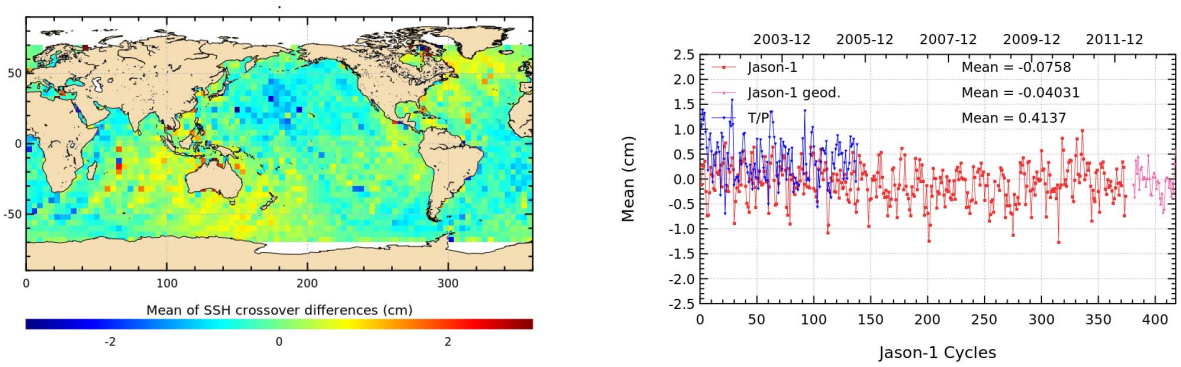

Figure 33: *Map of mean crossovers for Jason cycle 1 to 537 and cycle per cycle mean crossovers (right)*

5.2. Standard deviation of crossover differences

The cycle per cycle standard deviation of crossover differences are plotted in figure 34 (on the left) according to different crossover selections. 3 selections are applied:

- Red curve: no selection is applied. The mean value is 6.3 cm. It shows an annual signal linked to the sea ice extension variations in the Northern Hemisphere.
- Blue curve: shallow waters have been removed (bathy$\leq -1000m$). The previous annual signal has been removed by this selection even though a signal probably due to seasonal ocean variations remains.
- Green curve: the last selection allows monitoring the Jason-1 system performance. Indeed, areas with shallow waters (1000 m), of high ocean variability ($\geq 20cm$) and of high latitudes ($abs(lat) \geq 50$ degrees) have been removed. The standard deviation then provides reliable estimates of the altimeter system performances. In that case, no trend is observed in the standard deviation of Jason-1 SSH crossovers: good performances are obtained, with a standard deviation value of about 5.1 cm all along the mission.

The map of standard deviation of crossover differences overall the Jason-1 period, in figure 34 (on the right) shows usual results with high variability areas linked to ocean variability.

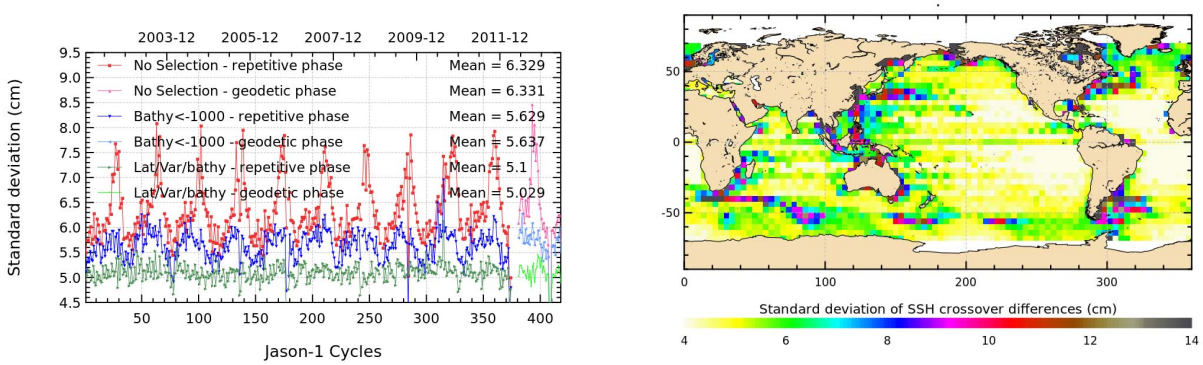

Figure 34: *Cycle per cycle standard deviation crossovers with different selections and map of Jason-1 standard deviation crossovers*

5.3. SSH bias between Jason-1 and T/P: focus on the tandem flight period

5.3.1. Temporal evolution of SSH bias between Jason-1 and T/P

The ECMWF wet troposphere correction is used in figure 35 which represents the temporal evolution of the SSH bias between T/P and Jason-1. This prevents from errors due to radiometer biases, as the model correction is the same for the two missions. When using radiometer wet troposphere correction, the bias differs by 7 to 8 mm. The impact of all geophysical corrections is also displayed in the figure. Results differ by 1.3 cm when applying or not corrections but signals seem to be homogeneous all over the time period. Notice that present results have been obtained using a dedicated TOPEX SSB estimation. Apart from higher variability for Jason-1 cycle 18 (Poseidon-1 was switched on for T/P cycle 361), the T/P to Jason-1 SSH bias nearly remains constant.

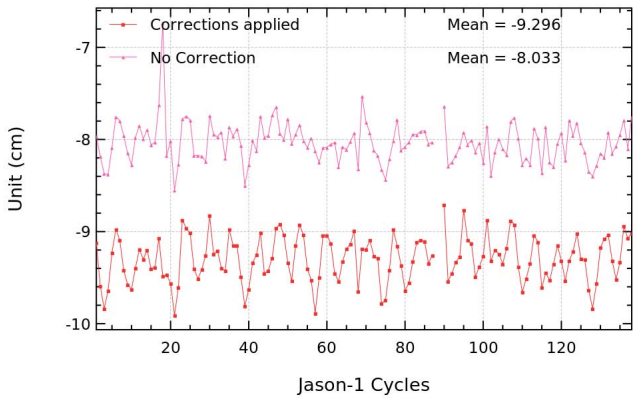

Figure 35: *Cycle per cycle mean of (T/P−Jason-1) SSH differences*

5.3.2. Spatial distribution of SSH bias between Jason-1 and T/P

Jason-1 and T/P have not been on the same track from cycle 22 onward. Consequently, the SSH differences can not be obtained directly as a result of the ocean variability. Thus, the map of the SSH differences between Jason-1 and T/P is obtained at the Jason-T/P crossovers in figure 36. The figure was generated using Jason-1 GDR version "c" (cycle 1 to 138) and updated corrections on T/P (GSFC orbit, Sea State Bias, ionospheric bias). The global map is much more homogeneous with these new standards, though there are still some visible structures, they are now much more consistent and have less amplitudes (generally less than ± 1 cm).
Using the official MGDR T/P standard (which was modified the last time in 1996, see handbook [54]), large differences were also visible, when looking on the verification phase of Jason-1 (cycles 1 to 21) (figure 37, left panel). Both satellites (T/P and Jason-1) were on the same ground track, which makes direct measurement comparison possible. For OSTST meetings in 2006 and 2007 retracked (new range,...) TOPEX cycles for the Jason-1 verification phase were already available (called RGDR). They contained also an orbit based on GRACE gravity model. This reduces the differences, as visible on figure 37 (right panel). The data of both missions are much more homogeneous, when looking at global maps. However, when separating ascending and descending passes during computing T/P - Jason-1 SLA differences, large hemispheric biases appear (see figure 38).

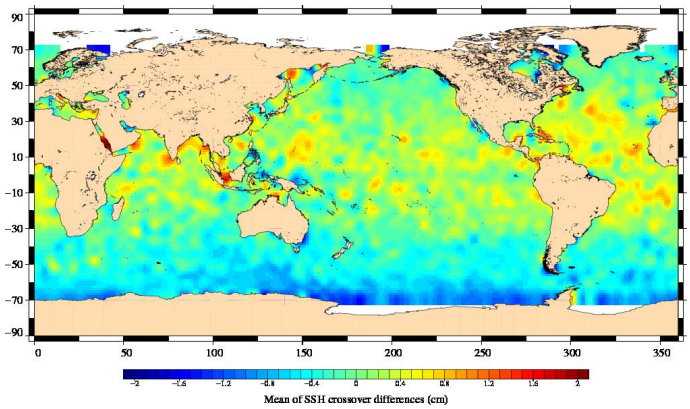

Figure 36: *Map of (T/P−Jason-1) SSH differences for Jason-1 GDR version "c" (cycles 1 to 138).*

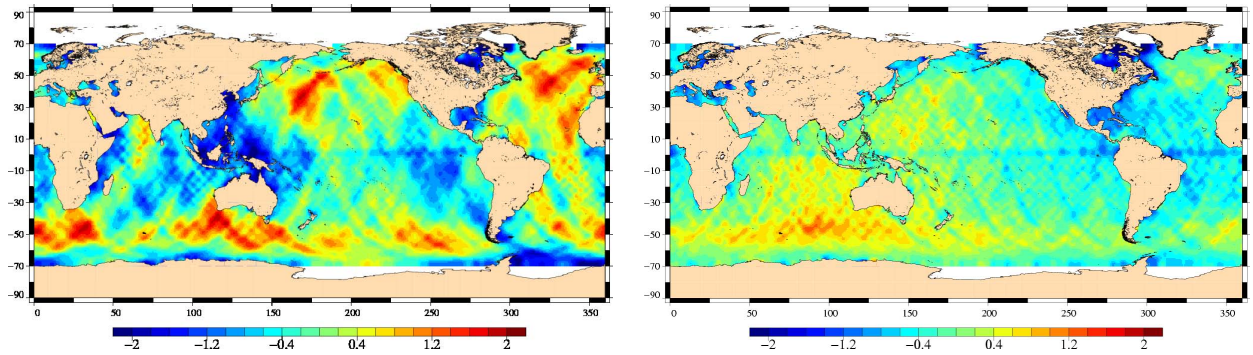

Figure 37: *Map of (T/P−Jason-1) SSH differences for Jason-1 cycles 1 - 21 (Jason-1 GDR version "b") , using orbit of MGDR (left) and GSFC orbit based on GRACE gravity model (right) for T/P.*

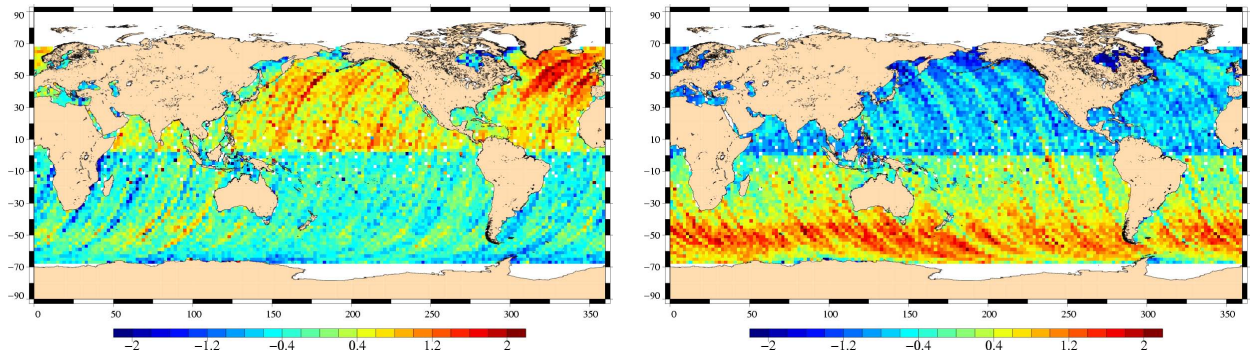

Figure 38: *Map of (T/P−Jason-1) SSH differences separating ascending and descending passes for cycles 1 - 21, using orbit based on GRACE gravity model for T/P and Jason-1 GDR version "b".*

Finally new SSB corrections have been computed on cycles 1-21 for TOPEX using RGDR, with the collinear method. For J1 the Venice 2006 SSB was used ([55]). These TOPEX and J1 SSB models are now much closer than before. When applying them in the SLA calculation in addition to the new orbits and the new ranges (Figure 39), the discrepancies between J1 and T/P are reduced. However, an East/West patch (< 1cm) remains, but it is not correlated with SWH. The origin of this signal is explained by CNES and GSFC orbit, used respectively for J1 and TOPEX. Indeed, using GSFC orbit for Jason-1 similar to those used in RGDR TOPEX data, allows to remove this East/West signal (see [56]).

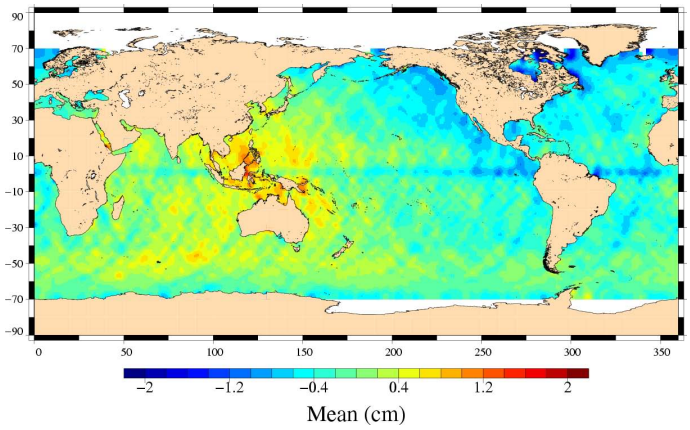

Figure 39: *Map of (T/P−Jason-1) SSH differences for Jason-1 cycles 1 - 21, using GSFC orbit based on GRACE gravity model for T/P, as well as recomputed Sea State Bias.*

5.3.3. Hemispheric SSH bias between Jason-1 and T/P

In order to further investigate hemispheric (T/P−Jason-1) SSH biases, its temporal evolution is presented in figure 40. It shows hemispheric differences between T/P and Jason-1, when separating northern and southern hemisphere. From the northern hemisphere to the southern hemisphere the (T/P−Jason-1) SSH bias estimates can thus differ by up to 1.5 cm. These hemispheric differences seem consistent from one cycle to another. The use of more homogeneous altimeter standards between Jason-1 and T/P has considerably lowered the difference between northern and southern hemisphere on the whole time period. Indeed, using orbits with ITRF 2005 reference system for both Jason-1 and T/P reduced these hemispheric differences.

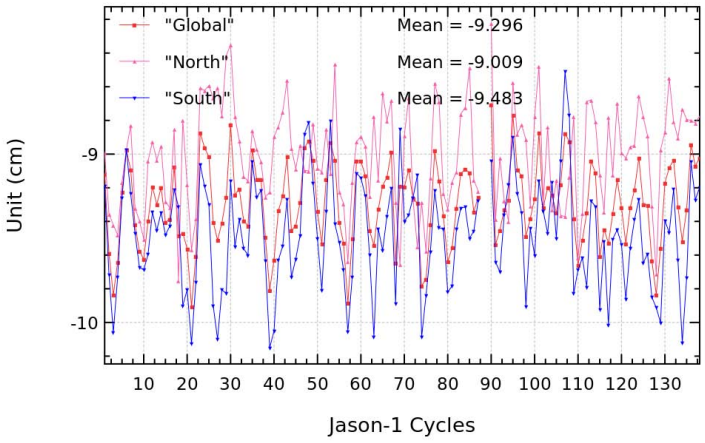

Figure 40: *Cycle per cycle mean of (T/P−Jason-1) SSH differences by hemisphere*

5.4. SSH differences at crossovers for Jason-1 and Jason-2

Figure 41 shows the mean of Jason-1 Jason-2 10-day SSH crossovers, using radiometer wet troposphere correction for both satellites or ECMWF model wet troposphere correction.
Since Jason-1 move to a geodetic orbit, the mean of Jason-1 minus Jason-2 SSH difference shows a jump, mainly due to a more precise PRF value for Jason-1 since may 2012, but also partly due to new JMR calibration file. A study about this jump is detailed in part 8.1..

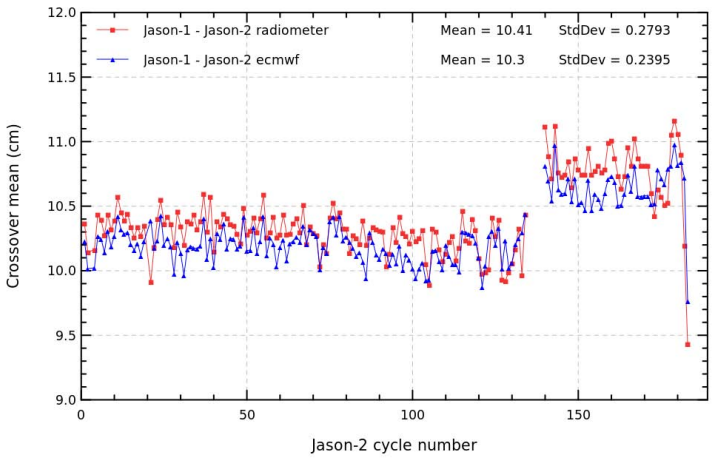

Figure 41: *Cycle per cycle mean of (Jason-1−Jason-2) SSH differences. Sea Surface Height are evaluated using homogeneous formulas (orbit, MSS, ocean tide)*

6. Along-track analysis

This analysis is used to compute Sea Level Anomalies (SLA) variability and thus to estimate data quality.

6.1. Along-track performances

Along track analyzes are also used to assess the altimeter system performances, by computing Sea Level Anomalies (SLA). The SLA variance gives an estimate of the errors of the system, even though the ocean variability fully contributes in this case. A comparison between Jason-1 and T/P has been performed computing the variance of SLA relative to the MSS. This allows global and direct calculations.
The SLA standard deviation is plotted in left side of figure 42 for Jason-1, Jason-2 and T/P. It exhibits similar and good performances for the satellites. After flight formation phases, SLA standard deviation increases for the satellite which is put on the interleaved ground track (T/P in 2002, Jason-1 in 2009). For TOPEX this is less visible, as its ground processing is different from the Jason's. Dorandeu et al. 2004 ([34]) shows that a clear increase in SLA standard deviation is visible for T/P interleaved ground-track when looking at wavelength shorter than 500km. This SLA standard deviation increase is due to the use of MSS CLS01 ([35]), as errors of this MSS are higher outside the historical T/P-Jason ground track ([34],[36]). Using a newer MSS, such as *CNES/CLS 2011* ([37]) which also used data from the interleaved ground track, decreases Jason-1 SLA standard deviation significantly for interleaved period (pink curve on right part of figure 42). As the mission is no longer on a repetitive orbit, it is important to have a Mean Sea Surface of good quality. The Jason-1 Mean Sea Surface has so been updated to *MSS CNES/CLS 2011* in the GDR product since the move to the geodetic orbit. As a consequence, in the left side of figure 42, the standard deviation of SLA is equivalent between Jason-1 and Jason-2 data for the Jason-1 geodetic period.

During summer and fall 2010 (around cycle 320), the SLA standard deviation has increased, not only for Jason-1, but also for Jason-2 and Envisat (not shown here). A part of this increase is probably related to "La Niña" episode occuring in Pacific ([39]). Focus on Pacific Ocean data (right side of figure 42) shows indeed an increase in SLA standard deviation until fall 2010, but also for second semester of 2011.

6.2. Sea level seasonal variations

From Sea Level Anomalies computed relative to the Mean Sea Surface CLS 2001 (Hernandez et al, 2001) until cycle 374, and relative to Mean Sea Surface CNES-CLS 2011 from cycle 500 onwards, the surface topography seasonal variations have been mapped from figure 43 to 53 for the overall Jason-1 data set. Major oceanic signals are showed clearly by these maps: it allow us to assess the data quality for oceanographic applications. The most important changes are observed in the equatorial band with the development of an El Niño in 2002-2003. The event peaked in the fourth quarter of 2002, and declined early in 2003. Conditions indicate an event of moderate intensity that is significantly weaker than the strong 1997-1998 El Niño (McPhaden,2003, [42]).
End of 2007, a La Niña event is visible in Eastern Pacific on figure 48. It lasted till the mid 2008 (see [41]). From mid 2009 to spring 2010 a moderate El Niño event occured (see [38]). In second

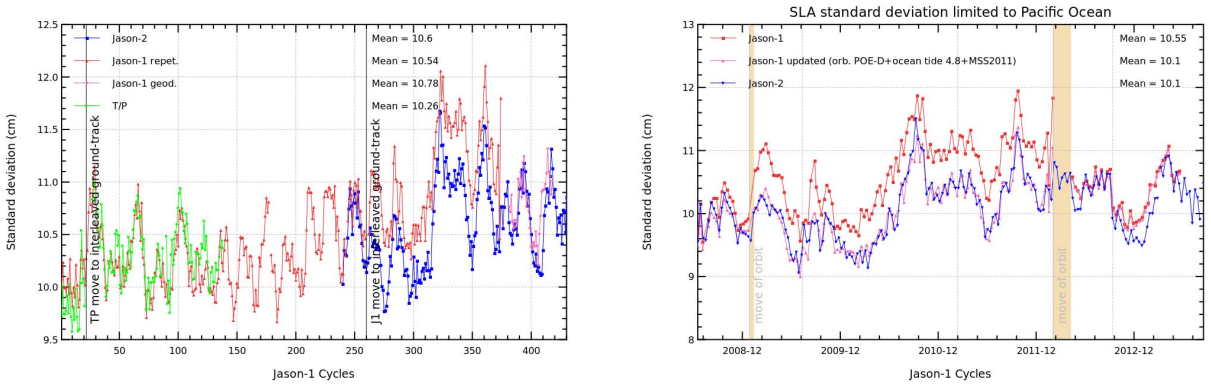

Figure 42: *Cycle per cycle SLA standard deviation. Left: showing T/P, Jason-1 and Jason-2 over whole Jason-1 period. Right: showing Jason-1 and Jason-2 over Jason-2 period and only for Pacific Ocean.*

half of 2010 a moderate to strong La Niña event developped (see [40]) until spring 2011.

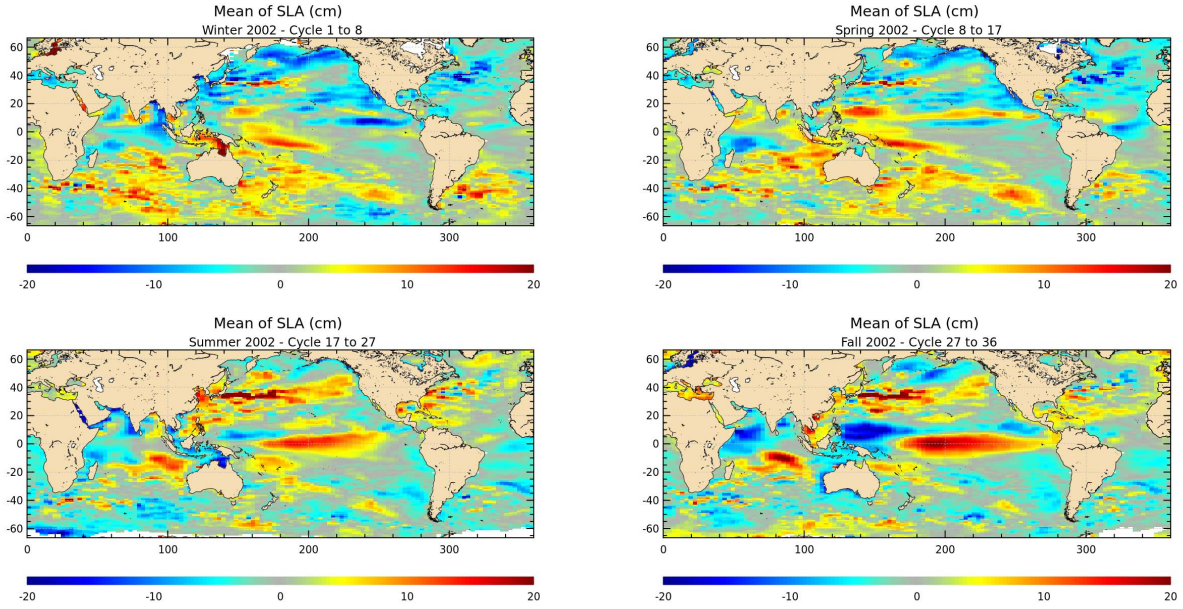

Figure 43: *Seasonal variations of Jason SLA (cm) for year 2002 relative to a MSS CLS 2001*

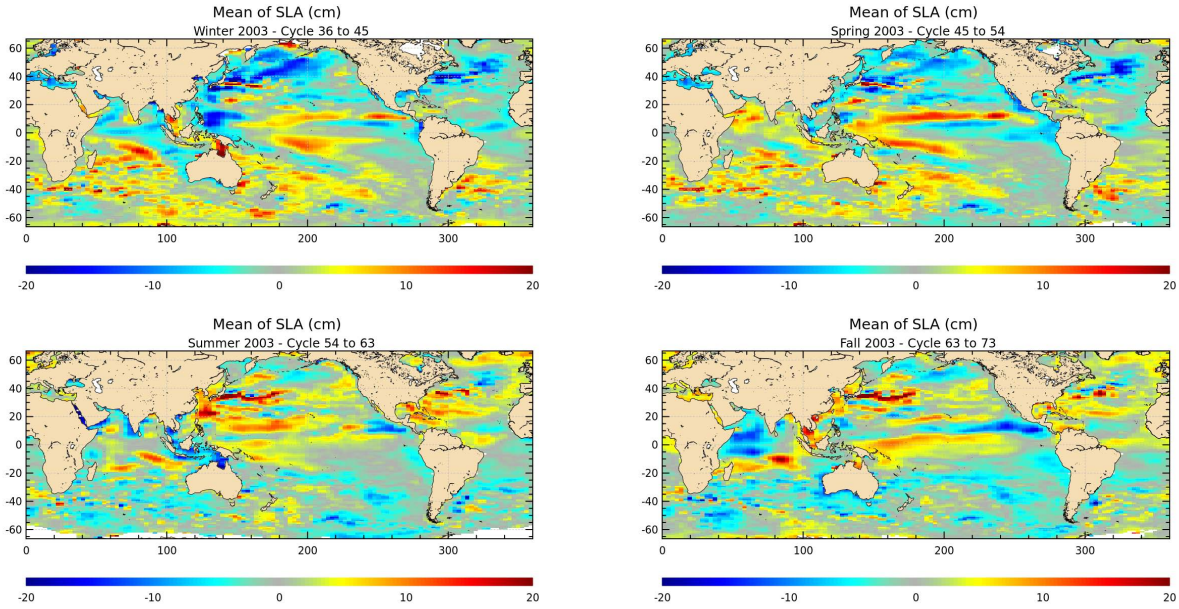

Figure 44: *Seasonal variations of Jason SLA (cm) for year 2003 relative to a MSS CLS 2001*

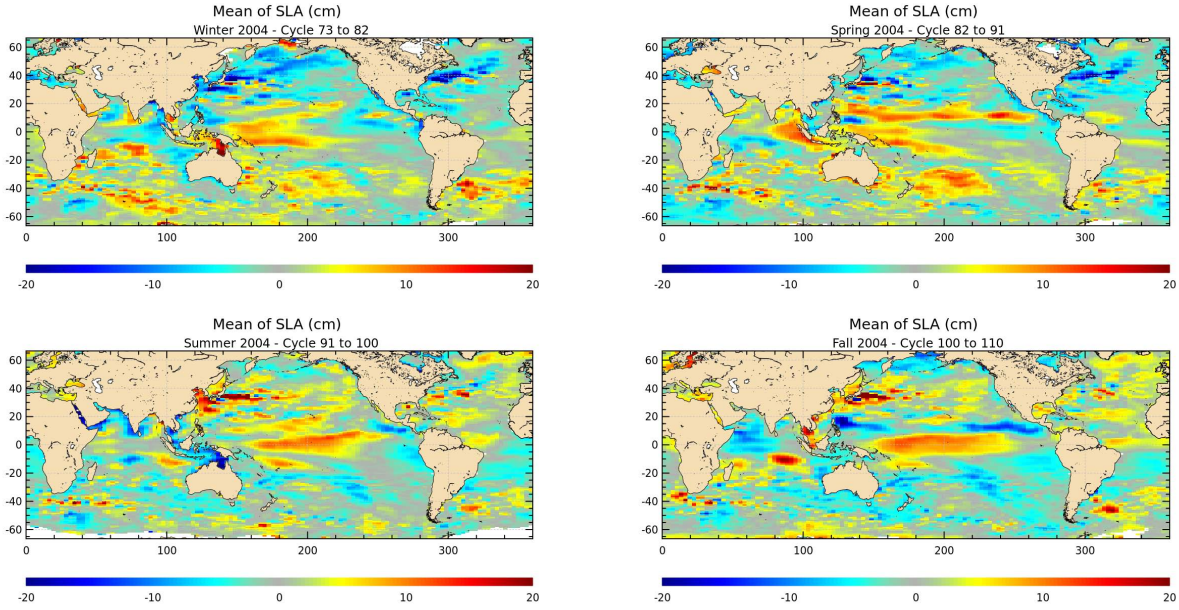

Figure 45: *Seasonal variations of Jason SLA (cm) for year 2004 relative to a MSS CLS 2001*

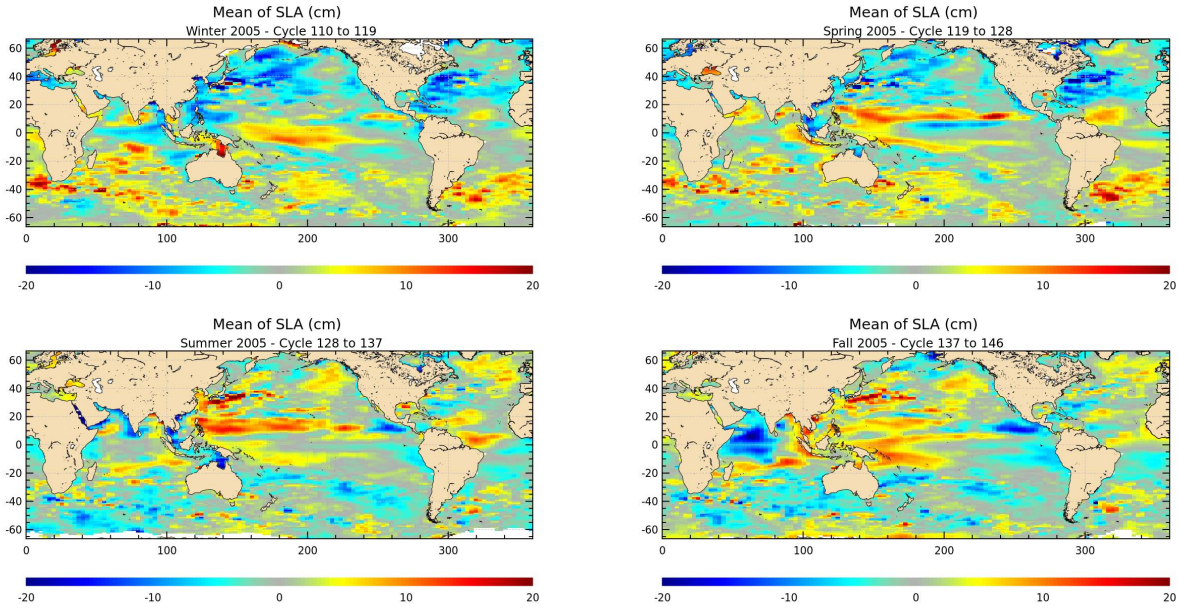

Figure 46: *Seasonal variations of Jason SLA (cm) for year 2005 relative to a MSS CLS 2001*

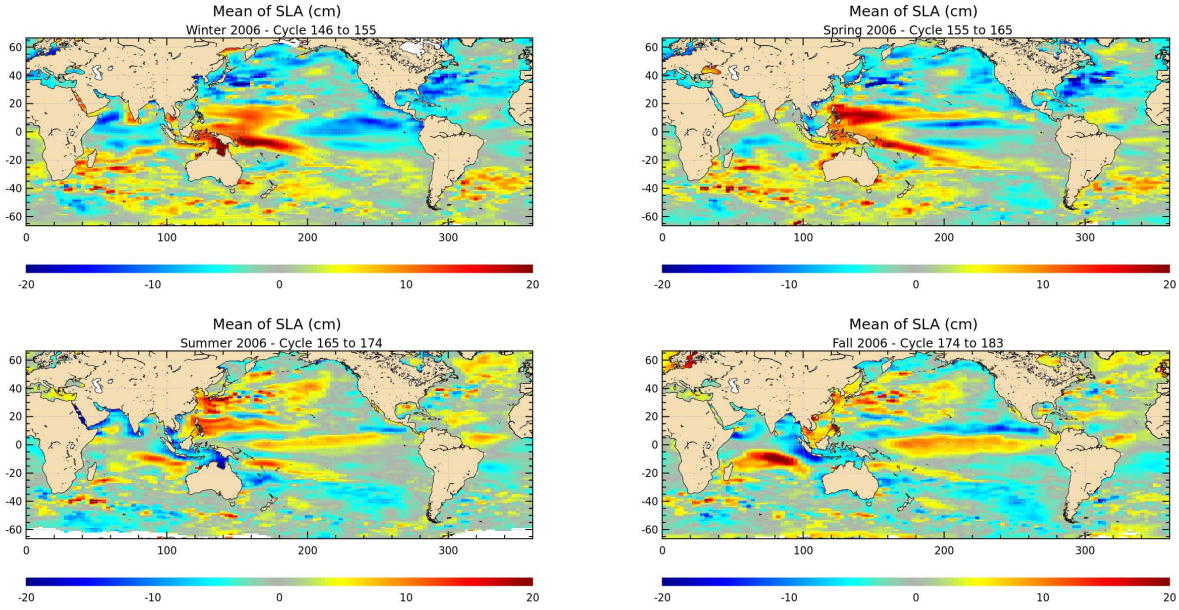

Figure 47: *Seasonal variations of Jason SLA (cm) for year 2006 relative to a MSS CLS 2001*

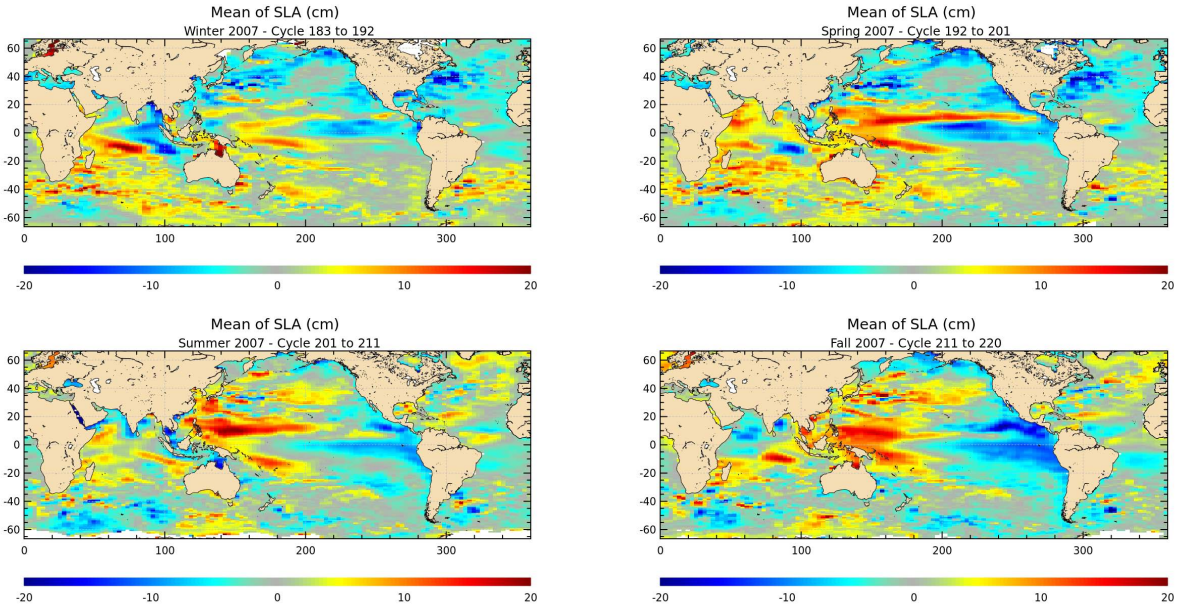

Figure 48: *Seasonal variations of Jason SLA (cm) for year 2007 relative to a MSS CLS 2001*

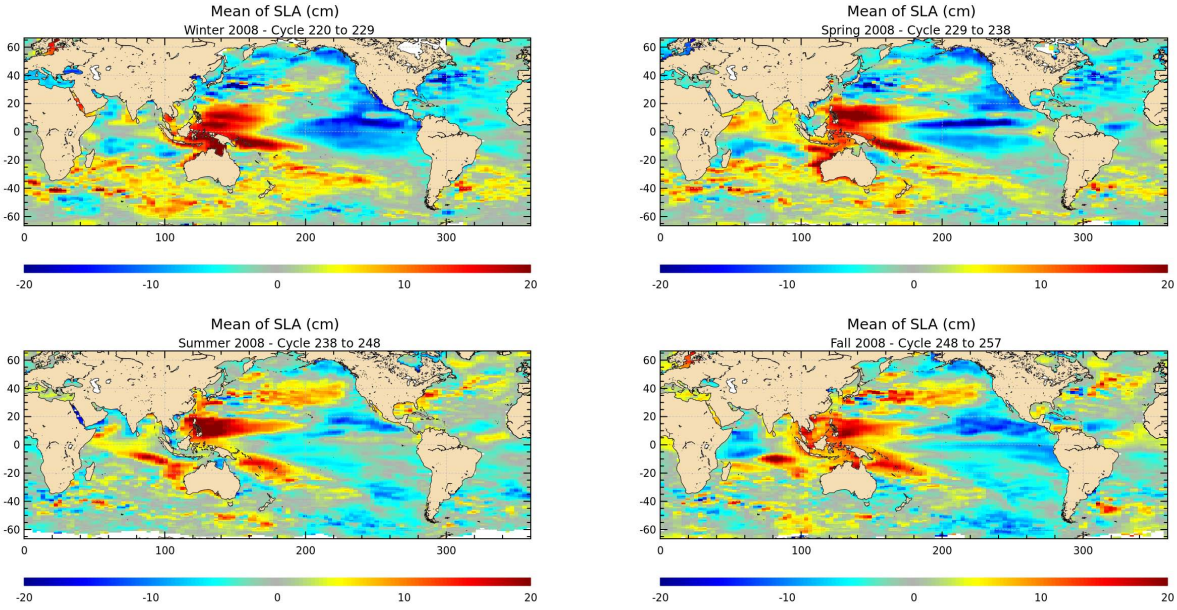

Figure 49: *Seasonal variations of Jason SLA (cm) for year 2008 relative to a MSS CLS 2001*

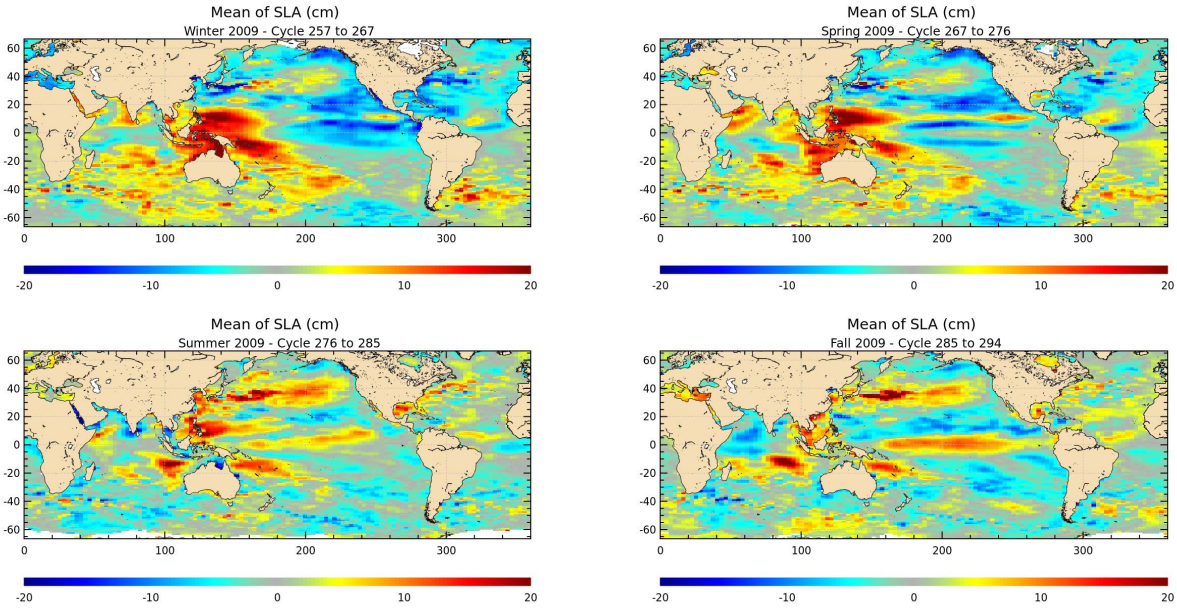

Figure 50: *Seasonal variations of Jason SLA (cm) for year 2009 relative to a MSS CLS 2001*

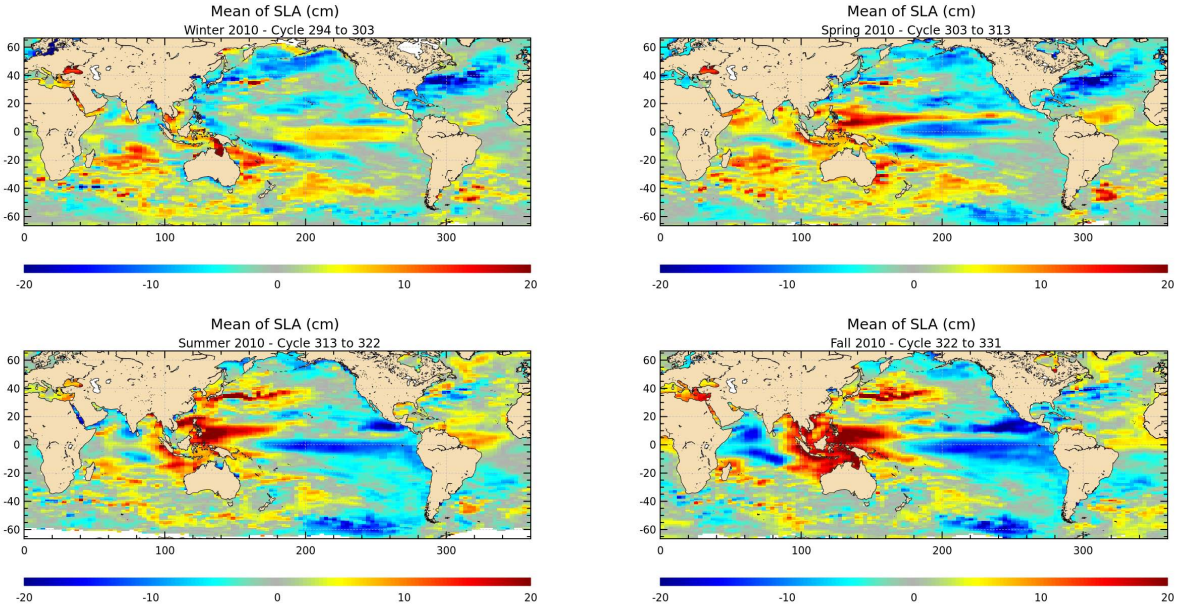

Figure 51: *Seasonal variations of Jason SLA (cm) for year 2010 relative to a MSS CLS 2001*

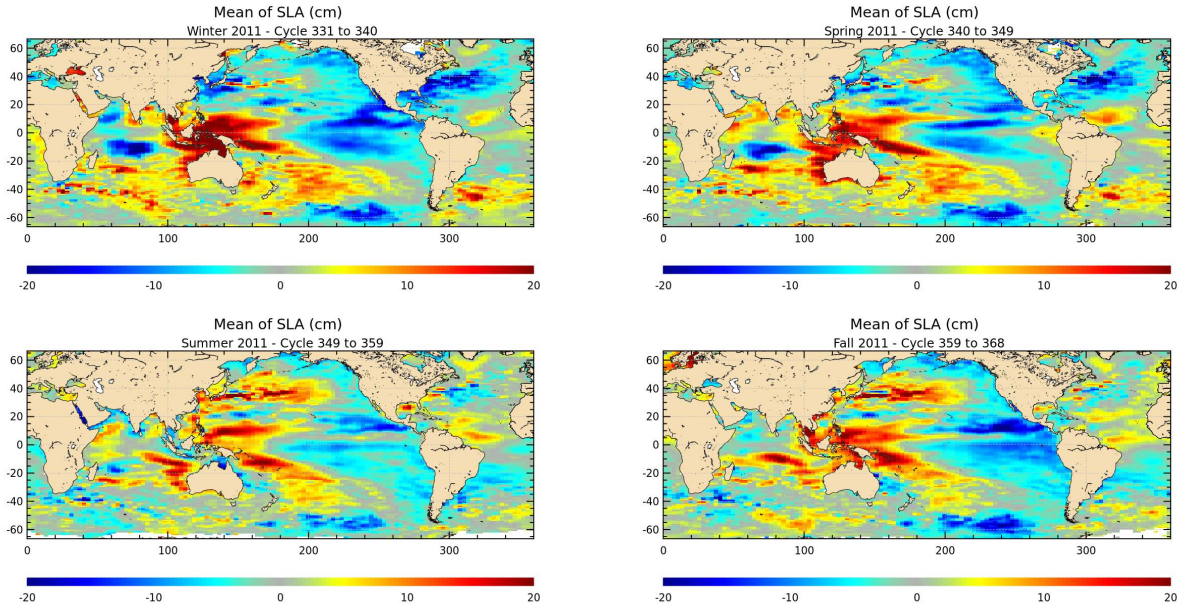

Figure 52: *Seasonal variations of Jason SLA (cm) for year 2011 relative to a MSS CLS 2001*

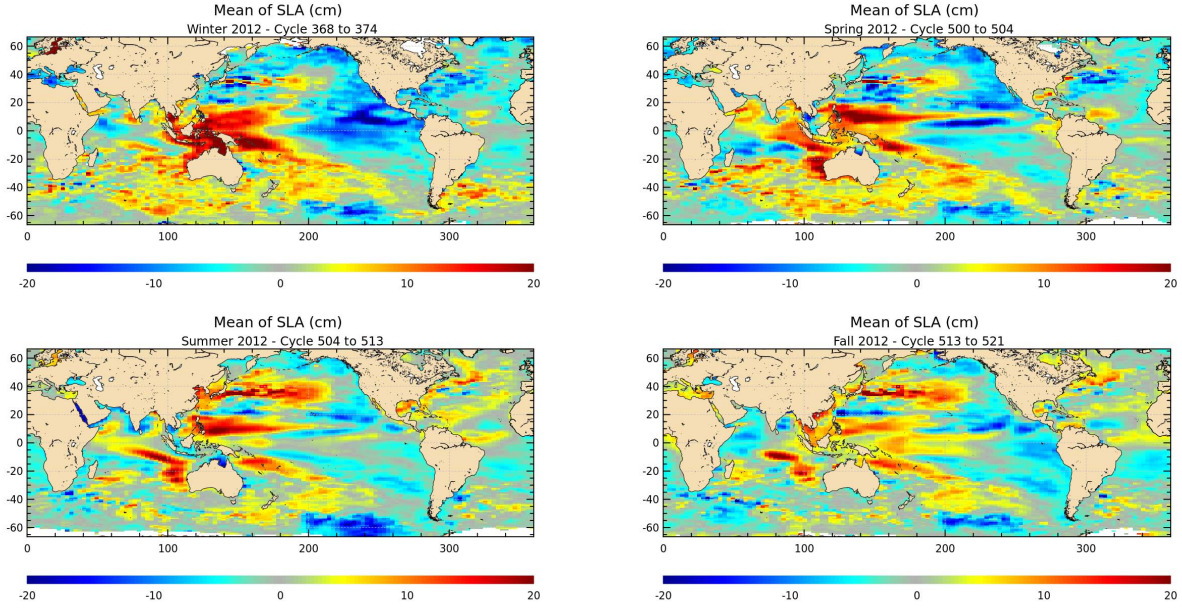

Figure 53: *Seasonal variations of Jason SLA (cm) for year 2012 (for winter: relative to MSS CLS 2001, Since cycle 500: relative to MSS CNES CLS 2011)*

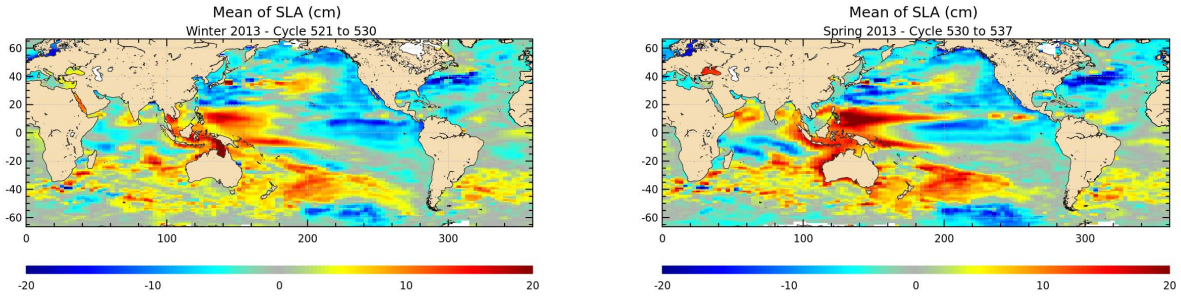

Figure 54: *Seasonal variations of Jason SLA (cm) for year 2013 relative to MSS CNES CLS 2011*

7. Global and regional Mean Sea Level (MSL) trends

7.1. Overview

Long-term MSL change is a variable of real interest in the studies of global climate change. Thus, a lot of work has been performed on the one hand to survey the mean sea level trend and on the other hand to assess the consistency between the MSL derived from all operational altimeter missions. Besides, external data sources such as tide gauges and Argo Temperature/Salinity (T/S) profiles have been used to assess the altimeter MSL evolution and thus detect potential MSL drift. The main works are summarized here.

Note that except if it is mentionned, no GIA correction is applied.

7.2. SSH applied for the MSL calculation

The SSH formula used to compute the MSL is defined for all the satellites as below :

$$SSH = Orbit - Altimeter\ Range - \sum_{i=1}^{n} Correction_i$$

with :

$$\begin{aligned}
\sum_{i=1}^{n} Correction_i \;=\; & Dry\ troposphere\ correction : S1\ and\ S2\ atmospheric\ tides\ applied \\
+\; & Combined\ high\ resolution\ dynamical\ atmospheric\ correction \\
+\; & Wet\ troposphere\ correction\ (radiometer\ or\ ECMWF\ model) \\
+\; & Filtered\ dual\ frequency\ ionospheric\ correction \\
+\; & Non\ parametric\ sea\ state\ bias\ correction \\
+\; & Geocentric\ ocean\ tide\ height,\ GOT\ 4.7 \\
+\; & Solid\ earth\ tide\ height \\
+\; & Geocentric\ pole\ tide\ height
\end{aligned}$$

The SSH formula has been modified or updated for each satellite in order to calculate the best MSL. Especially, stability problems of the radiometer wet troposphere correction have been taken into account :

- For Jason-1 : the radiometer wet troposphere correction is used although 60-days signals are still detected since 2006. The JMR replacement product that reduce instabilities is used between cycle 228 and cycle 259.
- For Envisat : the radiometer wet troposphere correction and a reprocessed orbit (GdrC standard) are used. Filtered dual frequency ionospheric correction is replaced by the gim model (+8mm) from cycle 65 onwards. Specific corrections for Envisat msl computation are: USO correction from GDR product, bias for side-B period (parts of cycles 047 and 048), sign of instrumental correction (PTR) corrected via external CLS input (impact of +2 mm/year drift)

- For T/P : the radiometer wet troposphere correction drift has been corrected with Scharroo's correction (Scharroo R., 2004 [47]), the relative bias between TOPEX and Poseidon and between TOPEX A and TOPEX B has been taken into account, the drift between the TOPEX and DORIS ionosphere corrections has been corrected on Poseidon cycles. GSFC std0809 orbit solution was used as well as a recomputed sea state bias (Tran et al., 2010 [45]).
- For Geosat Follow-On: the ECMWF model wet troposphere correction is used, the GIM model has been used for the ionospheric correction. Furthermore, GSFC std0809 orbits and an updated sea state bias were used.

7.3. Jason-1 Mean Sea Level

7.3.1. Global MSL trend derived from Jason-1 data

With the move to the geodetic orbit (cycle500), some Jason-1 GDR product standards switched:

- $OrbitPOE\_C \rightarrow OrbitPOE\_D$
- $MSS2001 \rightarrow MSS2011$

As a consequence, a particular study was needed in order to correctly link the MSL computations before and after the gap in Jason-1 data in May 2012. The result of this study are detailed in 8.1..

7.3.2. Sea surface height estimate

The assessment of the mean sea level trend is important for climate change studies. MSL estimation from Jason-1 and T/P are plotted in figure 55 (on the left), after reduction of the relative bias between the two time series. The results are obtained after area weighting (Dorandeu and Le Traon 1999 [48]), and using a global bias to correct the artificial jump between the repetitive and the geodetic part of Jason-1 mission (see part 8.1.).
The figure shows good agreement between the two missions and demonstrates that the Jason-1 mission ensures continuous precise MSL monitoring as it was done for more than a decade by the T/P mission. On both missions, seasonal signals are observed.
On figure 55, the red curve represents Jason-1 GMSL computed with the ECMWF model solution for wet troposphere correction. The blue and purple curves show Jason-1 GMSL computed with the radiometer solution for wet troposphere correction, using product corrections as concerned the blue curve and updated solutions (using GOT4.8 ocean tide, MSS2011 and orbit POE-D) as concerned the purple curve. The total impact of these updates on GMSL trend is about $+0.1mm/yr$ over the repetitive phase.

Several error sources can influence MSL evolution, one of them is the choice of wet troposphere correction. On the one hand ECMWF model wet troposphere correction might be influenced by model evolutions, on the other hand radiometer wet troposphere correction is influenced by yaw mode transitions or thermal instabilities after altimeter switch-off. Therefore MSL calculated with radiometer correction (blue curve) and with model correction (red curve) are shown in figure 55: using JMR or model wet troposphere correction has a slight impact on the slope of about 0.2 mm/year. Moreover (on right side of figure 55 after adjusting annual and semi-annual signals), almost 60-day signals are also detected on Jason-1 and T/P series, with nearly the same amplitude. A source of error could be from the largest tidal constituents at twice-daily periods which alias at periods close

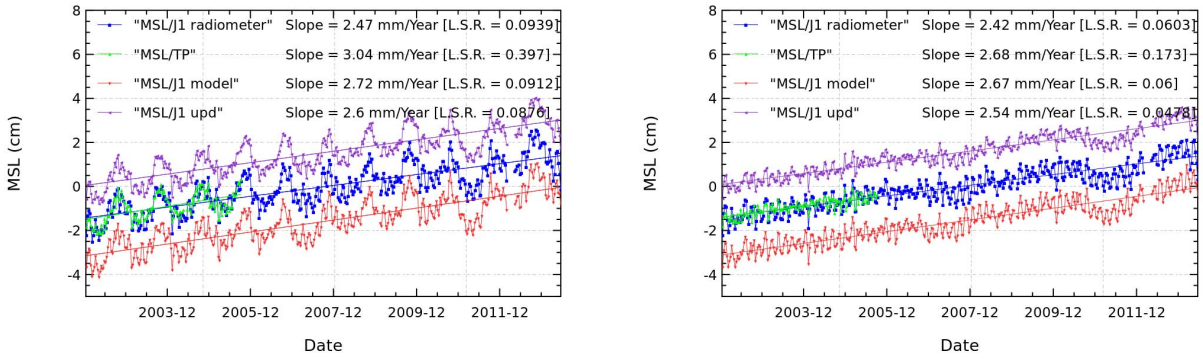

Figure 55: *Jason-1 and T/P mean sea level without (on the left) and with (on the right) annual and semi-annual adjustment*

to 60 days for Jason-1 and T/P (Marshall et al. 1995 [49]). Orbit errors in T/P altimeter series used to compute the tide solutions could also have contaminated these models (Luthcke et al. 2003 [50]). In this way, a study on the 58.77-day signal observed on the MSL derived from Jason-1&2 and TOPEX data has been performed in 2010 (see also [51]). The update of the ocean tide allows to decrease the 60-day signal (from blue curve (Got4.7 solution) to purple curve (GOT4.8 solution)). On figure 55 (right panel), annual and semi-annual signals have been adjusted. This allows to decrease the adjustment formal error for both satellites. The global MSL slopes for Jason-1 is almost 0.3mm/year lower than for T/P, but for Jason-1 the shown time period is more than 7.5 years longer than for T/P. Also, the MSL slope of Jason-1 shows a flattening at the end of 2006 and during 2007 (between cycles 183 and 219). Calibration with in-situ data (see section 7.5. and more detailed in annual reports [14] and [16]) shows no drift of altimeter MSL. Therefore this flattening is due to "La Niña" active during this period. It also shows a strong flattening during year 2011 (between cycles 326 and 359).
C.Boening & al. also wrote about the very strong effect of the "La Niña" event on global mean sea level between the beginning of 2010 and mid 2011 in [61]. J.T. Fasullo & al. suggest that Australia contributes uniquely and sustaintially to the intensity and persistance of global land hydrologic mass increase during the 2011 sea level drop in [62].

7.3.3. Even and odd passes coherence

The previous MSL trends were computed using as well ascending and descending passes, but when computing Jason-1 MSL slope separately for ascending and descending passes, small differences are noticed. Figure 56 shows SLA slopes using Jason-1 GDRs (with ECMWF model wet troposphere correction) and T/P MGDRs.

Jason-1 SLA slopes over the repetitive period are :

- 2.67 mm/yr using descending passes
- 2.59 mm/yr using ascending passes

Indeed, the difference between msl with ascending or descending passes is very dependant of the considered period. Here there is a difference lower than 0.1mm/yr, which differs from T/P (see right of figure 56). There were no difference in case of Jason-1 on its repetitive orbit period (see [53]), which differed from the 0.23mm/yr value calculated until the end of 2010 - from cycle 1 to

331 (see [52]).
There is no explanation concerning differences between ascending and descending passes. Indeed, ascending and descending passes cover the same geographical regions, so there is no reason why SLA slope should rise differently. A study using several orbit solutions showed, that the use of different orbits has an impact on those ascending/descending different SLA slopes.

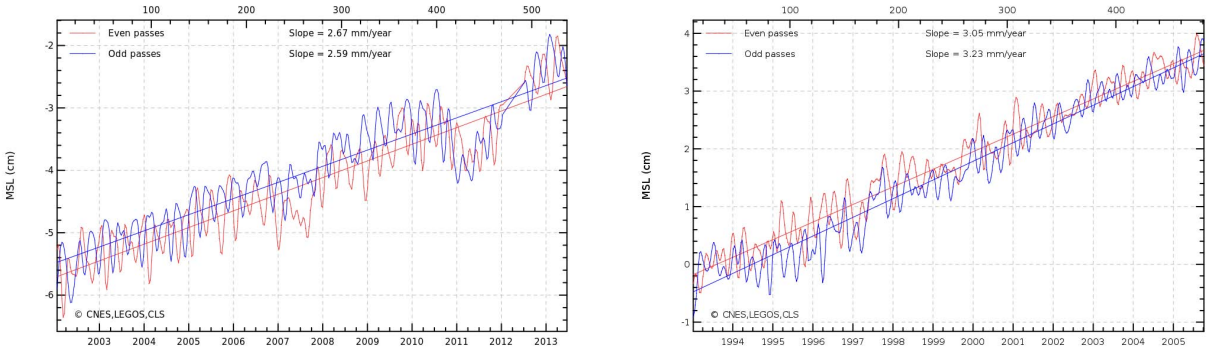

Figure 56: *J1 (left) and T/P (right) SLA slopes using only ascending (odd) or descending (even) passes.*

Note in addition that a particular investigation about the effect of orbit POE-D is detailed in 8.2.. The difference between msl with GdrC and updated standards on the repetitive period is about 0.1mm/yr (mainly due to the change of orbit, see figure 75 and more details in 8.2. and in [53]). Concerning MSL trends when seperating ascending and descending passes, MSL slopes differences between even and odd passes are slightly more homogeneous for POE_C orbit than POE_D orbit as shown in table 9.

7.4. Multi-mission comparisons of global MSL trends

Note that Jason-1 is no longer the reference mission for Global Mean Sea Level monitoring since it has been moved to Jason-2 on 29-10-2008.

7.4.1. Comparisons with other missions

The MSL has been monitored for each satellite altimeter over global ocean in order to assess the global MSL trend and also to detect any anomalies or any drifts on each MSL series. These different MSL have been plotted in figure 57, after removing annual and semi-annual signals, and filtering out signals lower than 60 days. Considering both T/P and GFO, the trends of global MSL are quite the same on their entire time period, around 3.1 mm/yr (figure 57 left). Moreover, since the beginning of Jason-1 (figure 57 right), results deduced from Jason-1 and GFO are in agreement with each other and slightly different from T/P, with respective slopes of 2.4 mm/yr, 2.2 mm/yr and 2.7 mm/yr). However, differences on the trends are partly explained by the different time periods considered, which is demonstrated on figure 57 bottom considering these 3 missions on the same time period. Indeed, between 2002 and 2006, Jason-1 is 0.3 mm/yr higher than T/P, which is 0.6 mm/yr higher than GFO. Finally, concerning Envisat mission, after the reprocessing of Envisat during 2011, the global MSL trend is now around 2.4 mm/year, in agreement with all altimeter

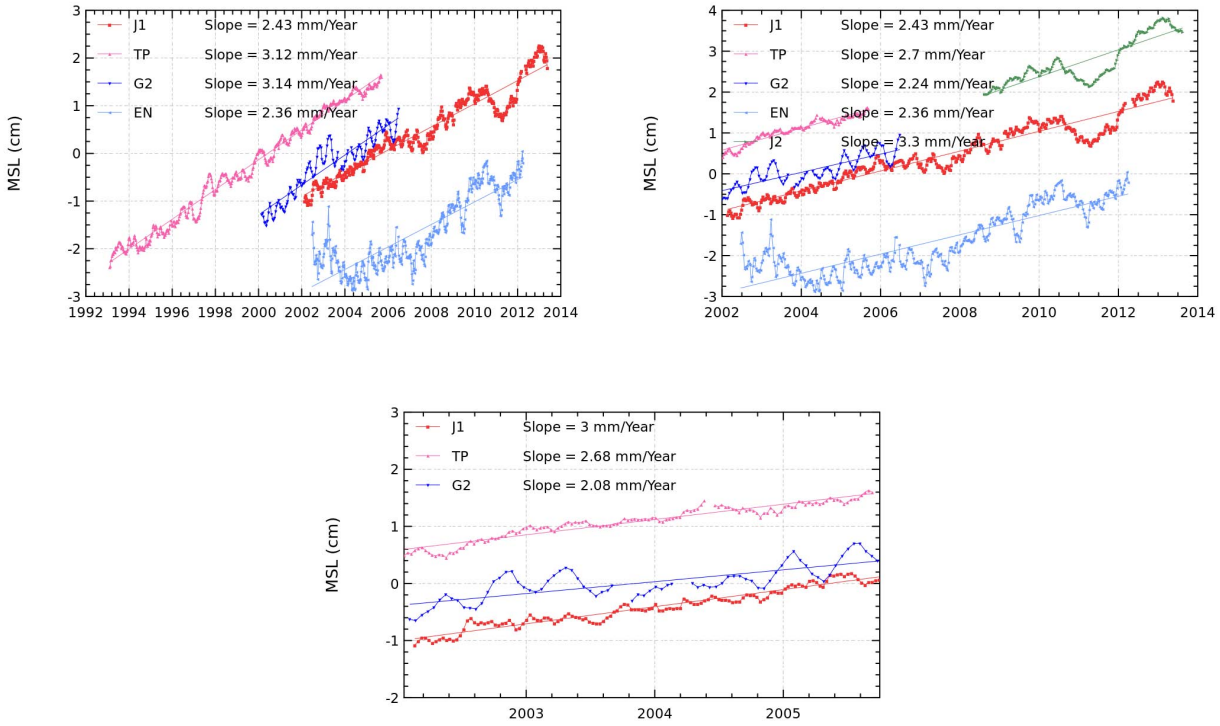

Figure 57: *Multi-mission MSL over global ocean since the beginning of T/P mission (**on the left**) and the beginning of Jason-1 mission (**on the right**) after removing annual and semi-annual signals, and over the common GFO-TP-J1 period (**on the bottom**). Post glacial rebound was not applied.*

missions (see Envisat annual report 2011 [5]).

7.4.2. Analyses of the long term Mean Sea Level trend

7.4.2.1. Global MSL trend derived from Jason-1&2 and T/P data

The global MSL trend derived from satellite altimetry - T/P, Jason-1 and Jason-2 - is now used as the reference for climate studies. Note that Jason-2 dataset is in version GDR-D. A SSH bias of 8.45 cm has been applied on Jason-1 data to be linked to TOPEX/Poseidon and of -10.67 cm between Jason-1 and Jason-2 (see also Aviso web site http://www.aviso.oceanobs.com/en/news/ocean-indicators/mean-sea-level/). These biases were accurately estimated during the verification phase where Jason-1 and T/P (respectively Jason-2 and Jason-1) were on the same orbit. This MSL plotted on figure 58 highlights a global trend of 3.18 mm/yr (post glacial rebound of -0.3 mm/yr was taken into account (Peltier, 2004 [57])). However, the MSL rise is lower and very weak from the end of 2005 to the end of 2007. During this period, only Jason-1 measurements are available, thus the comparisons with T/P MSL is not possible to confirm this behavior. However, comparisons with other satellites and in-situ data, do not highlight any abnormal drift on Jason-1. This MSL trend change might be explained by the very strong "La Niña" event which occurred in 2007 and beginning of 2008. Indeed, the MSL started to rise again in 2008. Note that the same behavior is observed in 2010-2011 on the global MSL, but with a stronger effect: global mean sea level dropped by 5 mm between the beginning of 2010 and mid 2011 (see [61] and [62]).

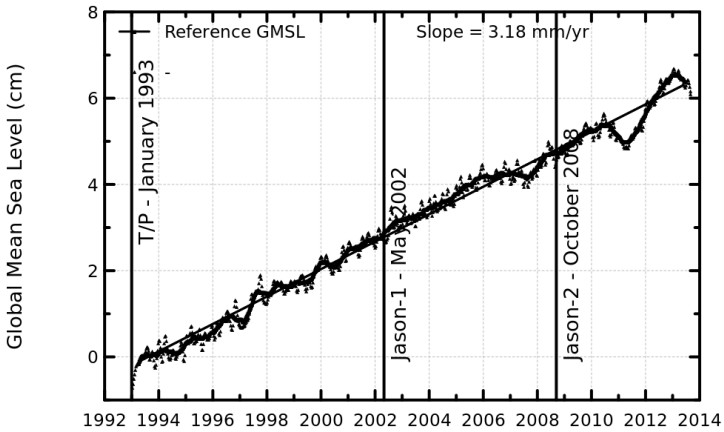

Figure 58: *Global MSL trend derived from Jason-2, Jason-1 and T/P data (GIA correction is applied)*

7.4.2.2. Regional MSL trends derived from AVISO merged products

The AVISO merged products are used to compute the regional MSL trends. Thanks to the high resolution of their grids (0.5 degrees), the MSL regional trends are accurate enough to assess the variability of regional slopes as plotted on map 59. Local slopes range between ±10mm/yr with

large structure in main oceans, especially in Pacific Ocean. This kind of map brings a lot of information about the regional MSL evolution, which have to be further studied for the long term evolution of oceanic circulation as well as the intensity of geostrophic currents and interannual oscillations (decadal, Madden-Julian oscillations for example).

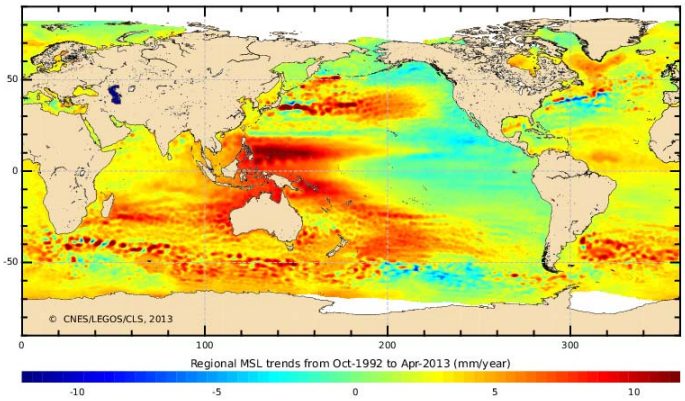

Figure 59: *Regional MSL trends derived from AVISO merged products*

7.5. External data comparisons

In order to assess the global MSL trend, comparisons to independent in-situ datasets are of great interest. Two methods have been developed in the frame of in-situ Calval studies and thoroughly described in both altimeter / tide gauges ([15]) and altimeter / Argo T/S profiles ([17]) annual reports. Note that both in-situ comparison methods complement each other since the first one using tide gauges only concerns coastal areas while the second one using T/S profiles is well widespread to get a regional assessment of the MSL.

7.5.1. Comparison with tide gauges

Firstly, Jason-1 altimeter data is compared with tide gauge measurements thanks to a dedicated method which aims at detecting potential drifts in sea surface heights (SSH). The tide gauge network processed is the GLOSS/CLIVAR "fast" sea level database, formerly known as the WOCE network.

Regarding tide gauges, the MSL bias has been computed taking into account the evolution in the method and data source as detailed in [15]. The result is shown on figure 60, which indicates an altimeter drift of 0.2 mm/yr with Jason-1 data, with a formal adjustment error of 0.1 mm/yr. On almost 10 years of consistent altimeter data delivery on repetitive phase and one year on geodetic phase, the coherence with in-situ measurements along coastal areas is pretty good, and rms differences is about 3.6 cm. In addition to the long-term trend differences observed here, some unexplained signals are observed. Currently, the accuracy of the method of comparison between

altimetry and tide gauge is not able to determine if these signals are due to errors on Jason-1 data or intrinsic uncertainties of the method.

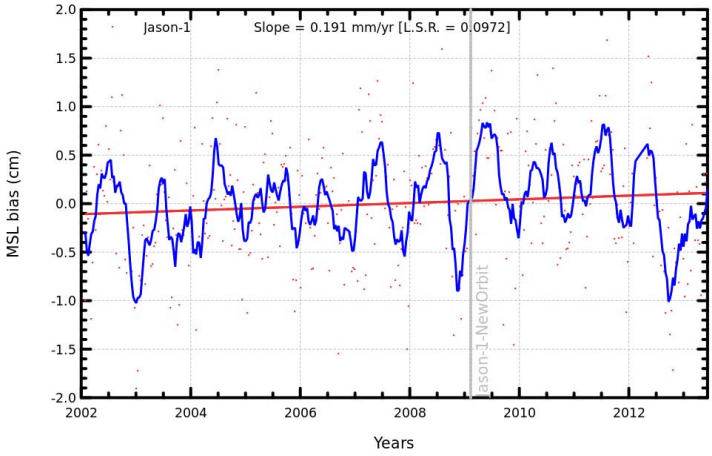

Figure 60: *Jason-1 altimeter MSL drifts compared with tide gauges measurements (post glacial rebound effect applied)*

In-situ tide gauges comparisons are also used to study the impact of the new GDR-D orbit (see 8.2.2.).

7.5.2. Comparison with Argo T/S profiles

The Argo network provides a coverage of almost the whole global ocean with more than 500 000 Temperature and Salinity (T/S) profiles available since 2004. The Dynamic Height Anomalies (DHA) derived from these profiles are representative of the thermohaline expansion of the water column from the surface to 900 dbar (i.e. baroclinic component). We combine these data with grids of the mass contribution to the sea level from GRACE to provide an estimation of the total height of the water column so that the same physical content is compared with altimetry. The monitoring of Jason-1 altimeter SLA and of the summed steric DHA and mass contributions are detailed in [15].

In-situ Argo T/S profiles comparisons are also used to study the impact of the new GDR-D orbit (see 8.2.2.).

8. Investigations

8.1. Analysis of the jump on Jason-1 GMSL after 2012 move to end-of-life orbit (from 03/2012 to 05/2012)

The global sea mean level (GMSL) of the oceans is one of the most important indicators of climate change. It incorporates the reactions from several different components of the climate system. Precise monitoring of changes in the mean level of the oceans, particularly through the use of altimetry satellites, is vitally important, for understanding not just the climate but also the socioeconomic consequences of any rise in sea level (for more information about the Global Mean Sea Level, see [63]).
Since May 2012, Jason-1 is on a geodetic orbit. To distiguish this geodetic phase from the previous repeat ground-track, numbering of the geodetic orbit period starts with cycle 500. Furthermore from cycle 500 onwards, the orbit standard is switched to POE standard D, the mean sea surface available in the GDRs is CNES-CLS-2011 and the JMR calibration file has been recomputed.
As regards the Jason-1 MSL monitoring, a jump seems to appear on the updated (homogeneous) dataset (see GMSL dedicated part 7.3., on figure 41, and on figure 62), but also on the product dataset (figure 66). This jump is mainly due to a more precise PRF value for Jason-1 since may 2012, but also partly due to new JMR calibration file in case radiometer wet troposphere solution is used. Nevertheless, a part of this jump is still unexplained.
The aim of this study is to estimate a precise value of this jump in Global Mean Sea Level between the repetitive and the geodetic Jason-1 missions.

8.1.1. Process

The Global Mean Sea level computed thanks to Jason-2 GDR-D data is used as a reference (see table 5) to evaluate the natural rise of global mean sea level during the Jason-1 safe hold mode period (from March to May 2012).
SSH is calculated for each altimetric measurement considered as valid according to the criteria applied either to the main altimetric parameters, the geophysical corrections or the SSH directly.
As the wet troposphere correction is an important source of uncertainties on MSL trend estimation, MSL using radiometer or ECMWF wet troposphere correction cases are both studied.

The SSH formula used to compute the MSL is defined for all the computation cases as below :

$$SSH = Orbit - Altimeter\ Range - \sum_{i=1}^{n} Correction_i$$

$$
\begin{aligned}
with \quad \sum_{i=1}^{n} Correction_i \;=\; & \textit{Dry troposphere correction} \\
& + \textit{Combined high resolution dynamical atmospheric correction} \\
& + \textit{Wet troposphere correction (radiometer or ECMWF model)} \\
& + \textit{Filtered dual frequency ionospheric correction} \\
& + \textit{Non parametric sea state bias correction} \\
& + \textit{Geocentric ocean tide height (GOT4.7 or GOT4.8)} \\
& + \textit{Solid earth tide height} \\
& + \textit{Geocentric pole tide height}
\end{aligned}
$$

The Sea Level Anomaly corresponds to the Sea Surface Height where the Mean Sea Surface is removed (SLA = SSH - MSS). Table 5, Table 7 and Table 6 present the differences in SSH formula and in MSS for each calculation case.
The two following Jason-2 MSL cases are used as references: $J2_{radiom}$ and $J2_{model}$.

MSL case	Wet Troposphere	Ocean tide	MSS	orbit
$J2_{radiom}$	radiometer	GOT4.8	CLS 2011	POE-D
$J2_{model}$	ECMWF model	GOT4.8	CLS 2011	POE-D

Table 5: Solutions used in mean sea level computation

The global mean sea level is computed over ten days periods using the same method as the one described on aviso website in 2013 (see [63]).

8.1.2. Jason-1 homogeneous product results

8.1.2.1. SSH formula

The two following Jason-1 MSL cases are studied: $J1^{updated}_{radiom}$, $J1^{updated}_{model}$. In these cases, updated homogeneous series of solutions are used (see Table 6).
Table 6 presents the differences in SSH formula and in MSS for each calculation case. (*Note that composite wet troposphere was computed using JMR Replacement Product for cycles 228 to 259.*)

MSL case	Wet Troposphere	Ocean tide	MSS	orbit
$J1^{updated}_{radiom}$	identical to $J1^{aviso}_{radiom}$ case	GOT4.8	CLS 2011	POE-D
$J1^{updated}_{model}$	ECMWF model	GOT4.8	CLS 2011	POE-D

Table 6: Solutions used in mean sea level computation

8.1.2.2. Time series

This part presents the time series per period for each mission, and the difference Jason-2 minus Jason-1, in the two cases of homogeneous Jason-1 ($J1^{updated}$).

It allows to visualize the jump in each case, these jumps will be evaluated more precisely in the following part.

Considering homogeneous Jason-1 SLA over the period, the difference between Jason-2 and Jason-1 evolutions is about 6 to 8 mm , using radiometer or model wet troposphere (see figure 62).

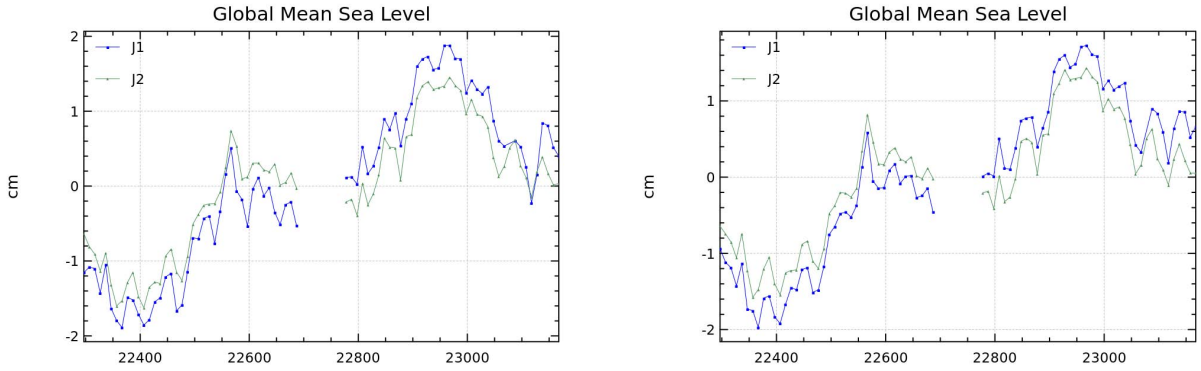

Figure 61: *Jason-2 and Jason-1 10-days MSL monitorings.* ***Left :*** $J2_{radiom}$ *and* $J1^{updated}_{radiom}$, ***Right :*** $J2_{model}$ *and* $J1^{updated}_{model}$. *Figures are centered.*

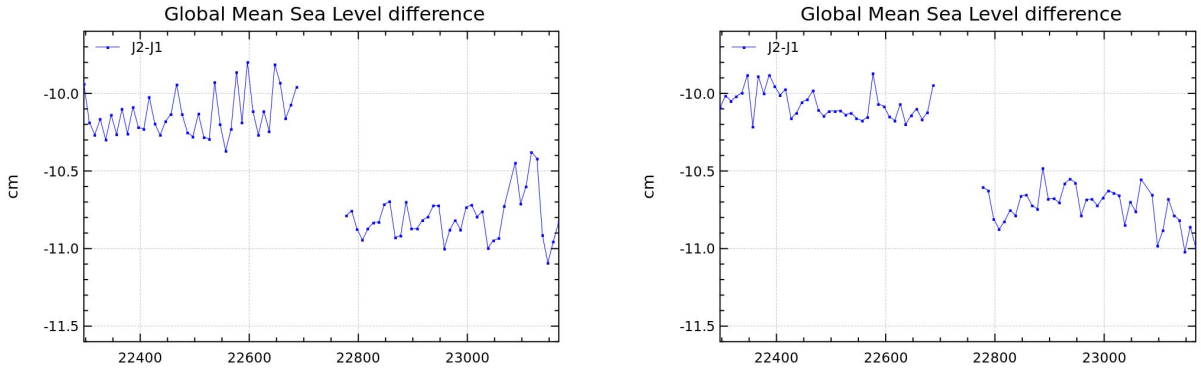

Figure 62: *Difference between Jason-2 and Jason-1 10-days MSL monitorings.* ***Left :*** $J2_{radiom}$ - $J1^{updated}_{radiom}$, ***Right :*** $J2_{model}$ - $J1^{updated}_{model}$.

8.1.2.3. Determination of the bias

In order to average the differences in the high frequencies signals between Jason-2 and Jason-1 data, we need to use at least 100 days data to evaluate the differences with a good accuracy.
On the other hand, a drift in Jason-2 minus Jason-1 difference is visible on figure 63 as the studied duration becomes longer. It is due to radiometer: this is not visible when the model solution is used as wet troposphere correction (see right of figure 63). As a consequence, the bias to apply is chosen for a period of 100days, in order to avoid the influence of this drift due to the radiometer.

In case of radiometer wet troposphere, homogeneous SLA, the difference is 7.8 mm.
In case of model wet troposphere, homogeneous SLA, the difference is 6.2 mm.

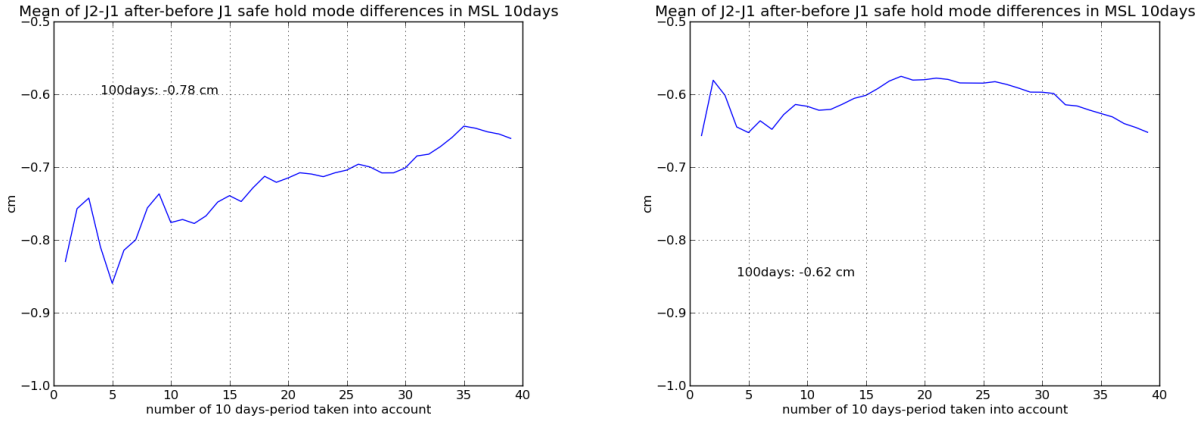

Figure 63: *Difference between global mean sea level after minus before SHM, versus the period used to compute this GMSL. Homogeneous SLA (with Orb POE-D and MSS11).* ***Left :*** *With radiometer Wet Troposphere.* ***Right :*** *With ECMWF Wet Troposphere.*

8.1.2.4. GMSL

The global mean sea level is calculated in case of homogeneous SLA, according to the following corrections:

- $SLA_{MSL} = SLA_{REF}$ as regards the repetitive period
- $SLA_{MSL} = SLA_{REF}$ - (7.8 mm) in case of SLA using radiometer wet troposphere as regards the geodetic period
- $SLA_{MSL} = SLA_{REF}$ - (6.2 mm) in case of SLA using model wet troposphere as regards the geodetic period

It leads to the following trends over the whole Jason-1 period after the remove of the annual and semi-annual signals. (see figure 64):

- 2.55 mm/yr in case of SLA using radiometer wet troposphere

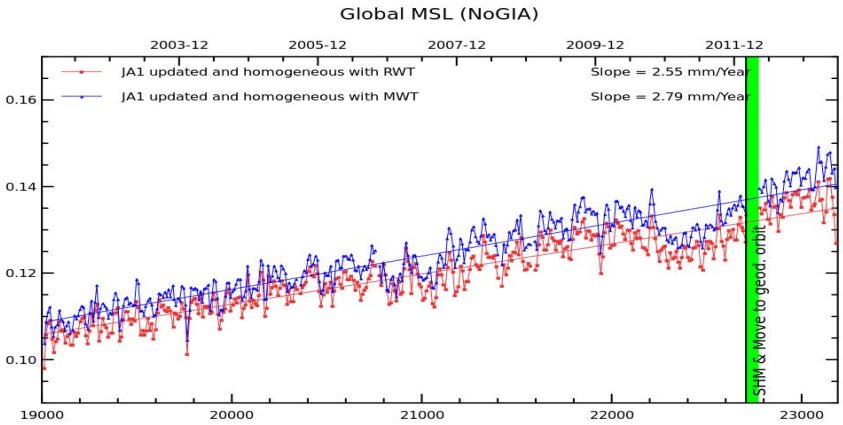

Figure 64: *Global Mean Sea Level. Annual signal has been removed. Updated solution.*

- 2.79 mm/yr in case of SLA using model wet troposphere

8.1.3. Jason-1 $Aviso_{(version2013)}$ product results

The Global Mean Sea Level available on Aviso website (early 2013) was limited to the repetitive period as concerned Jason-1 serie. In order to update the serie with the geodetic period data, the previous calculation was applied to the aviso solution (using different ocean tide, MSS and orbit solution since cycle 500 onwards).

8.1.3.1. SSH formula

The SLA computed like Jason-1 aviso GMSL product is mentioned as $J1^{aviso}_{radiom}$ and $J1^{aviso}_{model}$. Table 7 presents the differences in SSH formula and in MSS for each calculation case. (*Note that composite wet troposphere was computed using JMR Replacement Product for cycles 228 to 259.*) Note that these were the standards used for Aviso GMSL in 2013.

MSL case	Wet Troposphere	Ocean tide	MSS	orbit
$J1^{aviso}_{radiom}$				
on repetitive period (cycles 1 to 374)	composite wet troposphere	GOT4.7	CLS 2001	POE-C
on geodetic period (from cycle 500 onwards)	radiometer	GOT4.7	CLS 2011	POE-D
$J1^{aviso}_{model}$				
on repetitive period cycles 1 to 374)	ECMWF model	GOT4.7	CLS 2001	POE-C

.../...

MSL case	Wet Troposphere	Ocean tide	MSS	orbit
on geodetic period (from cycle 500 onwards)	ECMWF model	GOT4.7	CLS 2011	POE-D

Table 7: Solutions used in mean sea level computation as aviso GMSL product (in 2013)

8.1.3.2. Time series

This part presents the time series per period for each mission, and the difference Jason-2 minus Jason-1, in case of non homogeneous Jason-1 SSH ($J1^{aviso}$) (as it was the case in 2013 on Aviso). It allows to visualize the jump in each case, these jumps will be evaluated more precisely in the following part.

Considering non homogeneous Jason-1 SLA over the period, the difference between Jason-2 and Jason-1 evolutions is lower than in the previous cases, and is about 2 mm to 3 mm in both cases, using radiometer or model wet troposphere (see figure 66). On figure 66, a 60days signal is visible on the J2 minus J1 SLA difference because of the use of a different tide solution (GOT4.8 for J2 instead of GOT4.7 for J1).

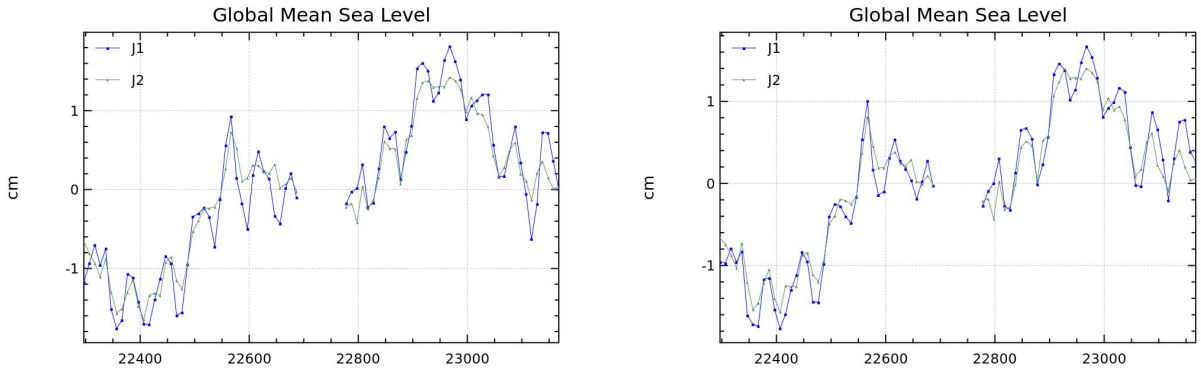

Figure 65: *Jason-2 and Jason-1 10-days MSL monitorings.* ***Left :*** $J2_{radiom}$ *and* $J1^{aviso}_{radiom}$, ***Right :*** $J2_{model}$ *and* $J1^{aviso}_{model}$. *Figures are centered.*

8.1.3.3. Determination of the bias

In order to average the differences in the high frequencies signals between Jason-2 and Jason-1 data, we need to use at least 100 days data to evaluate the differences with a good accuracy.
On the other hand, a drift in Jason-2 minus Jason-1 difference is visible on figure 67 as the studied duration becomes longer. It is due to radiometer: this is not visible when the model solution is used as wet troposphere correction (see figure 67). As a consequence, the bias to apply is chosen for a period of 100days, in order to avoid the influence of this drift due to the radiometer.

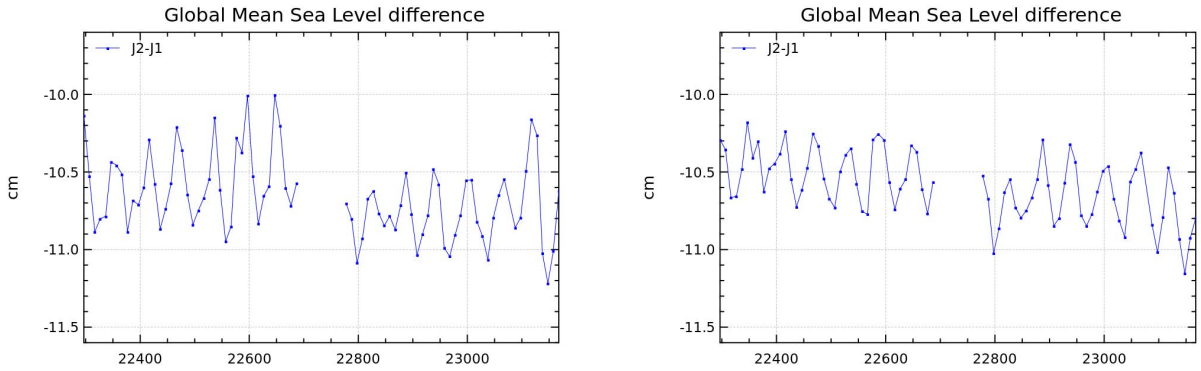

Figure 66: *Difference between Jason-2 and Jason-1 10-days MSL monitorings.* ***Left :*** $J2_{radiom}$ - $J1^{aviso}_{radiom}$, ***Right :***$J2_{model}$ - $J1^{aviso}_{model}$.

In case of radiometer wet troposphere, non homogeneous SLA, the difference is 3.4 mm.
In case of model wet troposphere, non homogeneous SLA, the difference is 1.8 mm.

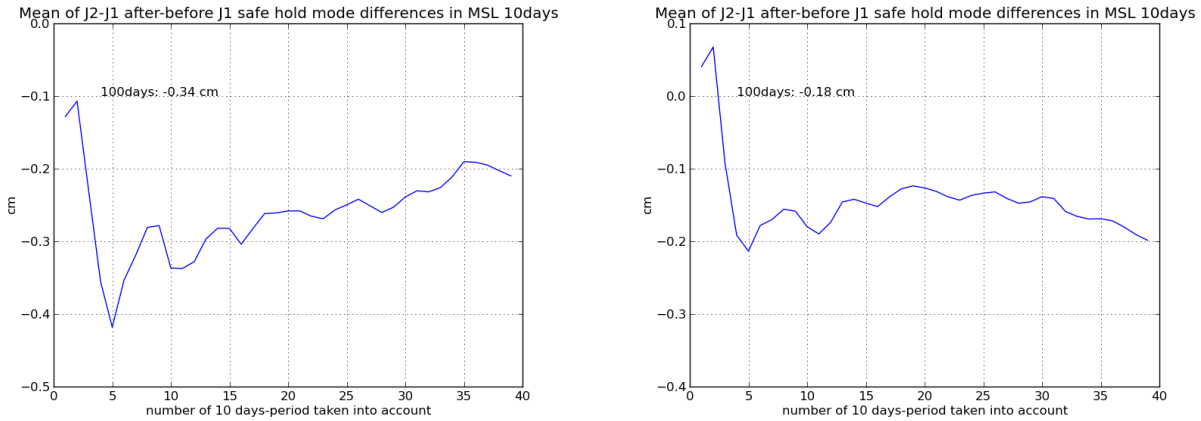

Figure 67: *Difference between global mean sea level after minus before SHM, versus the period used to compute this GMSL. Orb POE-C and MSS01 until cycle 374, Orb POE-D and MSS11 since cycle 500.****Left :*** *With radiometer Wet Troposphere.* ***Right :*** *With ECMWF Wet Troposphere.*

8.1.3.4. GMSL

The global mean sea level is calculated in case of like aviso SLA (2013), according to the following corrections:

- $SLA_{MSL} = SLA_{REF}$ as regards the repetitive period
- $SLA_{MSL} = SLA_{REF}$ - (3.4 mm) in case of SLA using radiometer wet troposphere as regards the geodetic period
- $SLA_{MSL} = SLA_{REF}$ - (1.8 mm) in case of SLA using model wet troposphere as regards the geodetic period

which leads to the following trends over the whole Jason-1 period after the remove of the annual and semi-annual signals. (see figure 68):

- 2.43 mm/yr in case of SLA using radiometer wet troposphere
- 2.68 mm/yr in case of SLA using model wet troposphere

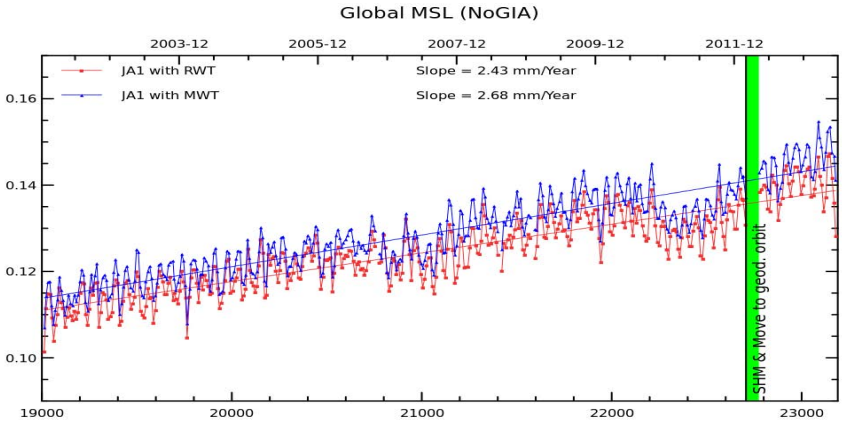

Figure 68: *Global Mean Sea Level. Annual signal has been removed. Aviso*$_{(version2013)}$ *data.*

8.1.4. Conclusion

This study allows to evaluate the global jump in Jason-1 MSL after the move of the satellite to its geodetic orbit, no regional study has been done yet. Nonetheless, such a study is ongoing and first results reveals a difference in behaviour between northern and southern hemispheres. On left of figure 69 the global bias with the updated and homogeneous solution and using radiometer wet troposphere is 7.8mm globally whereas it is 4.6mm in northern hemisphere and 10.2mm in southern hemisphere. On right of figure 69 the global bias with the updated and homogeneous solution and using model wet troposphere is 6.2mm globally whereas it is 2.8mm in northern hemisphere and 8.8mm in southern hemisphere.

Note that this study was done with Aviso GMSL from 2013. In the meantime (January 2014), Aviso GMSL was reprocessed with also homogeneous standards for Jason-1.

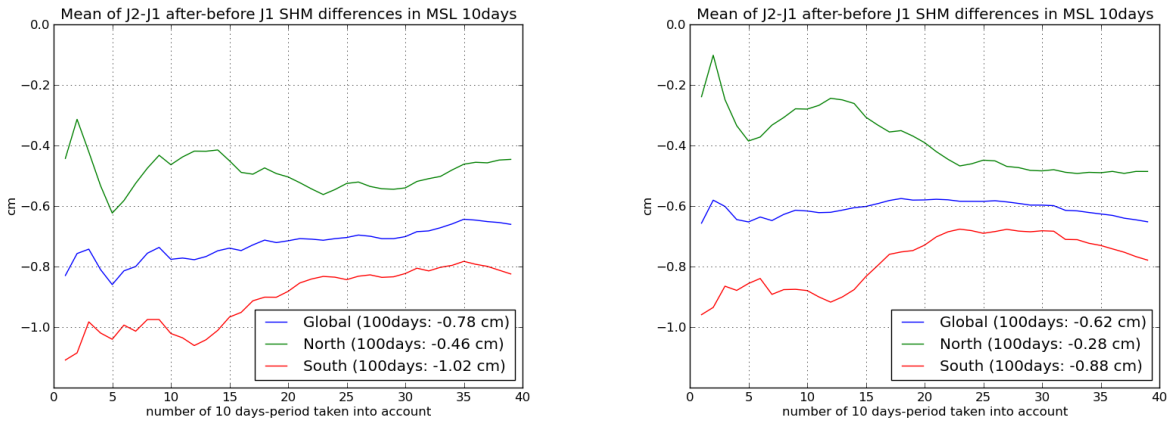

Figure 69: *Mean Sea Level difference between* $JA2 - JA1_{after-beforeSHM}$. *JA1 updated. Global, in northern atmosphere, and in southern atmosphere.* ***Left:*** *with radiometer wet troposphere* ***Right:*** *with model wet troposphere*

8.2. Comparison between GDR-D orbit and GDR-C orbit

The quality of Precise Orbit Ephemeris is crucial for the quality of altimeter data products and the studies based upon these data. Inversely, studies using Sea Surface Height (SSH) calculation from altimeter or in-situ data enable:
- to give insight on orbit quality for the different missions,
- to compare different orbit solutions for one mission,
- and to give hints which mission is impacted by suspicious behavior, when comparing several missions.

This analysis concerns the POE CNES standard D orbit for Jason-1 over the period from cycle 1 to 374. It has been compared to POE CNES standard C orbit standard (used for Jason-1 GDR-C products up to cycle 374) with the objective to characterize the spatial and temporal differences between the two orbit solutions (resumed in table 8 and complete in figure 70) and to analyse the impact on the Mean Sea Level trends.
Note that the CNES POE-D solution is available in the GDR-C products from cycle 500 onwards.

Orbit	Type	Cycles used for figures	ITRF	Gravity field
POE CNES standard C (called POE_C in this part)	using Doris, GPS (less available since 2006, August) and Laser	1 to 374	2005	EIGEN-GL04S
POE CNES standard D (called POE_D in this part)	using Doris, GPS (less available since 2006, August) and Laser	1 to 374	2008	EIGEN-GRGS_RL02bis_MEAN-FIELD

Table 8: *U*sed orbits

	GDR-C version "c" products	GDR-D version "c" Geodetic orbit products
Gravity model	EIGEN-GL04S-ANNUAL (2008) Non-tidal TVG : drifts in degree 2,3,4 zonal coeffs, C21/S21; Annual and semi-annual terms up to deg/ord 50 Solid Earth Tides: from IERS2003 conventions Ocean tides FES2004 Atmospheric gravity : 6hr NCEP pressure fields + tides from Horwitz-Cowley model Pole Tide: solid Earth and ocean from IERS2003 conventions Third bodies: Sun, Moon, Venus, Mars and Jupiter	**EIGEN-GRGS_RL02bis_MEAN-FIELD (2011)** Non-tidal TVG : Annual, Semi-annual, and **drifts up to deg/ord 50** Solid Earth Tides: from IERS2003 conventions Ocean tides FES2004 Atmospheric gravity : 6hr NCEP pressure fields **+ tides from Biancale-Bode model** Pole Tide: solid Earth and ocean from IERS2010 conventions Third bodies: Sun, Moon, Venus, Mars and Jupiter
Surface forces	Radiation Pressure model: thermo-optical coefficient from pre-launch box and wing model, with smoothed Earth shadow model Earth Radiation : Knocke-Ries albedo and IR satellite model Atmospheric density model : DTM-94 for Jason, and MSIS-86 for Envisat	Unchanged
Estimated dynamical parameters	Drag coefficient every 2 or 3 revolutions Along-track and Cross-track 1/rev per day or every 12 hours	Unchanged
Satellite reference	Mass and Center of gravity: Post-Launch values + variations generated by Control Center Attitude Model : For Jason-1 and Jason-2 : Quaternions and Solar Panel orientation from control center, completed by nominal yaw steering law when necessary For Envisat: nominal attitude law	Unchanged
Doris Weight	1.5 mm/s (1.5 cm over 10 sec) For Jason-1 , Doris Weight is reduced by a factor 10 before Doris instrument change	Unchanged
SLR Weight	10 cm	**15 cm**
GPS Weight	10 cm (phase) / 10 m (code)	**2 cm (phase) / 2 m (code)**

	GDR-C version "c" products	GDR-D version "c" Geodetic orbit products
Displacement of reference points	Earth tides: IERS2003 conventions Ocean Loading: FES2004 Pole tide : solid earth pole tides (Pole tide and ocean loading applied to both SLR stations and DORIS beacons) Reference GPS constellation: JPL solution at IGS (orbits and clocks) , consistent with IGS05; before GPS week 1400, JPL solution has been aligned with IGS05; IGS00 clocks are unchanged	Earth tides: IERS2003 conventions Ocean Loading: FES2004 Pole tide : solid earth pole tide (Pole tide and ocean loading applied to both SLR stations and DORIS beacons) Reference GPS constellation: JPL solution at IGS (orbits and clocks) – **fully consistent with IGS08**
Terrestrial Reference Frame	Extended ITRF2005 (SLRF/LPOD2005, DPOD2005, IGS05)	**Extended ITRF2008 (SLRF/ITRF2008, DPOD2008, IGS08)**
Earth orientation	Consistent with IERS2003 conventions and ITRF2005	**Consistent with IERS2010 conventions and ITRF2008**
Propagations delays	SLR Troposphere correction: Mendes-Pavlis SLR range correction: constant 5.0 cm range correction for Envisat, elevation dependent range correction for Jason DORIS Troposphere correction : CNET model GPS PCO/PCV (Emitter and Receiver) consistent with constellation orbits and clocks (IGS05 Antex after GPS week 1400) GPS : Phase wind-up correction	SLR Troposphere correction: Mendes-Pavlis SLR range correction: constant 5.0 cm range correction for Envisat, elevation dependent range correction for Jason **DORIS Troposphere correction : GPT/GMF model** GPS PCO/PCV (Emitter and Receiver) consistent with constellation orbits and clocks **(IGS08 Antex)** GPS : Phase wind-up correction
Estimated measurement parameters	DORIS: 1 Frequency bias per pass, 1 troposphere zenith bias per pass SLR : bias per arc solved for a few stations, bias per pass for a few stations GPS: Floating ambiguity per pass, receiver clock adjusted per epoch	Unchanged
Tracking Data corrections	Jason-1 Doris data: South Atlantic Anomaly Model (JM Lemoine et al.) applied before and after DORIS instrument change DORIS datation bias for Envisat and Jason aligned with SLR before and after instrument change	Unchanged

Figure 70: *Differences between GDR-C and GDR-D precise orbit determination (POD) standards, used respectively for the computation of the version "c" products and version "c" Geodetic Orbit products orbit field.*

8.2.1. SSH crossover differences

Orbits of Jason-1 GDR products (POE-C solution until cycle 374) are fully compliant with requirement. Nevertheless, small geographical correlated patterns of amplitudes up to ± 2 cm (positive in North-Atlantic and South-Pacific, negative in South-Atlantic and North-Pacific) are visible on maps of mean SSH differences at crossovers (see right of figure 71). Using orbits based on a new version of gravity field reduces these small geographical correlated pattern (see left of figure 71).

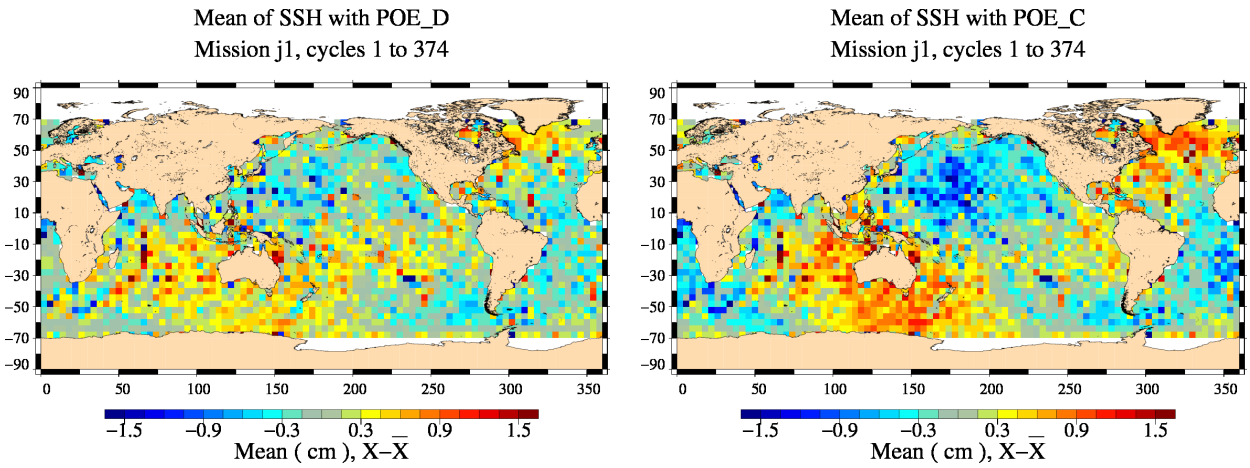

Figure 71: *Map of mean of SSH crossovers differences using POE_D (left) and using POE_C (right). Global mean values are respectively -0.1063m and -0.1632m Data cover Jason-1 cycles 1 to 374.*

Figure 72 shows temporal evolution of mean SSH differences at crossovers. We can observe a 120 days signal (related to β' angle) for the both orbit solutions but the signal is more centered with a higher amplitude for CNES POE_D orbit. Furthermore, CNES POE_C orbit solution shows strong ascending/descending geographically correlated SSH differences (see figure 71). So the temporal and spatial differences of mean SSH at crossovers observed indicates an improvement of the tested orbit versus POE_C.

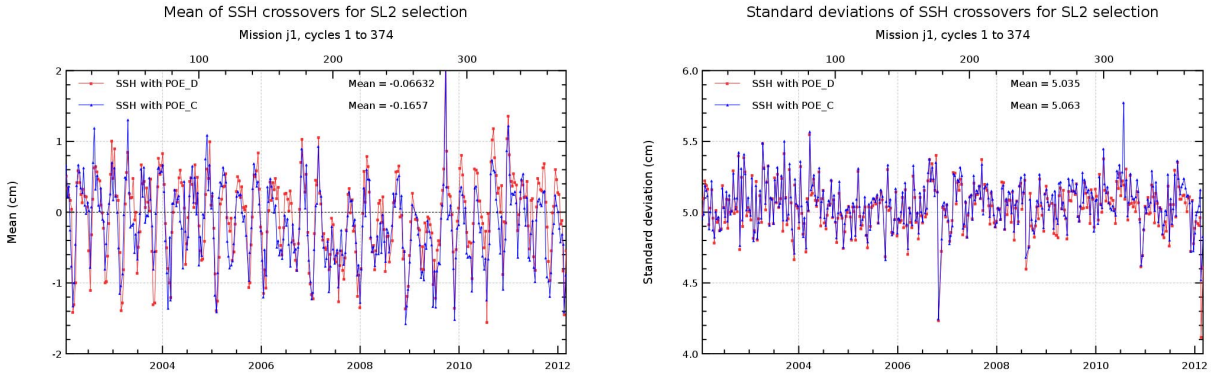

Figure 72: *Cyclic monitoring of mean (left) and standard deviation (right) SSH differences at crossovers using selection with |Lat| < 50, Bathy < -1000m and low variability, for respectively POE_D and POE_C. Data cover Jason-1 cycles 1 to 374.*

An other diagnosis (figure 73) show the differences of SSH variances (using POE_D orbit - using POE_C orbit) at crossovers. Negative values indicate a variance reduction (hence an improvement) of the test orbit (POE_D in this case) in comparison to the reference orbit (POE_C in this case). So POE_D orbit solution shows an improvement at crossovers versus the POE_C orbit, but it is quite small.

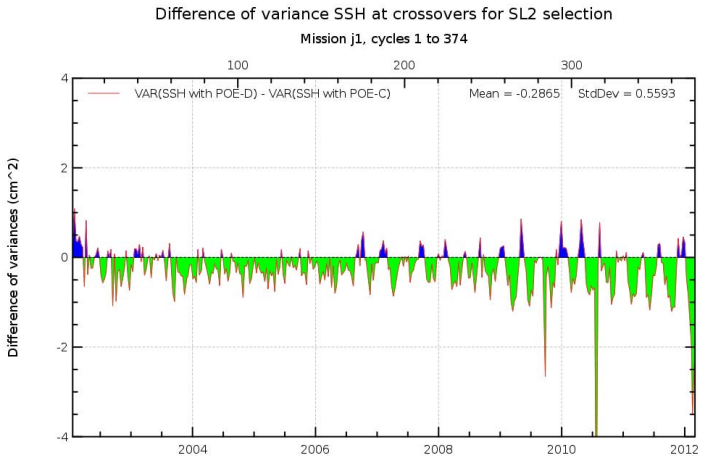

Figure 73: *Cyclic monitoring of differences of SSH variances at crossovers using |Lat| < 50, Bathy < -1000m and low variability: (variance(SSH using POE_D) - variance(SSH using POE_C)). Data cover Jason-1 cycles 1 to 374.*

SSH differences at EN/J1 crossovers showed East/West bias using POE-C orbit solution. Geographically correlated patterns are reduced using POE-D orbit solution for Envisat, and further with POE-D on both missions.

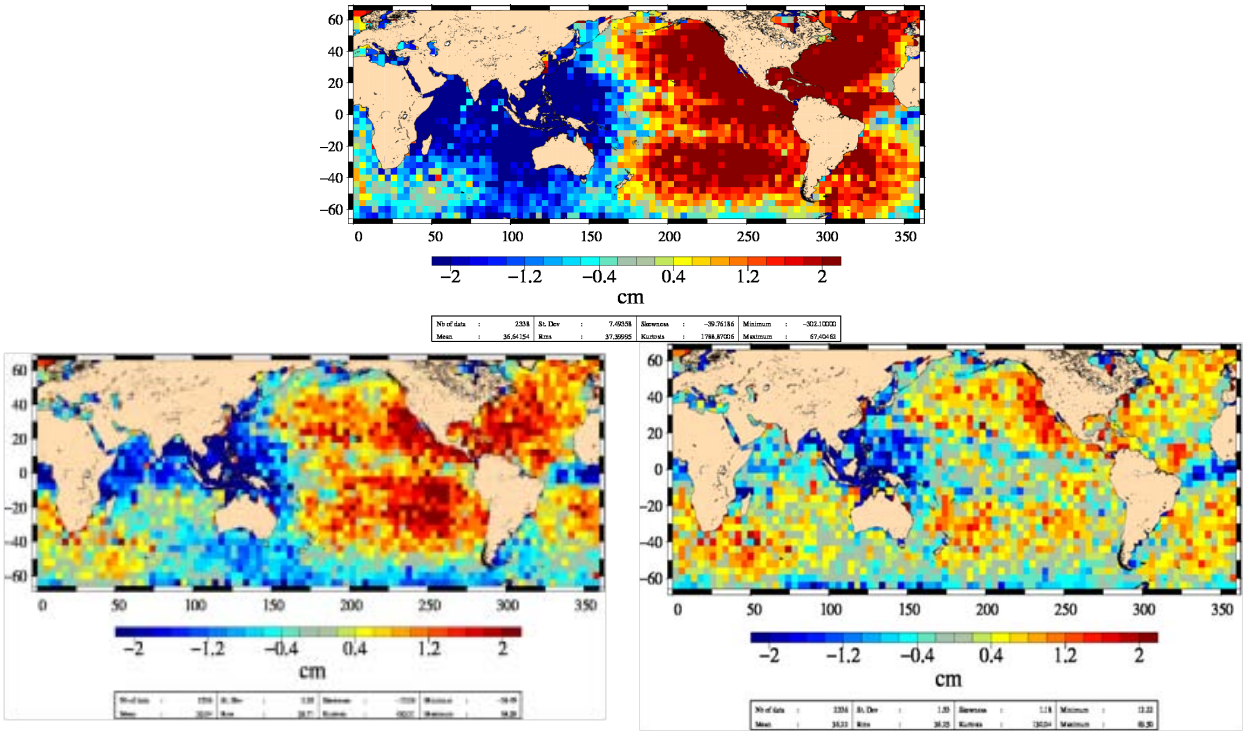

Figure 74: *Map of mean of SSH EN/J1 crossovers differences over year 2011.* ***Top:*** *using POE-C orbit for both missions* ***Bottom:*** *using POE-D orbit for Envisat in both cases, and POE-C (left) or POE-D (right) orbit for Jason-1.*

8.2.2. Global Mean Sea Level

Concerning global Mean Sea Level slope (see figure 75), use of CNES POE_D orbit versus use of CNES POE_C orbit has a small impact on the slope: lower than 0.1 mm/year. When seperating ascending and descending passes, MSL slopes differences between even and odd passes are more homogeneous for POE_C orbit than POE_D orbit as shown values in table 9.

MSL	MSL slope using POE_D	MSL slope using POE_C
global	2.34 mm/yr	2.27 mm/yr
even passes	2.40 mm/yr	2.21 mm/yr
odd passes	2.20 mm/yr	2.24 mm/yr
difference between odd and even passes	0.20 mm/yr	-0.03 mm/yr

Table 9: *M*ean sea level slopes

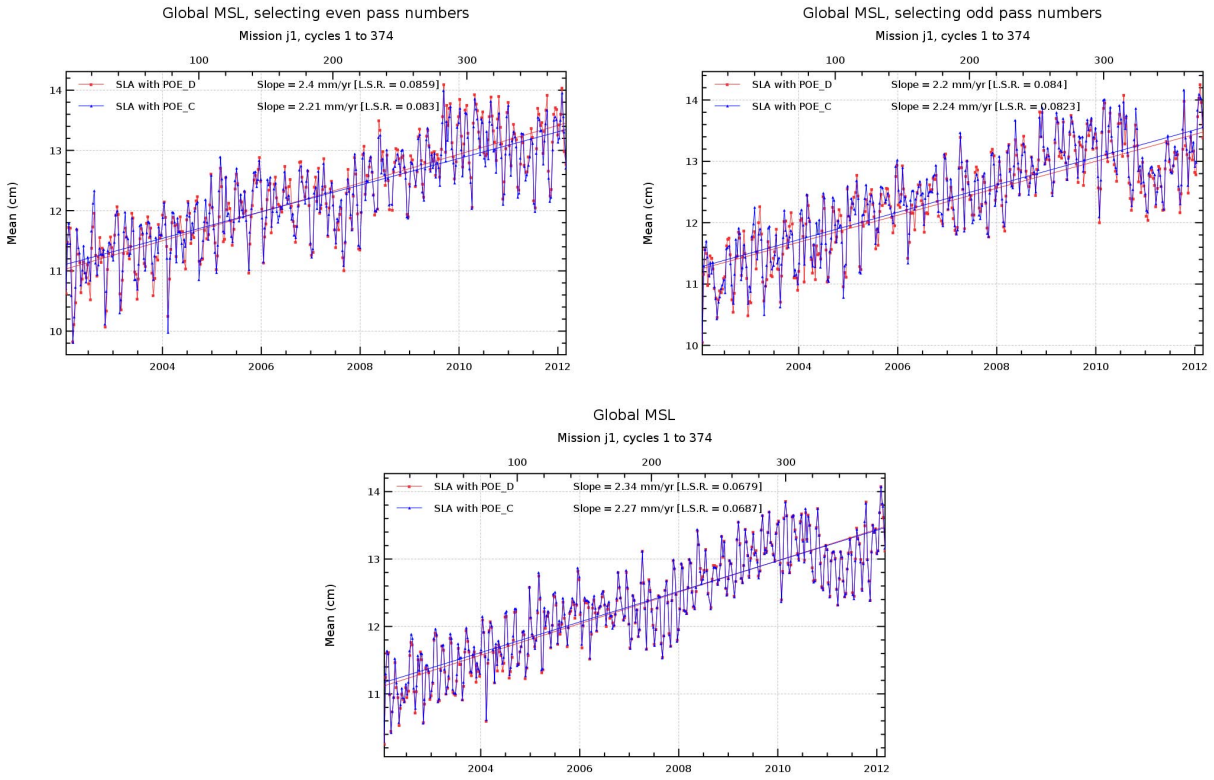

Figure 75: *Cyclic monitoring of global mean sea level separating even and odd passes (top) and all passes mixed-up (bottom) using respectively POE_D and POE_C. Data cover Jason-1 cycles 1 to 374.*

The impact of the new GDR-D orbit on Jason-1 altimeter data and tide gauges comparisons is presented in [14]. Regarding the trend differences, results are coherent between both standards, the consistency of Jason-1 GDR-D orbit is slightly improved with regard to the previous GDR-C (see figure 76).

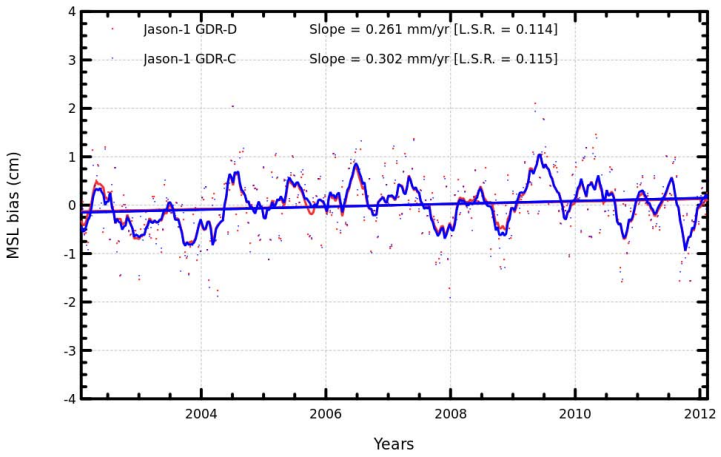

Figure 76: *Monitoring of SSH trend differences between in-situ TG and altimeter data computed with CNES-POE GDR-C and GDR-D orbits for Jason-1.*

The impact of the new GDR-D orbit on Jason-1 altimeter data and in-situ Argo T/S profiles comparisons is detailed in [16]. The altimeter MSL drift refered to the independant in-situ measurements is increased by 0.2mm/yr with the use of the preliminary GDR-D orbit solution instead of the GDR-C orbit solution. Concerning the East/West bias (figure 74), figure 77 first shows that the comparison of altimetry (GDR-C, left graphs) with Argo + GRACE data indicates that the hemispheric MSL trend difference is more attributed to the Envisat mission. This is indeed associated with the GDR-C orbit solution since Envisat has a lower altitude and is more sensitive to gravity effects. Secondly, the use of the GDR-D orbit solution which includes a time-varying gravity effect (figure 77, right graphs) strongly reduces the hemispheric bias observed with Envisat and it makes both missions more homogeneous. However, a residual hemispheric bias is detected for Jason-1 (1.3 mm/yr - top right- whereas it was -0.1 mm/yr with the POE-C orbit -top left-). This could be related with a residual error of the method concerning the regional estimation of the MSL trends but also with a residual error in the orbit determination (see [16]).

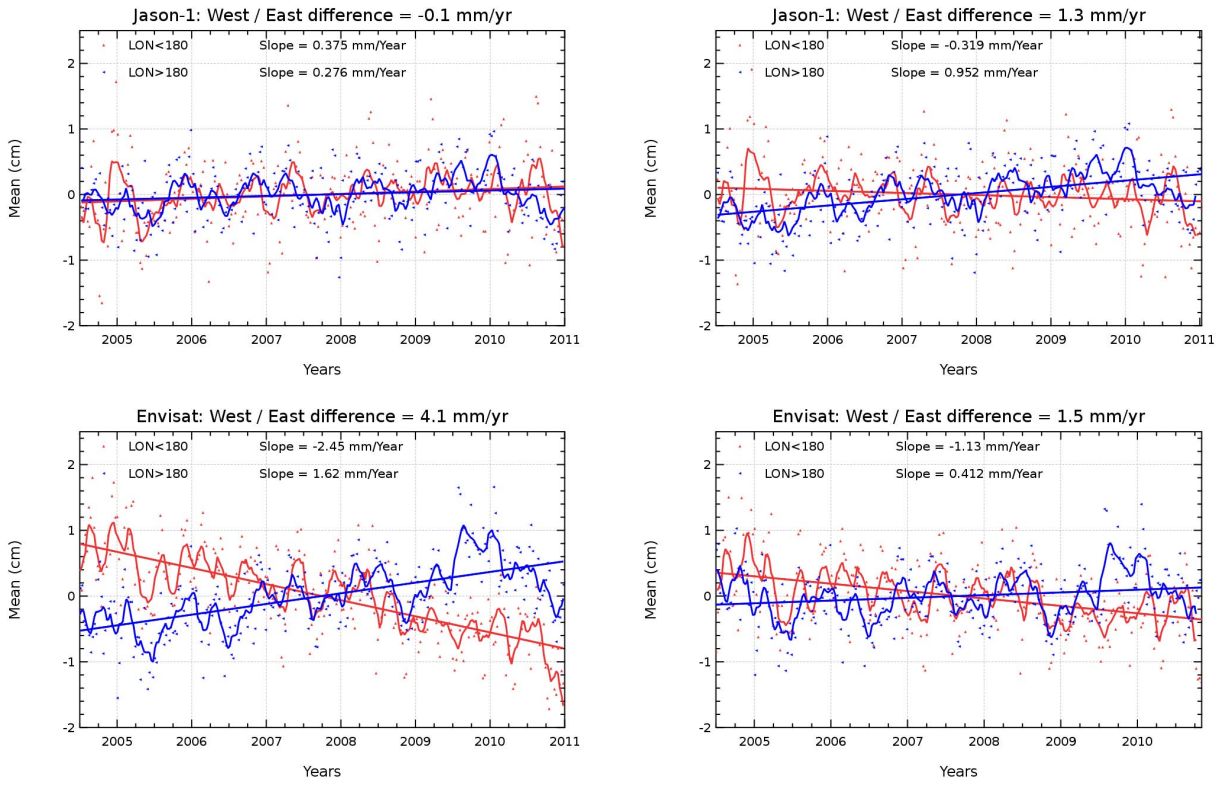

Figure 77: *SSH difference (cm) between altimeter data and Argo + GRACE measurements for Envisat (bottom) and Jason-1 (top) computed with CNES POE-C orbit (left) and POE-D orbit (right), separating east ($\leq 180^{\circ}$) and west ($\geq 180^{\circ}$) longitudes. Corresponding annual and semi-annual signals are removed. Trends of raw data are indicated and the 2-month filtered signal is added.*

8.3. Towards a new Jason-1 orbit solution for climate studies

The consistency between Jason-1 and Jason-2 during the tamdem formation phase is very good. Using CNES POE_D solutions for the orbit, a fine North/South signature is visible yet, with impact on the long term trend estimation at regional scales when connecting the two consecutive missions (it can be corrected empirically afterwards but datasets without this regional differences are preferable for climate studies). Those fine North/South descrepencies are observed using CNES GDR-D solutions (top left of figure 78) but not with GSFC_0905 solutions neither with GSFC_1204 solutions (bottom right of figure 78, only GSFC_0905 solutions results are shown).
Investigations proved it was not due to the lack of GPS on Jason-1 (from mid-2006 onwards) as they are still observable when using Doris/Laser orbits for both Jason-1 and Jason-2 (bottom left of figure 78).
Doris instrument onboard Jason-1 (unlike Jason-2) is sensitive to the South Atlantic Anomaly (SAA). A solution for this problem consists in down-weighting of the Doris station in the SAA zone in addition to the use of an corrective model of the anomalous behavior of the DORIS ultra-stable-oscillator (USO) related to the SAA, see [44]. This solution reduces efficiently the variance at crossovers. In order to explain these North/South differences between Jason-1 and Jason-2, tests have been done concerning the weighting strategy of Doris stations in South Atlantic Anomaly region.

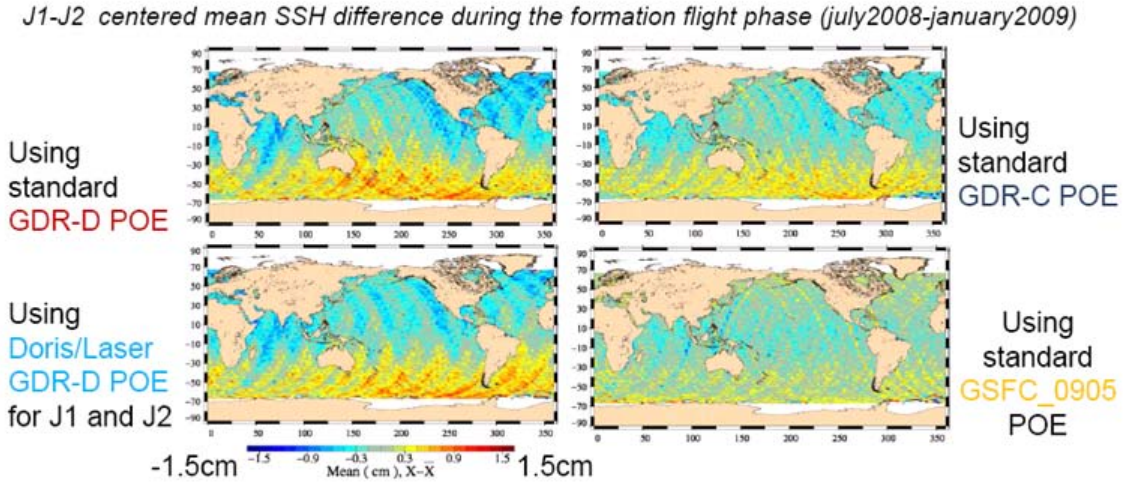

Figure 78: *Jason-1 minus Jason-2 centered mean of SSH difference at crossovers during the formation flight phase using different orbit solutions*

The tests were performed on pure Doris solutions to study only the impact of the weighting strategy of SAA stations for Jason-1. The impact of the use of the down-weighting of SAA stations is studied on Jason-1 data from cycles 1 to 516, and via a comparison with the Jason-2 data (no down-weighting of the SAA Doris stations).

In this section, $ORBITJ1_{PONDJA1}$ refers to a Doris solution where down-weighting of the SAA stations is applied, and $ORBITJ1_{PONDJA2}$ refers to a Doris solution using the same weighting as for the Jason-2 orbit (no down-weighting).

8.3.1. Comparison between Jason-1 Doris only orbit solutions with and without down-weighting of SAA stations

The total effect of the differences between CNES POE-D solution and Doris only without down-weighting of the SAA stations over Jason-1 cycles 240 to 259 (bottom of figure 79) is detailed with:

- the differences between CNES POE-D solution and Doris Only solution with down-weighting of the SAA stations (top left of figure 79)
- and the impact of the down-weighting on a Doris only solution (top right of figure 79)

The North / South bias is mainly due to differences in SAA modeling (top right of the figure), and not to the reduction to a Doris only solution (top left of the figure).

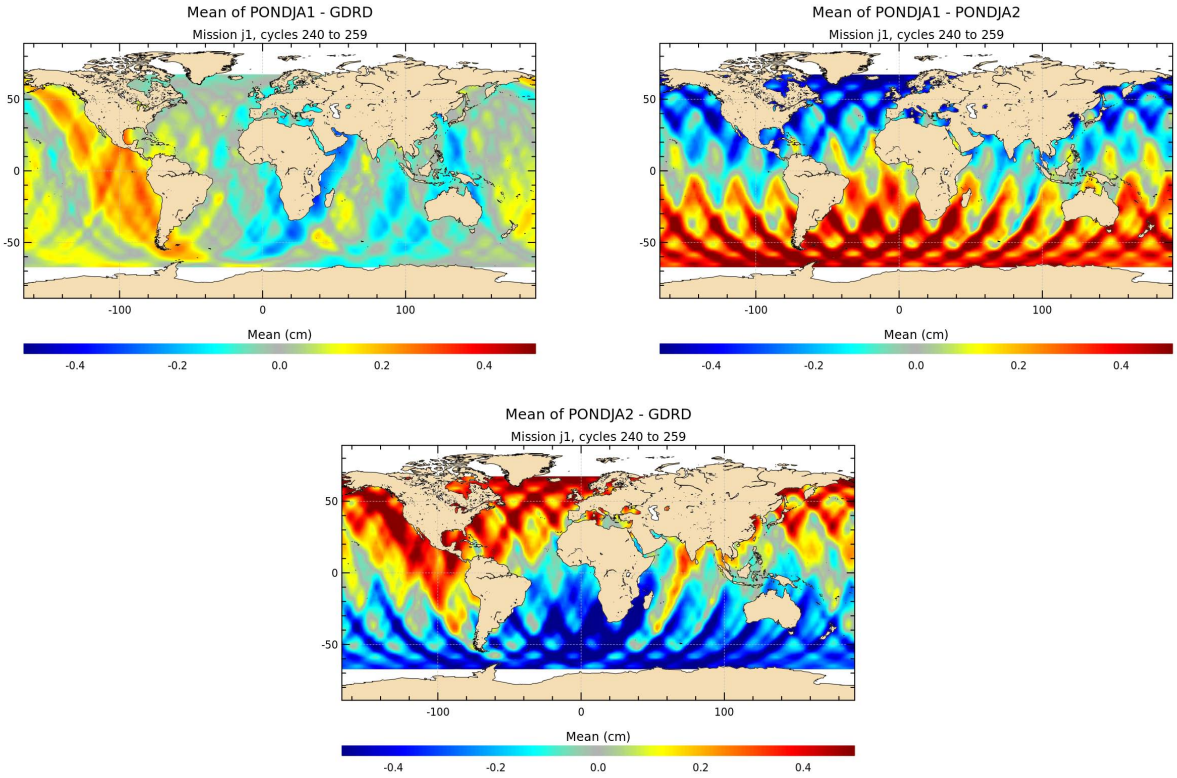

Figure 79: ***Top left:*** *Comparison between tritechnique / Doris only.* ***Top right:*** *down-weighting effect.* ***Bottom:*** *total effect*

8.3.2. Comparison with Jason-2

8.3.2.1. During the flight formation phase

Jason-1 minus Jason-2 SLA differences during the formation flight phase (see on figure 80) are studied in order to evaluate the North/South effect taking into account an orbit or another. Here, in both cases a Doris only "like GdrD" solution is used for Jason-2 (no down-weighting of the SAA stations), the difference in the two maps is that the Jason-1 solution includes down-weighting of

the SAA stations on the left whereas the there is NO down-weighting of the SAA stations on the right. As a result the North/South effect disappears, which can so be explained by the particular down-weighting applied on Jason-1.

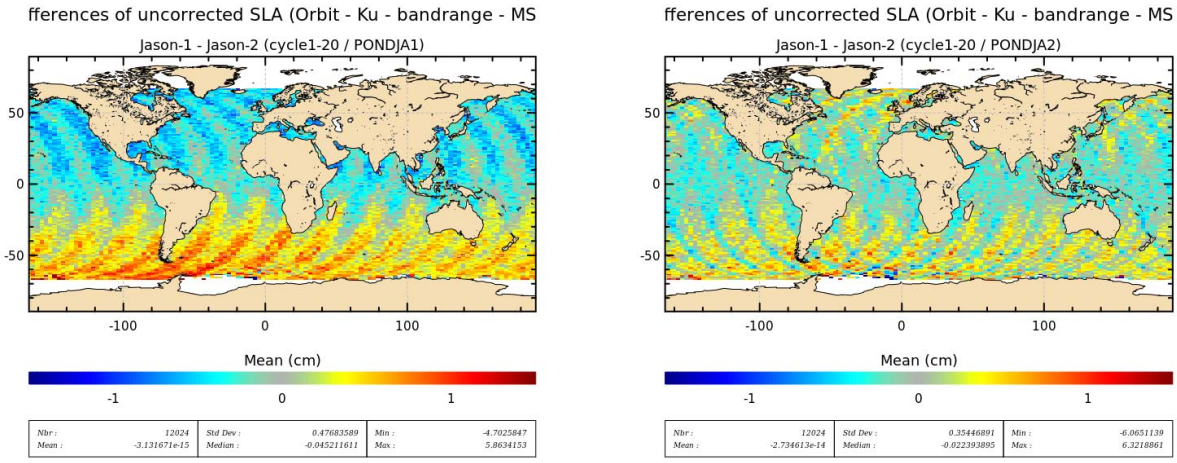

Figure 80: *Jason-1 minus Jason-2 centered mean of uncorrected SLA difference during the formation flight phase (between July 2008 and January 2009, Jason-2 cycles 1 to 20 and Jason-1 cycles 239 to 259)* ***Left:*** *with down-weighting* ***Right:*** *without down-weighting*

8.3.2.2. Outside the flight formation phase

Outside of the flight formation phase, direct comparisons between Jason-1 and Jason-2 (measurement by measurement) are no longer possible, but maps of SSH differences at JA1/JA2 crossover points can be computed. As the satellites no longer fly over the same place at only 55seconds interval, the SSH has to be corrected for the geophysical corrections (tides, troposphere, ...). Therefore the difference maps between Jason-1 and Jason-2 at crossovers may not only show differences related to orbit computation, but also due to the geophysical corrections. Therefore a particular attention has been payed, in order to use the same corrections (tides, SSB 2012, model wet troposphere) for Jason-1 and Jason-2.
The Jason-1 minus Jason-2 SSH differences at crossovers are computed per year (2008 to 2012) and shown on figures 81 to 85. Three combinations of orbit solutions are used:

- top left: POE-D for JA1 and JA2
- top right: Doris only orbits with down-weighting of SAA Doris stations for Jason-1, and without down-weighting for Jason-2
- bottom: Doris only orbits without down-weighting of SAA Doris stations for both Jason-1 and Jason-2

The top left map of figure 81 showing the JA1 - JA2 crossover differences for 2008 displays the same North/South differences (tough a bit noisier) as the direct orbit minus range minus MSS differences between Jason-1 and Jason-2 computed during the flight formation phase (on top left of figure 80). This shows that Jason-1 minus Jason-2 SSH crossover maps are a useful and valid tool to observe regional biaises related to orbit solutions between the two missions.
The top left figures (using POE-D for both missions) show in addition to the North / South bias

a superposed (kind of sinusoidal pattern). This is related to the fact that Jason-2 POE-D uses in addition to Doris and Laser measuremetns also GPS data, whereas Jason-1 POE-D, since mid-2006) no longer has GPS data. When using doris only orbits (with down-weighting for Jason-1) at crossovers, the sinusoidal signature has disapeared and only the North / South difference remains. Nevertheless it is more or less strong in function of the year.
Using Doris only orbits without down-weighting of SAA Doris stations for both missions (bottom part of the figures) shows that the North / South bias disappears, or is at least reduced (in case of year 2011).

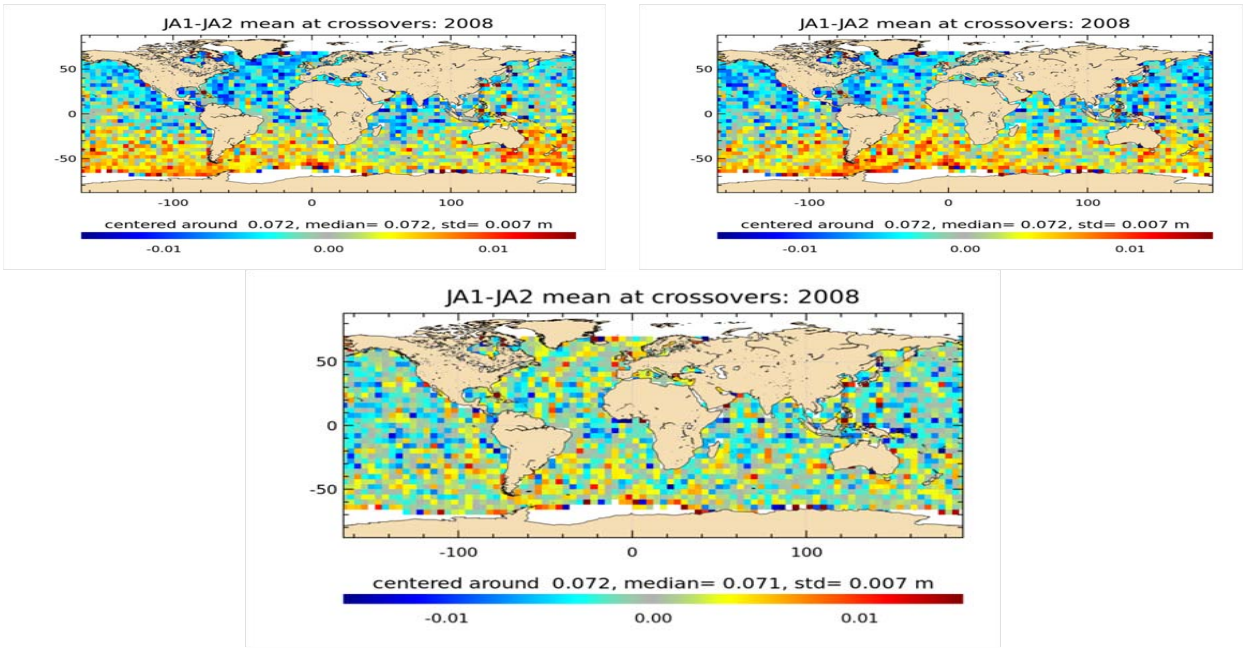

Figure 81: *Jason-1 minus Jason-2 centered mean of SSH difference at crossovers over year 2008, from july onwards (using Model Wet Troposphere, Got4.8 ocean tide, SSB2012).* ***Left:*** *POE-D orbit* ***Right:*** *Doris Only with down-weighting for Jason-1 orbit* ***Bottom:*** *Doris Only without down-weighting for Jason-1 orbit*

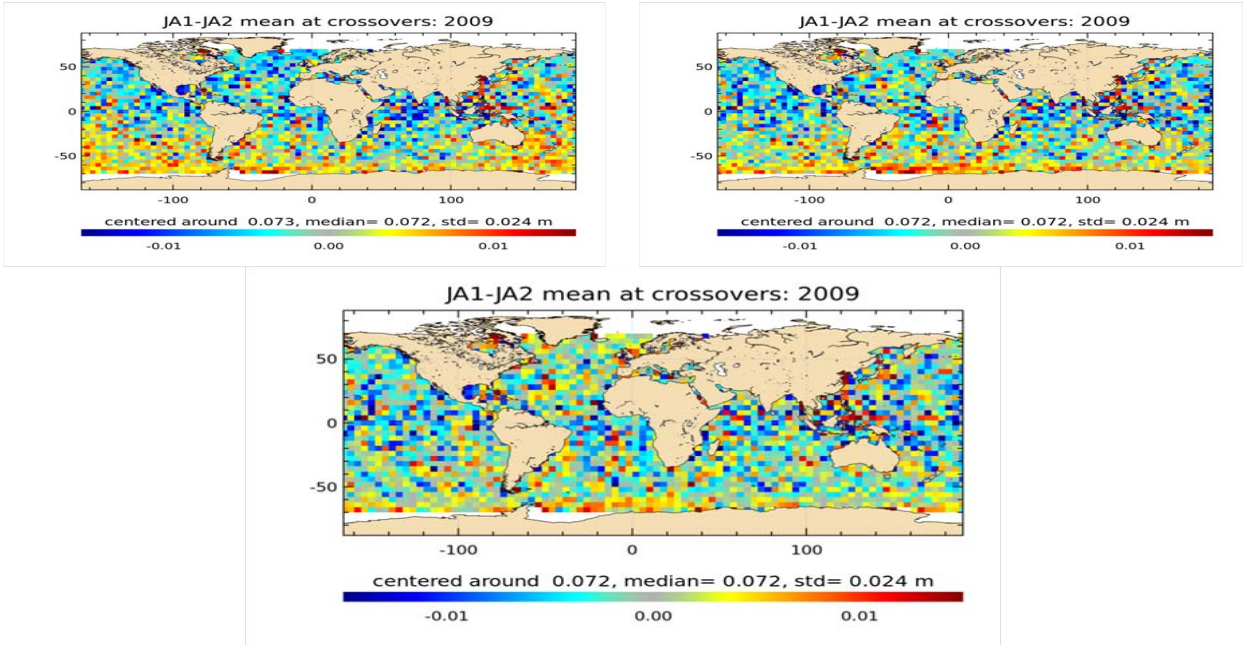

Figure 82: *Jason-1 minus Jason-2 centered mean of SSH difference at crossovers over year 2009 (using Model Wet Troposphere, Got4.8 ocean tide, SSB2012).* ***Left:*** *POE-D orbit* ***Right:*** *Doris Only with down-weighting for Jason-1 orbit* ***Bottom:*** *Doris Only without down-weighting for Jason-1 orbit*

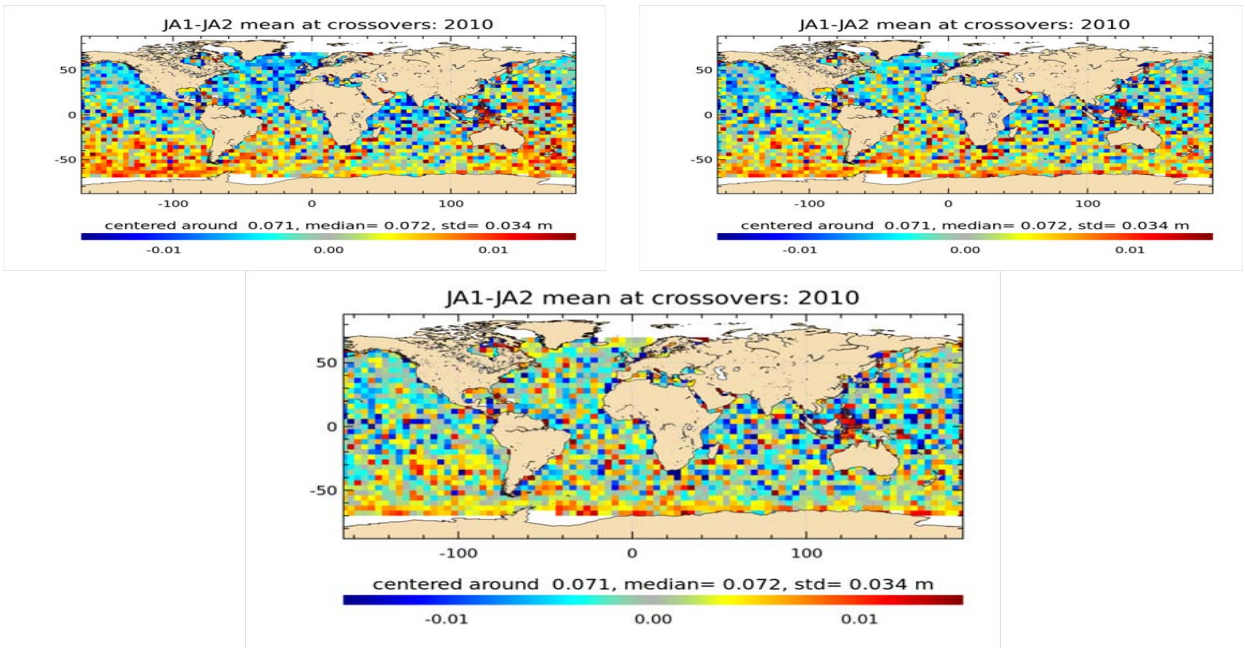

Figure 83: *Jason-1 minus Jason-2 centered mean of SSH difference at crossovers over year 2010 (using Model Wet Troposphere, Got4.8 ocean tide, SSB2012).* ***Left:*** *POE-D orbit* ***Right:*** *Doris Only with down-weighting for Jason-1 orbit* ***Bottom:*** *Doris Only without down-weighting for Jason-1 orbit*

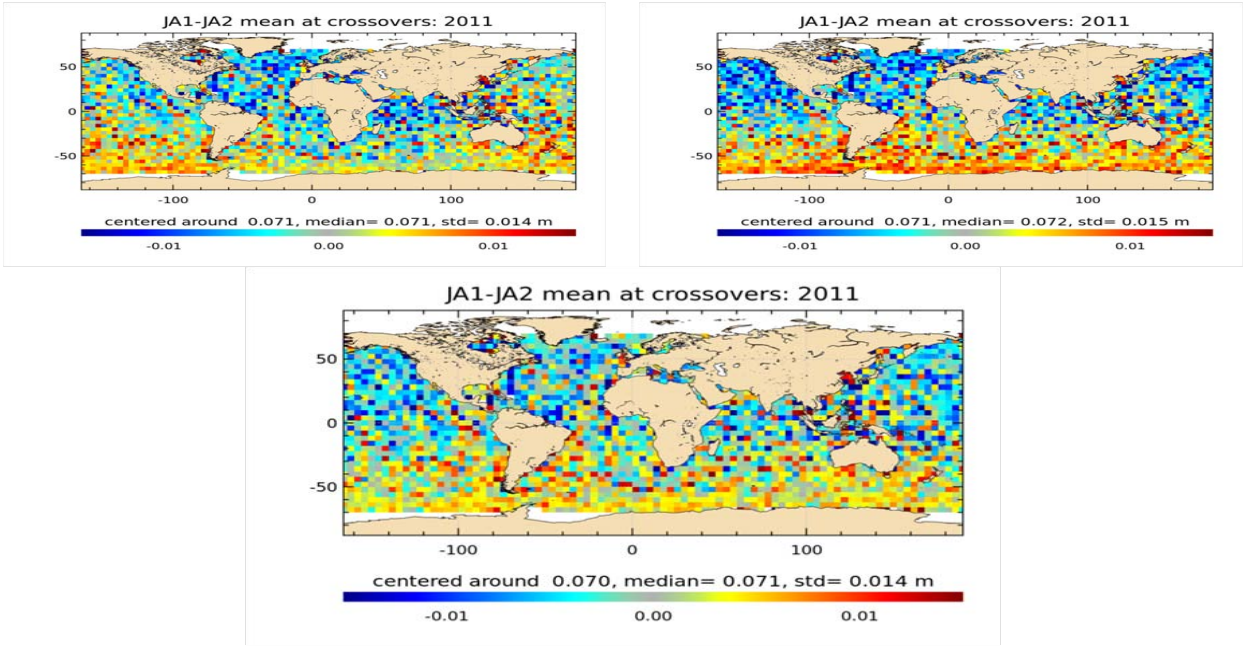

Figure 84: *Jason-1 minus Jason-2 centered mean of SSH difference at crossovers over year 2011 (using Model Wet Troposphere, Got4.8 ocean tide, SSB2012).* ***Left:*** *POE-D orbit* ***Right:*** *Doris Only with down-weighting for Jason-1 orbit* ***Bottom:*** *Doris Only without down-weighting for Jason-1 orbit*

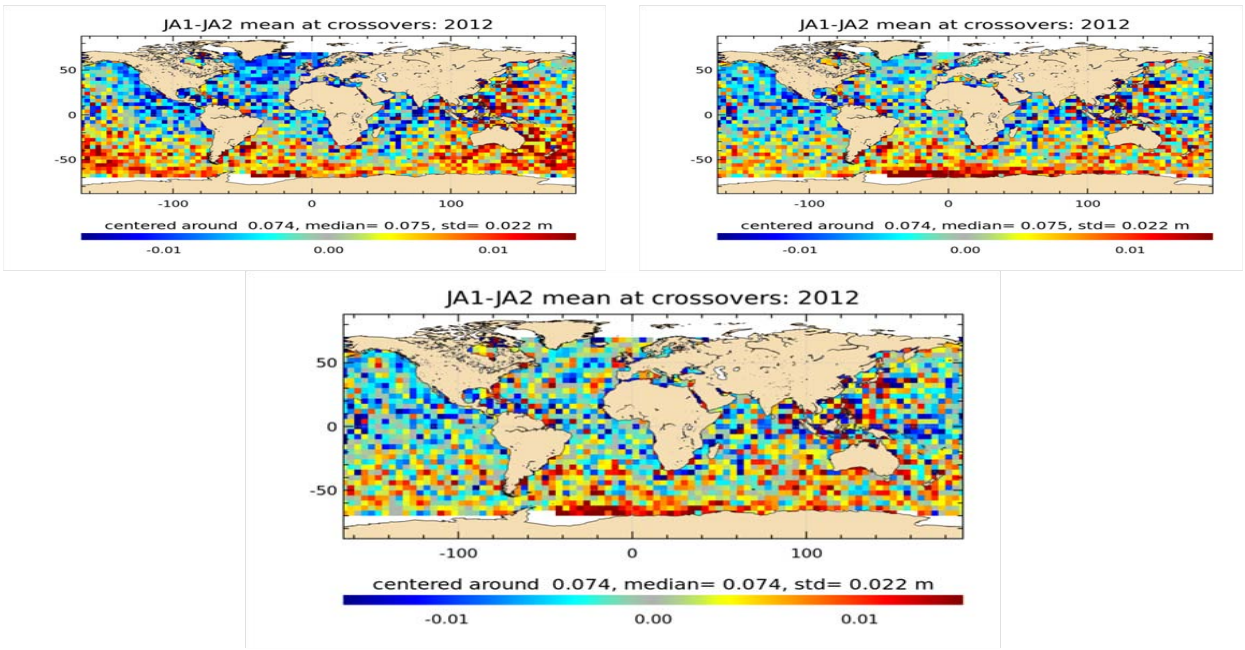

Figure 85: *Jason-1 minus Jason-2 centered mean of SSH difference at crossovers over year 2012 (using Model Wet Troposphere, Got4.8 ocean tide, SSB2012).* ***Left:*** *POE-D orbit* ***Right:*** *Doris Only with down-weighting for Jason-1 orbit* ***Bottom:*** *Doris Only without down-weighting for Jason-1 orbit*

Finally, Jason-2 and Jason-1 GMSL are computed on one hand for the northern hemisphere and on the other hand for the southern hemisphere using each orbit solution, then differences between the two missions MSL are done, and trends of these differences are calculated as an indicator of long term consistency between Jason-1 and Jason-2 GMSL (see figure 86). The difference between the north trend and the south trend is slightly lower using both solutions without down-weighting of the SAA stations (1.39mm/yr versus 1.26mm/yr). The bias between northern and southern MSL is lower in case of homogeneous down-weighting (without downweighting for Jason-1, right part of the figure), but a difference is still noticeable for the second part of year 2011 (which is coherent with the previous result about SSH crossovers).

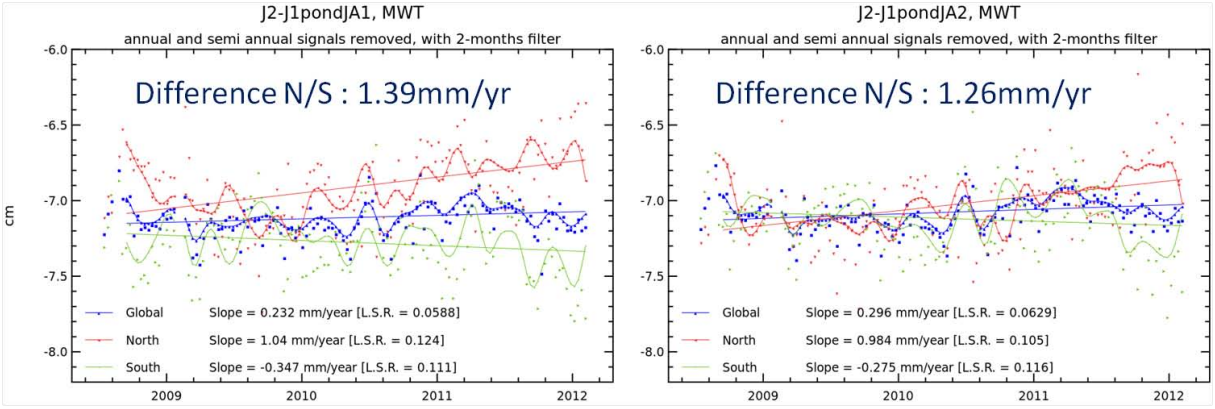

Figure 86: *Comparison between Jason-1 GMSL and MSL separating northern and southern hemisphere* ***Left:*** *with down-weighting of the SAA stations.* ***Right:*** *without down-weighting of the SAA stations.*

8.3.3. Impact on Jason-1 mono-mission performances

8.3.3.1. Mesoscale

The down-weighting of the SAA stations was introduced to improve the Jason-1 mesocale performance. Computing and comparing the SSH at crossover variance using one solution and the other allows to evaluate the solutions at time scales lower than 10 days. The figure 87 shows the map of variance difference of Sea Surface Height at crossovers between **Doris only orbit computed as Jason-2 mission (without down-weighting of SAA stations)** and **Doris only orbit with down-weighting of SAA stations**.
Over the whole mission, Jason-1 mono-mission performance at mesoscale is better using a solution that takes into account the down-weighting than without. The impact of the down-weighting is not significant before 2004 and the switch from the redundant to the nominal DORIS instrument in June 2004 (right of figure 87), but it is growing with time.
Note that at mesoscale, CNES POE-D solution (multitechnique) is better than Doris only solution.

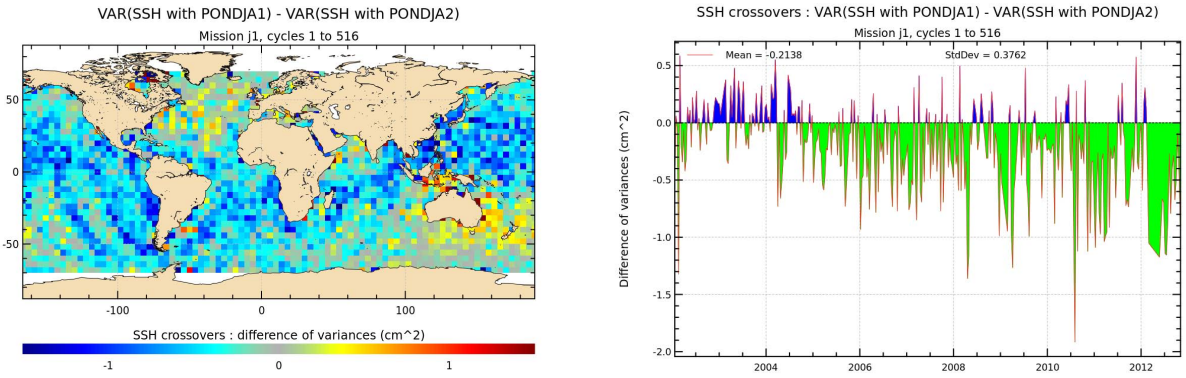

Figure 87: *Variance differences of Sea Surface Height at crossovers. Comparison between Doris only orbit with and without down-weighting of the SAA stations.* ***Left:*** *Map of these differences.* ***Right:*** *Temporal evolution of these differences.*

8.3.3.2. Global Mean Sea Level

The impact of the down-weighting on inter annual signals as well as on the global mean sea level trend is very low (see figure 88).

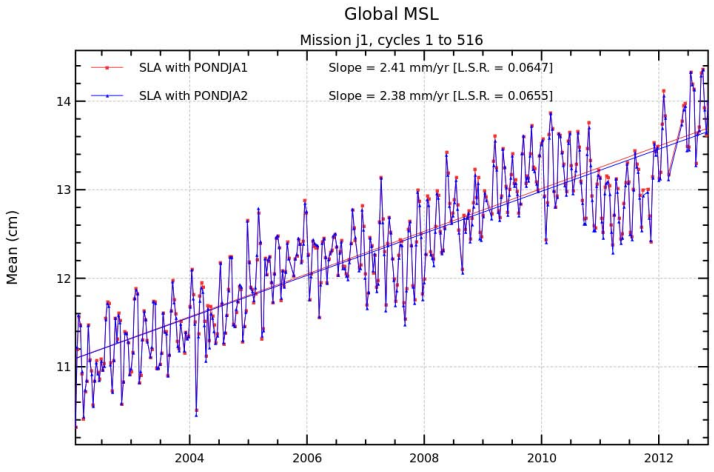

Figure 88: *Jason-1 Global Mean Sea Level difference using two orbit solutions with or without the down-weighting of the SAA stations.*

8.3.3.3. Regional Mean Sea Level

Figure 89 shows the map of sea level anomaly difference of trends between Jason-1 with and without down-weighting of SAA stations. The North/South bias between solutions with or without down-weighting of SAA Doris stations varies locally (+/- 1mm/yr) in time (over the whole Jason-1 time series).

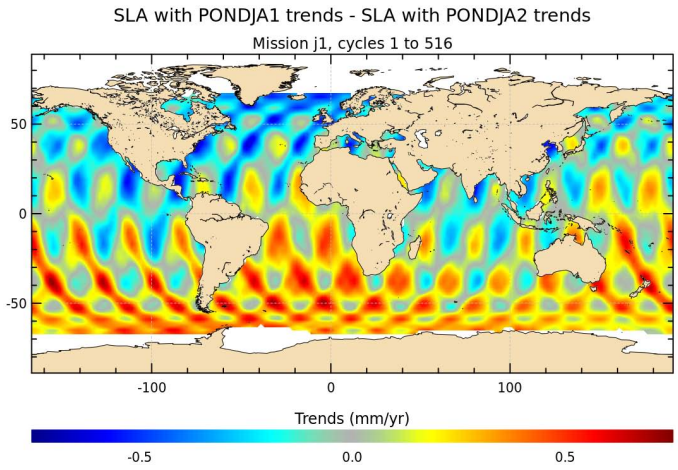

Figure 89: *Sea Level Anomaly difference between Jason-1 with and without down-weighting of SAA stations*

Concerning the north/south differences, the MSL trend differences between south and north hemispheres have been calculated from graphics 90. Hemispheric MSL trend differences between South and North hemispheres for the two orbit solutions are:

- Jason-1 Doris without down-weighting: $\Delta = 0.54 mm/yr$ (see top of figure90)
- Jason-1 Doris with down-weighting: $\Delta = 0.80 mm/yr$ (see top of figure90)

It leads to the result that Jason-1 Doris orbit with down-weighting of SAA stations is less homogeneous than Jason-1 Doris without down-weighting by approximately 0.26mm/yr, which represents a low impact. On the bottom part of figure 90 showing the difference of SLA computing with one solution or the other, for both northern and southern hemispheres, the impact of the SAA down-weighting is not important before the switch of the DORIS instrument in June 2004. There is a stabilisation of the parameters of the SAA model in february 2009, (indeed the drift between the two curves seem to become less important). Note that the SAA model might be less good since the move to geodetic orbit in May 2012.

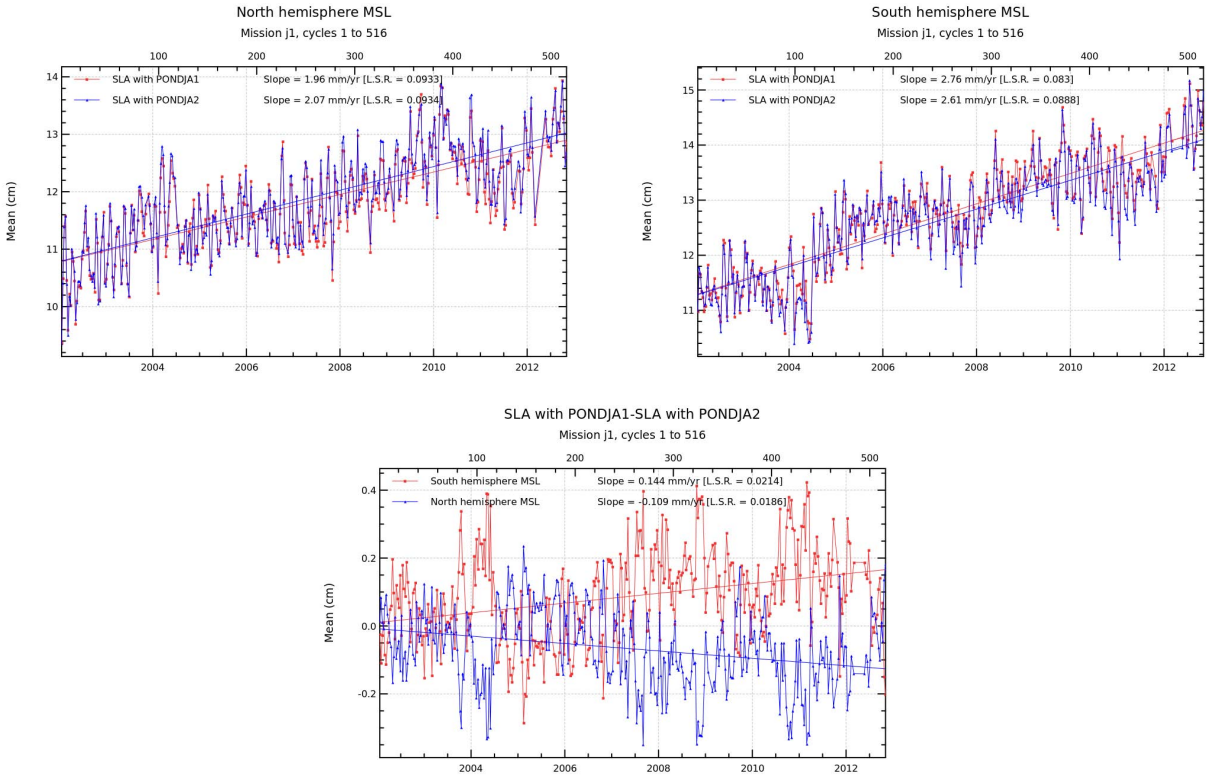

Figure 90: *GMSL on Jason-1 mission from cycle 1 to 516 for North or South hemisphere.* ***Left:*** *North hemisphere* ***Right:*** *South hemisphere* ***Bottom:*** *Differences "with down-weighting" minus "without down-weighting" on each hemisphere.*

To determine if the trend is more relevant with one solution or the other, a comparison of trends (above 20°N and below 20°S) with an external data source can also be used (Argo Temperature Salinity Profiles). The difference between North and South results are lower than the error of the methods, so that it is not possible to determine with this method which down-weighting solution is better compared to external T/S profiles.

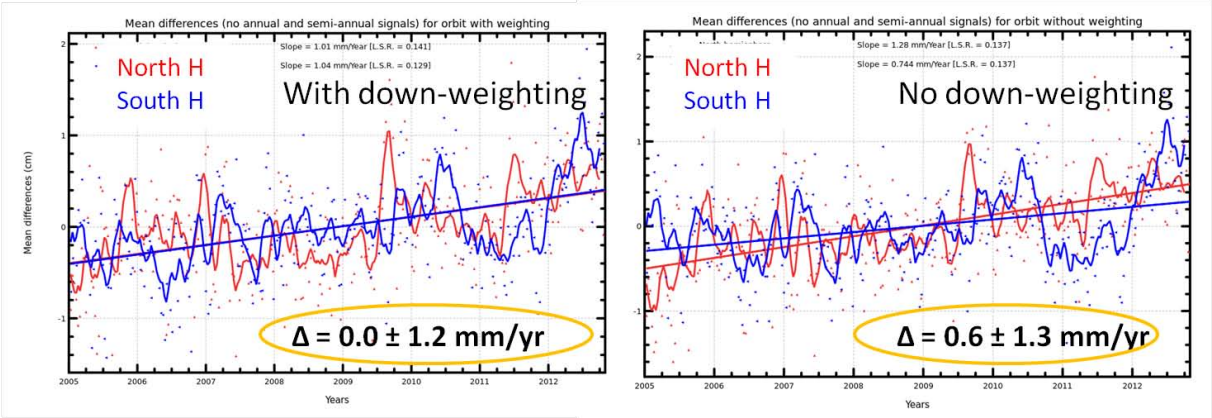

Figure 91: *Comparison between Jason-1 altimetry and T/S profiles separating North/South hemisphere (for $|lat| > 20^{\circ}$) **Left:** with down-weighting of the SAA stations. **Right:** without down-weighting of the SAA stations.*

8.3.4. Conclusion

As Jason-1 (unlike Jason-2) is sensitive to the South Atlantic Anomaly, the solution used consists in down-weighting of the Doris station in the SAA zone that reduces efficiently the variance at crossovers, in addition to the use of a corrective model of the anomalous behavior of the DORIS ultra-stable-oscillator (USO) related to the SAA (see [44]). Today, a drawback of this evolution seems to appear with an impact on the long term trend estimation at regional scales when connecting two consecutive missions: a North/South difference between Jason-1 and Jason-2 has to be taken into account for regional trend estimation of multimission dataset. It can be corrected empirically afterwards but datasets without this regional differences are preferable for climate studies. This study has shown that removing the down-weighting of the Doris stations in the South Atlantic Anomaly for Jason-1 reduces efficiently the small North/South bias between Jason-1 and Jason-2 (when unsing Doris only orbits) both during the flight formation phase and afterwards. This would much more increase the consistency between Jason-1 and Jason-2 for climatological studies than the constant bias map (computed over the flight formation phase) currently used. Regional sea level trends (separating North and South hemisphere) between Jason-1 and Jason2 are much more consistent when not down-weighting SAA stations for Jason-1.
Concerning comparison with in-situ data (T/S profiles), taking into account the error of the method, it is currently not possible to determine which weighting strategy is better for Jason-1.
Nevertheless, when Jason-1 Doris SAA stations are no longer down-weighted, the performance at mesoscale (100-days crossovers) is degradated. Further points in this study could be:

- to test an intermediate weighting strategy to find a trade off between Jason-1 performances and consistency between Jason-1 and Jason-2,
- to test a multi-technique solution for Jason-1 (Doris, Laser and GPS when available) without (or with reduced) down-weighting of the SAA stations, in order to assess the performance and the consistency with Jason-2 (Doris/LaserLGPS) of such a modified multi-technique orbit solution.

9. Jason-1 and Jason-2 altimeter validation activities over ocean in the framework of the SALP project

Jason-1 and Jason-2 altimeter validation activities over ocean in the framework of the SALP project were presented at OSTST in October 2013 and the following poster is available at: http://www.aviso.oceanobs.com/fileadmin/documents/OSTST/2013/posters/Philipps_Poster_OSTST13_PerfoJ1J2.pdf

Jason-1 and Jason-2 altimeter validation activities over ocean in the framework of the SALP project

Sabine Philipps (CLS), Michaël Ablain (CLS), Hélène Roinard (CLS), J. Legeais (CLS), Nicolas Picot (CNES)
CLS, Space Oceanography Division, Toulouse, France, (mablain@cls.fr)
CNES, Centre National d'Etudes Spatiales, Toulouse, France

SALP Service Altimetrie & Localisation Precise

Overview

Global data quality assessment of Jason-1 and Jason-2 data are performed by CNES and CLS in the framework of the SALP project since the Jason-1 launch in 2002.
Our purpose is to underline the importance and the complexity of performance missions activities ("Cal/Val") through 3 relevant examples.

Cal/Val objectives are :
- -To check the data availability and validity
- -To analyze the physical content quality of product parameters
- -To estimate the system performances
- -To contribute to a better knowledge of the sea-level physical content
- -To check the system improvement
- -To provide information for users and production centre (My Ocean/DUCAS)

Example 1 : Mono-mission analyses

Check the internal consistency of an altimetric system by analysing the Sea Surface Height (SSH), its parameters and geophysical corrections

TIME

- 2005: detection of an hemispheric north/south bias on mono-mission crossover maps due to a time-tag bias of ~0.28 ms
- 2008: reprocessing of Jason-1 data in GDR-C version including a new parameter to correct empirically this time-tag bias, time-tag bias is also observable on Jason-2 data
- 2010: CNES experts find the explanation for the time-tag bias on Jason
- 2012: Reprocessing of Jason-2 data in GDR-D version: the datation in the GDR product is corrected for this time-tag bias

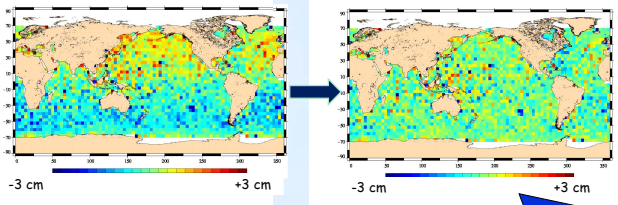

Example 2: Altimeter missions cross comparisons

Evaluate the coherence between two altimeter systems by comparing their SSH and estimate the potential improvement of the computation of a new altimeter standard in the SSH calculation.

TIME

- 2008: detection of an hemispheric north/south bias between JA1 and JA2 during flight formation phase for CNES POE_C - range - MSS. This bias was reduced using GSFC Doris/Laser orbit
- 2012: reprocessing of Jason-2 in GDR-D standard. Outside of formation flight phase geographically correlated bias observable on JA1-JA2 crossover points using : POE-D, GOT4V8, model WTC, SSB from products

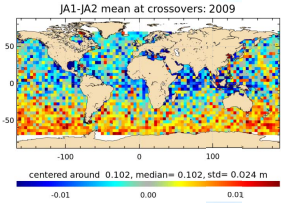

Hemispheric SSH bias: +/- 1 cm

- POE-D, GOT4V8, model WTC, **2012 SSB**: amplitude of geographically correlated bias is reduced (around Indonesia, around 50° S). Small North/South bias remains

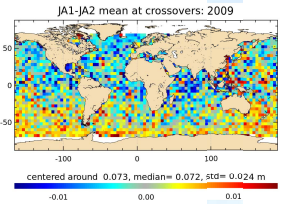

Hemispheric SSH bias: +/- 0.5 cm

- **Doris only orbit (without down-weighting of SAA stations for JA1)**, GOT4V8, model WTC, 2012 SSB

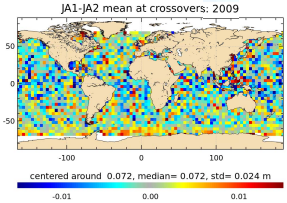

Hemispheric SSH bias: not detectable

Mono-mission analyses
Cross-comparisons
Cal/Val
In-Situ comparisons

Example 3 : In-Situ Comparisons

Compute the SSH differences between altimeter data and in-situ measurements (tide gauges, Argo T/S profiles,...) to detect potential drifts or jumps on the long-term time series

TIME

- 2005: Down-weighting of SAA stations for JA1 orbit solution improves performances at mesoscale, but creates a small North/South bias between JA1 and JA2 data. Compared to insitu data (T/S profile), which weighting solution is more coherent?
- 2013: Down-weighting of SAA stations for JA1 Doris only orbit shows North/South trend differences (between JA1 and T/S) of 0.6 mm/yr
- 2013: Without down-weighting of SAA stations for JA1 Doris only orbit the North/South trend differences (between JA1 and T/S) is reduced to 0.2 mm/yr

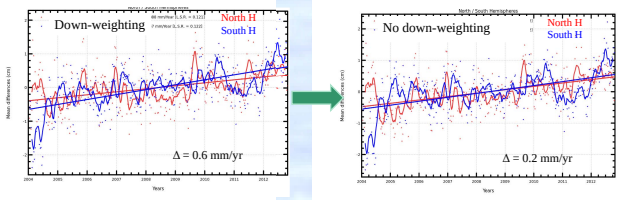

Conclusions

- Jason-1 and Jason-2 altimeter ocean validation activities performed by CNES and CLS have allowed us to strongly contribute to the improvement and the very good data quality
- The 3 examples presented here show that :
  - Altimeter Validation activities over ocean is not a "simple" data quality control but a very complex and exhaustive activity
  - The communication with experts is crucial to understand and correct the anomalies
- The key of success of these validation activities are :
  - Use other altimetry missions in operation
  - Use independent external data sources
  - Agility: iterate quickly : reactivity is essential in crises and commissioning
  - Skill diversity: integrating a wide panel of scientific & technical skills in the validation
  - Skills maintained on time : over all the altimetry period
- For future altimeter missions, 2 main recommendations should be applied for ocean validation activities:

Recommendation 1 "A strong effort is mandatory for the altimeter ocean validation activities"
- To provide for users and productions centers (My Ocean/DUACS, ECMWF) the best altimeter datasets possible for all the applications: oceanic variability, climate studies,...

- **Recommendation 2:** "An integrated team gathering validation & instrumental experts is necessary"
  - To have short feedback loops
  - To correct/validate the anomalies as soon as possible

These recommendations are emphasized with the upcoming launch of Sentinel-3A:
The SARM altimeter on board provides a new potential for high resolution topography but also many questions and challenges for Calibration / Validation activities.

Collecte Localisation Satellites
8-10 rue Hermes
31520 Ramonville Saint-Agne - France

OSTST
8-11 October 2013 | Boulder, US

CNES Centre National d'Etudes Spatiales

10. Conclusion

Jason-1 celebrated its 11th anniversary in December 2012. Since the beginning of the Jason-1 mission and until the end of the T/P mission in October 2005, T/P and Jason-1 overflew the ocean over 2 parallel passes except the 21 first cycles, when they were on the same pass. Thanks to this long flight configuration, performances comparisons between both missions have been performed with success during 4 years, proving that the major objective of the Jason-1 mission to continue the T/P high precision has been reached.

The good quality of Jason-1 data has been shown in this report : the main altimeter parameters are stable and have the same behaviors as T/P ones, the crossover and along-track performances remain very good. Since mid-2008 Jason-1 flew in tandem with Jason-2. After the flight formation phase with Jason-2, Jason-1 was moved in February 2009 on its interleaved orbit. This is the same ground track as Topex/Poseidon during its tandem phase with Jason-1, but there is a time shift of 5 days. Cross-over and along-track performances remain good.

In 2010 and 2011, fuel depletion maneuvers have been performed, in order to reduce the risk of explosion in case of a collision with debris or other satellites.

In 2012, two successive safe hold modes in February and March led to the decision to move Jason-1 on an end-of-life orbit. Since May 2012, Jason-1 has been on a geodetic orbit. This will allow to improve the accuracy and resolution of the marine geoid, as it provides valuable new information about the marine gravity field. Nonetheless, data from the new orbit are still used for oceanographic purposes:
In 2013, Jason-1 entered a new safe hold mode event in March. Jason-1 continued to gather valuable altimeter data for the first half of this year. Comparisons between both Jason missions are consistent, which is a good indicator of the performance of both satellites. Finally, contact was lost with the Jason-1 spacecraft at some point after the last good downlink at 0114 UTC on 21 June 2013. Jason-1 was passivated and decommissioned on 01 July 2013, with the last command sent at 16:37:40 UTC; terminating the Jason-1 mission after 11.5 years of operations. After 53,535 orbits, the Jason-1 science data mission ended on 21 June 2013 – four days after the successful completion of the first full 406-day geodetic cycle on 17 June 2013, at sub-cycle 537. Jason-1 continued to meet all Level 1 mission requirements until its final signal was transmitted.
During 2014, the whole Jason-1 data will be reprocessed using the last improvements and homogeneous solutions.

11. References

References

[1] AVISO and PODAAC User Handbook. IGDR and GDR Jason-1 Products, 2012: Edition 4.2, June. SMM-MU-M5-OP-13184-CN (AVISO), JPL D-21352 (PODAAC). Available at http://www.aviso.oceanobs.com/fileadmin/documents/data/tools/hdbk_j1_gdr.pdf.

[2] E. Bronner and G. Dibarboure, May 24th, 2012: Technical Note about the Jason-1 Geodetic Mission. *SALP-NT-MA-EA-16267-CNv1.0*. Available at: http://www.aviso.oceanobs.com/fileadmin/documents/data/duacs/Technical_Note_J1_Geodetic_Mission.pdf

[3] S. Philipps, G. Valladeau, J.F. Legeais and M. Ablain, 2013: Jason-2 validation and cross calibration activities 2012. SALP-RP-MA-EA-22139-CLS.

[4] H. Roinard, S. Philipps, G. Valladeau, J.F. Legeais and M. Ablain, 2013: Jason-2 validation and cross calibration activities 2013. SALP-RP-MA-EA-22270-CLS.

[5] Ollivier, A., M. Guibbaud, 2012: Envisat RA2/MWR ocean data validation and cross-calibration activities. Yearly report 2012. SALP-RP-MA-EA-22163-CLS

[6] Ollivier, A., M. Guibbaud, 2013: Envisat RA2/MWR ocean data validation and cross-calibration activities. Yearly report 2013.

[7] Ablain, M., H. Roinard, S. Philipps, P. Thibaut, and N. Picot, 2013: Jason-1 GDR Quality Assessment Report. Cycle 525. SALP-RP-P2-EX-21072-CLS525. http://www.aviso.oceanobs.com/fileadmin/documents/calval/validation_report/J1/BilanCalval_J1_Cycle_525.pdf

[8] Queffeulou, P., 2004: Long Term Validation of Wave Height Measurements from Altimeters. *Mar. Geod.***27:295-510.**

[9] Ray, R. D., 2003: Benefits of the joint T/P−Jason mission for improving knowledge of coastal tides. Paper presented at the Jason-1 and TOPEX/Poseidon Science Working Team Meeting, Arles (France), November.

[10] Arnault, S., N. Chouaib, D. Diverres, S. Jaquin, and O. Coze, 2004: Comparison of TOPEX/Poseidon and JASON Altimetry with ARAMIS In Situ Observations in the Tropical Atlantic Ocean. *Mar. Geod.***27 (1-2): 15-30.**

[11] Provost., C. Arnault, N. Chouaib, A. Kartavtseff, L. Bunge, and E. Sultan, 2004: TOPEX/Poseidon and Jason Equatorial Sea Surface Slope Anomaly in the Atlantic in 2002: Comparison with Wind and Current Measurements at 23W. *Mar. Geod.***27(1-2) 31-45.**

[12] Durrant, T.H., J.M. Greenslade, I. Simmonds, 2009: Validation of Jason-1 and Envisat Remotly Sensed Wave Heights. *JAOT.***26, 123-134.**

[13] Abdalla, S., P. A.E.M. Janssen, and J.-R. Bidlot, 2010: Jason-2 OGDR Wind and Wave Products: Monitoring, Validation and Assimilation. *Mar. Geod.*, **33 (S1), 239-255.**

[14] Valladeau, G., 2012: Validation of altimeter data by comparison with tide gauge measurements for TOPEX/Poseidon, Jason-1, Jason-2 and Envisat (Annual report 2012). SALP-NT-MA-EA-22157-CLS, CLS.DOS/NT/12-259.

[15] Valladeau G. and Prandi P., 2013:Validation of altimeter data by comparison with tide gauge measurements for TOPEX/Poseidon, Jason-1, Jason-2 and Envisat (Annual report 2013). [CLS.DOS/NT/13-262].

[16] Legeais, J.F. and Ablain M., 2012: Validation of altimetric data by comparison with in-situ T/S Argo profiles for TOPEX/Poseidon, Jason-1, Envisat and Jason-2 (Annual report 2012). SALP-RP-MA-EA-22176-CLS, CLS.DOS/NT/12-261.

[17] Legeais J.F. and Ablain M., 2013: Validation of altimetric data by comparison with in-situ T/S Argo profiles (Annual Report 2013) [SALP-RP-MA-EA-22281-CLS, CLS.DOS/NT/13-256]

[18] Philipps, S. and M. Ablain,2007 : SALP - BC 60453-6-04: Retraitement des GDRs Jason-1 en version 'B' pour les cycles 022 à 127, SALP/BC60453-6-04. September.

[19] Ablain, M., S. Philipps, J. Dorandeu, P. Thibaut and N. Picot, 2006: SSALTO CALVAL Performance assessment Jason-1 GDR 'B'/ GDR 'A'. Poster presented at OSTST meeting, Venice, Italy, 16-18 march 2006. Available at: http://www.aviso.oceanobs.com/fileadmin/documents/OSTST/2006/ablain1.pdf

[20] Ablain, M., S. Philipps, J. Dorandeu, and N. Picot, 2007: SSALTO CALVAL Performance assessment Jason-1 data. Poster presented at OSTST meeting, Hobart, Australia, 12-15 march 2007. Available at: http://www.aviso.oceanobs.com/fileadmin/documents/OSTST/2007/ablain_J1.pdf

[21] Commien, L., S. Philipps, M. Ablain, and N. Picot, 2008: SSALTO CALVAL Performance assessment Jason-1 GDR-C / GDR-B. Poster presented at OSTST meeting, Nice, France, 09-12 November 2008. Available at: http://www.aviso.oceanobs.com/fileadmin/documents/OSTST/2008/commien.pdf

[22] Valladeau, G., S. Philipps and M. Ablain, 2010: Jason-1 Validation and cross-calibration activities (Annual report 2009). SALP-RP-MA-EA-21795-CLS, CLS.DOS/NT/10-005.

[23] Brown G.S., 1977: The average impulse response of a rough surface and its application, IEEE Transactions on Antenna and Propagation, Vol. AP 25, N1, pp. 67-74, Jan.

[24] Thibaut, P. O.Z. Zanifé, J.P. Dumont, J. Dorandeu, N. Picot, and P. Vincent, 2002: Data editing: The MQE criterion. Paper presented at the Jason-1 and TOPEX/Poseidon Science Working Team Meeting, New-Orleans (USA), 21-23 October.

[25] Amarouche, L., P. Thibaut, O.Z. Zanife, P. Vincent, and N. Steunou. 2004: Improving the Jason-1 Ground Retracking to Better Account or Attitude Effects. *Mar. Geod.***27 (1-2): 171-197.**

[26] Ablain, M., S. Philipps, M. Urvoy, N. Tran, and N. Picot, 2012: Detection of Long-Term Instabilities on Altimeter Backscatter Coefficient Thanks to Wind Speed Data Comparisons from Altimeters and Models (Marine Geodesy Vol. 35, Iss. sup1, 2012)

[27] Ablain, M. and J. Dorandeu, 2005: TOPEX/Poseidon validation activities, 13 years of T/P data (GDR-Ms), Available at: http://www.jason.oceanobs.com/documents/calval/validation_report/tp/annual_report_tp_2005.pdf

[28] Le Traon, P.-Y., J. Stum, J. Dorandeu, P. Gaspar, and P. Vincent, 1994: Global statistical analysis of TOPEX and POSEIDON data. *J. Geophys. Res.,***99, 24619-24631.**

.

[29] Chambers, D., P., J. Ries, T. Urban, and S. Hayes, 2002: Results of global intercomparison between TOPEX and Jason measurements and models. Paper presented at the Jason-1 and TOPEX/Poseidon Science Working Team Meeting, Biarritz (France), 10-12 June.

[30] Obligis, E., L. Eymard, M. Ablain, B. Picard, J.F. Legeais, Y. Faugere and N. Picot, 2010: The wet tropospheric correction for altimetry missions: A mean sea level issue. *Oral presentation at OSTST meeting, Lisbon, Portugal*. Available at http://www.aviso.oceanobs.com/fileadmin/documents/OSTST/2010/oral/19_Tuesday/OBLIGIS.pdf.

[31] Brown, S., S. Desai, W. Lu, and A. Sibthorpe. 2009. Performance Assessment of the Advanced Microwave Radiometer after 1 Year in Orbit. *Oral presentation at OSTST meeting, Seattle, USA*. Available at: http://www.aviso.oceanobs.com/fileadmin/documents/OSTST/2009/oral/Brown.pdf

[32] Legeais, J.F., 2010: On the stability of the altimetric wet tropospheric correction. CLS.DOS/NT/11-033.

[33] Boy, François and Jean-Damien Desjonqueres. 2010: Note technique datation de l'instant de reflexion des échos altimètres pour POSEIDON2 et POSEIDON3 *Reference: TP3-JPOS3-NT-1616-CNES*

[34] Dorandeu.,J., M. Ablain, Y. Faugère, F. Mertz, 2004: Jason-1 global statistical evaluation and performance assessment. Calibration and cross-calibration results. *Mar. Geod.***This issue.**

[35] Hernandez, F. and P. Schaeffer, 2000: Altimetric Mean Sea Surfaces and Gravity Anomaly maps inter-comparisons AVI-NT-011-5242-CLS, 48 pp. CLS Ramonville St Agne.

[36] Ablain, M., S. Philipps, N. Picot, and E. Bronner, 2010: Jason-2 Global Statistical Assessment and Cross-Calibration with Jason-1. *Marine Geodesy*, **33(S1), 162-185**. Available at http://pdfserve.informaworld.com/807580__925506316.pdf

[37] P .Schaeffer, Y. Faugère, JF. Legeais, A. Ollivier, T. Guinle, N. Picot. 2012. The CNES_CLS11 Global Mean Sea Surface computed from 16 years of satellite altimeter data. Special Issue on Jason2 of Marine Geodesy

[38] World Meteorological Organization, 2010: El Nino/ La Nina Update (30 March 2010). Available at http://www.wmo.ch/pages/prog/wcp/wcasp/documents/El_Nino_Mar10_Eng.pdf.

[39] World Meteorological Organization, 2010: El Nino/ La Nina Update (30 October 2010). Available at http://www.wmo.ch/pages/prog/wcp/wcasp/documents/El_Nino_Oct10_Eng.pdf.

[40] World Meteorological Organization, 2011: El Nino/ La Nina Update (25 January 2011). Available at http://www.wmo.ch/pages/prog/wcp/wcasp/documents/El-Nino_Jan11_Eng.pdf.

[41] World Meteorological Organization, 2008: El Nino/ La Nina Update (24 June 2008). Available at http://www.wmo.ch/pages/prog/wcp/wcasp/documents/El_Nino_Jun08_Eng.pdf.

[42] Phaden Mc.J., 2003: Evolution of the 2002-03 El Nino, *UCLA Tropical Meteorology and Climate Newsletter,***No57**. April.

[43] Lemoine, F. G., Zelensky, N.P., Chinn, D.S., Pavlis, D.E., Rowlands, D.D., Beckley, B.D., Luthcke, S.B., Willis, P., Ziebart, M., Sibthorpe, A., Boy, J.P., Luceri, V., Towards development of a consistent orbit series for TOPEX, Jason-1, and Jason-2. *Advances in*

Space Research, Volume 46, Issue 12, 15 December 2010, Pages 1513-1540, **ISSN 0273-1177, 10.1016/j.asr.2010.05.007.** http://www.sciencedirect.com/science/article/pii/S0273117710003224

[44] Lemoine J.M. and H. Capdeville, 2006. A corrective model for Jason-1 DORIS doppler data in relation to the South Atlantic anomaly.*J. Geodesy*, 80:507-523.

[45] Tran, N. , Labroue, S. , Philipps, S. , Bronner, E. and Picot, N., 2010: Overview and Update of the Sea State Bias Corrections for the Jason-2, Jason-1 and TOPEX Missions, *Marine Geodesy*,**33:1, 348 - 362**. Available at http://pdfserve.informaworld.com/804727__925502357.pdf

[46] Y.Faugere, N.Granier, and A.Ollivier, 2007: Envisat validation activities. 2007 yearly report, Available at: http://www.jason.oceanobs.com/documents/calval/validation_report/en/annual_report_en_2007.pdf

[47] Scharroo R., J. L. Lillibridge, and W. H. F. Smith, 2004: Cross-Calibration and Long-term Monitoring of the Microwave Radiometers of ERS, TOPEX, GFO, Jason-1, and Envisat, **Marine Geodesy, 27:279-297**.

[48] Dorandeu, J. and P.Y. Le Traon, 1999: Effects of Global Atmospheric Pressure Variations on Mean Sea Level Changes from TOPEX/Poseidon. *J. Atmos. Technol.,***16, 1279-1283.**

[49] Marshall, J. A., N. P. Zelinsky, S. B. Luthcke, K. E., Rachlin, and R. G. Williamson, 1995: The temporal and spatial characterustics of TOPEX/Poseidon radial orbit error. *J. Geophys. Res.* **100(C2):25331-25352.**

[50] Luthcke. S. B., N. P. Zelinsky, D. D. Rowlands, F. G. Lemoine, and T. A. Williams, 2003: The 1-Centimeter Orbit: jason-1 Precision Orbit Determination Using GPS, SLR, DORIS, and Altimeter Data. *Mar. Geod.***26(3-4): 399-421.**

[51] Valladeau, G., S. Philipps and M. Ablain, 2011: Jason-1 validation and cross calibration activities (Annual report 2010). SALP-RP-MA-EA-21903-CLS, CLS.DOS/NT/10-332.

[52] H. Roinard, G. Valladeau, S. Philipps and M. Ablain, 2012: Jason-1 validation and cross calibration activities (Annual report 2011). SALP-RP-MA-EA-22056-CLS, CLS.DOS/NT/12-017.

[53] H. Roinard, D. Alexandre, G. Valladeau, J.F. Legeais, S. Philipps and M. Ablain, 2013: Jason-1 validation and cross calibration activities (Annual report 2012). SALP-RP-MA-EA-22139-CLS, CLS.DOS/NT/12-221.

[54] Aviso User Handbook: Merged Topex/Poseidon Products (1996). AVI-NT-02-101-CN, edition 3.0. Available at http://www.aviso.oceanobs.com/fileadmin/documents/data/tools/hdbk_tp_gdrm.pdf

[55] Labroue, S., Ph. Gaspar, J. Dorandeu, O.Z. Zanife, 2006: Latest Results on Jason-1 Sea State Bias with the Non-Parametric Technique. *Talk presented at OSTST meeting, Venice, Italy, 16-18 March.*

[56] Ablain, M., S. Philipps, S. Labroue, J. Dorandeu, and N. Picot, 2007: SSALTO CALVAL Consistency assessment between Jason-1 and TOPEX. poster presented at OSTST meeting, Hobart, Australia, 12-15 march 2007. Available at: http://www.aviso.oceanobs.com/fileadmin/documents/OSTST/2007/ablain_J1TP.pdf

[57] Peltier, 2004: Global Glacial Isostasy And The Surface of The Ice-Age Earth: The ICE-5G (VM2) Model and GRACE. *Annual Review of Earth and Planetary Sciences*, May 2004, **Vol. 32, Pages 111-149**, doi: 10.1146/annurev.earth.32.082503.144359

[58] Cerri L., A. Couhert, S. Houry and F. Mercier, 2011: Improving the long-term stability of the GDR orbit solutions. OSTST presentation, San Diego.

[59] Brown, S. "A Novel Near-Land Radiometer Wet Path Delay Retrieval Algorithm: Application to the Jason-2/OSTM Advanced Microwave Radiometer", submitted to IEEE Trans. Geosci. Rem. Sens. March 2009

[60] "The enhanced Jason-1 Microwave Radiometer (JMR) corrections contains better wet tropospheric path delay corrections along with better land, rain and ice flagging for coastal regions than that found in the Jason-1 Geophysical Data Records" (based on GdrC). available at http://podaac.jpl.nasa.gov/dataset/JASON-1_JMR_ENH

[61] Boening, C., J. K. Willis, F. W. Landerer, R. S. Nerem, and J. Fasullo (2012), The 2011 La Niña: So Strong, the Oceans Fell, Geophys. Res. Lett., doi:10.1029/2012GL053055, in press.

[62] Fasullo JT., Boening C., Landerer F.W., Nerem R.S. (2013), Australia's unique influence on Global Sea Level in 2010-2011, Geophys. Res. Lett., doi:10.1002/grl.50834.

[63] http://www.aviso.oceanobs.com/en/news/ocean-indicators/mean-sea-level.html

[64] http://www.aviso.oceanobs.com/en/calval/systematic-calval/validation-reports.html

[65] Impact of GDR_D standards on SSB corrections (http://www.aviso.oceanobs.com/fileadmin/documents/OSTST/2012/oral/02_friday_28/01_instr_processing_I/01_IP1_Tran.pdf)